Analytical study of the direct initiation of gaseous detonations for small heat release.

Paul Clavin, Bruno Denet

Analytical study of the direct initiation of gaseous detonations for small heat release.

Paul Clavin and Bruno Denet

Aix Marseille Université, CNRS, Centrale Marseille, IRPHE UMR7342,
49 Rue F. Joliot Curie, 13384 Marseille, France

(Received ?; revised ?; accepted ?. - To be entered by editorial office)

An analysis of the direct initiation of gaseous detonations in spherical geometry is presented. The full set of constitutive equations is analyzed by an asymptotic analysis in the double limit of Mach number close to unity (small heat release) and large thermal sensitivity. The quasi-steady curvature-induced quenching phenomenon is first revisited in this limit. Considering a realistic decrease rate of the rarefaction wave, the unsteady problem is reduced to a single nonlinear hyperbolic equation. The time-dependent velocity of the lead shock is an eigenfunction of the problem when two boundary conditions are imposed to the flow at the lead shock and at the burnt gas side. Following Liñan *et al.* (2012), the boundary condition in the quasi-transonic flow of burnt gas is expressed in terms of the curvature. Focusing the attention on successful initiation, the time-dependent velocity of the lead shock of a detonation approaching the CJ regime is solution of a nonlinear integral equation investigated for stable and marginally unstable detonations. By comparison with the quasi-steady trajectories in the phase space "*propagation velocity vs radius*", the solution exhibits the unsteady effect produced upon the detonation decay by the long time delay of the upward running mode for transferring the rarefaction-wave-induced deceleration across the inner detonation structure from the burnt gas to the lead shock. In addition, a new and intriguing phenomenon concerning pulsating detonations is described. Even if the results are not quantitatively accurate, they are qualitatively relevant for real detonations.

Key words: Authors should not enter keywords on the manuscript, as these must be chosen by the author during the online submission process and will then be added during the typesetting process

1. Introduction

As suggested long ago by Vieille (1900), gaseous detonations are supersonic combustion waves whose internal structure is a reactive layer following a non-reactive shock wave. This is called the ZND structure to honor the works of Zeldovich (1940), Von Neumann (1942) and Döring (1943). The shocked gas velocity relative to the lead shock is of the same order of magnitude as the sound speed a_u and, thanks to a large activation energy, the reaction rate t_r^{-1} is smaller than the collision frequency $1/t_r \ll 1/t_{coll}$. Consequently, the molecular diffusivities (viscosity and molecular diffusion) are negligible in the reactive layer as shown by the large Reynolds number la_u/ν based on the thickness of the reactive layer $l \approx a_u t_r$ and the viscous diffusivity $\nu \approx a_u^2 t_{coll}$, $a_u^2 t_r/\nu \approx t_r/t_{coll} \gg 1$. Even when the propagation Mach number is close to unity $0 < M-1 \ll 1$ as it is the case in the forthcoming asymptotic analysis, the thickness of the lead shock $a_u t_{coll}/(M-1)$ is

smaller than the thickness of the reaction layer l provided that the ratio of the reaction time to the collision time is sufficiently large, $(M-1)t_r/t_{coll} \gg 1$. In such a condition, the lead shock can be considered as an inert discontinuity even when the heat release is small $0 < M-1 \ll 1$, see Clavin & Searby (2016).

The direct initiation of gaseous detonation refers to the formation of a self-sustained detonation in the decay of a blast wave when a large amount of energy E is deposited quasi-instantaneously in a small region of space (radius r_E) of an unconfined combustible gas mixture. Here, attention is limited to spherical geometry. At the very beginning, the density of deposited energy is larger than the density of chemical energy available in the gas mixture $E/r_E^3 \gg \rho_u q_m$, ρ_u and q_m denoting the density and the chemical energy per unit mass in the initial gaseous mixture. Therefore the initial condition is the Sedov (1946) - Taylor (1950*b*) self-similar solution of a strong blast wave in an inert gas, expressing how the propagation velocity $\mathcal{D}$ decreases with the shock radius r_f, $\mathcal{D} \propto (E/\rho_u)^{1/2}/r_f^{3/2}$. A critical radius r^* larger than the detonation thickness, $r^* \gg l$, $r^*/l \approx 300$, and a critical energy $E^* \propto \rho_u q_m r^{*3}$ have been identified for a long time by numerous experiments, see Lee (1977) and Lee (1984). For $E > E^*$ the self-sustained Chapman-Jouguet detonation (CJ regime characterized by a sonic condition at the exit of the reaction zone and a minimum propagation velocity $\mathcal{D}_{_{CJ}}$) is reached at a radius $\approx (E/\rho_u q_m)^{1/3}$ larger than r^*. For $E < E^*$ a progressive decoupling of the reaction zone from the lead shock produces the failure of initiation; the shock intensity continuously decreases and no detonation occurs.

Pioneering numerical solutions of direct initiation were performed by Korobeinikov (1971) assuming that the detonation wave is a discontinuity across which the planar jump conditions are satisfied. This problem was reconsidered more recently by Liñan *et al.* (2012) providing us with new insights into the transition between two self-similar solutions, namely the solution of Sedov (1946) and Taylor (1950*b*) for a strong non reactive blast wave and the solution of Zeldovich (1942) and Taylor (1950*a*) for a spherical CJ detonation. Under the approximation of the discontinuous model there is no critical energy: the overdriven detonation that is initially generated by the blast wave relaxes systematically to a planar CJ wave at a finite radius proportional to $(E/\rho_u q_m)^{1/3}$ no matter the value of E. This indicates clearly that the critical energy should be related to small modifications of the inner structure of the detonation wave (finite thickness effect).

A first criterion was proposed by Zeldovich *et al.* (1956). Considering that the time taken by the blast wave for reaching the planar CJ velocity $\mathcal{D}_{o_{CJ}} \approx 2\sqrt{q_m}$ should be larger than the reaction time t_r, the order of magnitude of the critical radius predicted by Zeldovich *et al.* (1956) is of the same order of magnitude as the thickness of the planar CJ wave $l_{o_{CJ}}$, $r^* \approx l_{o_{CJ}}$. This is in contradiction with experiments. Using a relevant value of t_r, this criterion leads to a critical energy which is smaller than the experimental data by a factor 10^{-5} to 10^{-6}. A further step was achieved forty years later by He & Clavin (1994) who considered the modification of the inner structure generated by a small curvature of the wave amplified by the strong thermal sensitivity of the induction length governed by an Arrhenius law with a large activation energy $\mathcal{E}/k_BT \gg 1$. The He & Clavin (1994) analysis of curved CJ detonations was performed for a large Mach number $M \gg 1$ in the limit $\mathcal{E}/k_BT \to \infty$, using a quasi-steady inner structure modeled by a crude square-wave model (chemical energy released instantaneously after the induction delay). The analysis leads to a non linear relation between the propagation velocity $\mathcal{D}_{_{CJ}}$ of a curved CJ detonation and the curvature $1/r_f$. The corresponding curve $\mathcal{D}_{_{CJ}}/\mathcal{D}_{o_{CJ}}$ versus $r_f/l_{o_{CJ}}$ presents a C-shaped exhibiting a quasi-steady curvature-induced quenching; there is no quasi-steady solution of spherical CJ wave with a radius smaller than a critical r_f^* which

is is larger than l_{oCJ} by a factor of few hundreds, essentially because the activation energy is large $\mathcal{E}/k_BT \gg 1$. The energy varying like r_f^3, the order of magnitude of the experimental critical energy is recovered.

The quasi-steady analysis is not fully satisfactory, even though the numerical simulations of He & Clavin (1994) (one-step model) and of He (1996) (detailed chemical scheme for the combustion of hydrogen-oxygen mixtures) are in satisfactory agreement with the critical radius r_f^*, at least the order of magnitude. The unsteady effects are important near criticality. For example, a quasi-quenching of the detonation with a propagation velocity decreasing well below $\mathcal{D}_{oCJ}$, followed by a sudden re-ignition, is exhibited near criticality. This illustrates that the initiation process is different from the quassi-steady decay of an overdriven detonation. The corresponding interplay of pressure waves and reaction rate was analyzed numerically by Lee & Higgins (1999). The importance of unsteadiness was emphasized by Eckert *et al.* (2000) whose numerical simulations (for a one-step exothermal reaction governed by an Arrhenius law) show that the unsteady terms are larger than the geometrical terms. However the critical radius r_f^* is not much different from that in He & Clavin (1994), it is smaller by a factor between 2 and 4. Considering the difference of detonation model, the agreement is satisfactory since the square-wave model in He & Clavin (1994) overestimates the critical radius. Nevertheless the behavior of the dynamics near criticality cannot be reproduced by the quasi-steady approximation. The specific effect of a small curvature was pointed out in He & Clavin (1994) by comparing the numerical simulations in spherical geometry with those in planar geometry. In the latter case the critical distance r^* is still larger than the detonation thickness but ten times smaller than the critical radius in spherical geometry. Therefore both curvature and unsteadiness are important near criticality. A somewhat different point of view is presented by Eckert *et al.* (2000), who concluded that "*the primary failure mechanism is found to be unsteadiness*".

The purpose of the present analytical study is to investigate the role of unsteadiness combined with the curvature effects. There are two different unsteady effects. One is inherent to the driving mechanism of the detonation decay, namely the rarefaction wave in the burnt gas. The other is the intrinsic dynamics of the inner detonation structure controlling the response to variation of the flow of burnt gas. The corresponding hyperbolic problem is too complicated for general analytical solutions to be obtained. Not only the dynamics of the inner structure of the detonation is a tough problem but also the rarefaction wave (the cause) depends on the dynamics of the detonation decay (the effect). Moreover separating the inner structure from the inert rarefaction wave is not an easy task in spherical geometry. According to the Sedov-Taylor self-similar solution, the characteristic time of evolution of the blast wave $\mathcal{D}/(\mathrm{d}\mathcal{D}/\mathrm{d}t)$ is of order $r/\mathcal{D}$ which is is larger than the transit time of a fluid particle through the detonation structure $(l/\mathcal{D})$ by a factor r/l (a large number near criticality $r^*/l \gg 1$). This does not insure that a quasi-steady approximation is accurate since, according to Clavin & Williams (2002), the response time of the inner structure is also larger than $l/\mathcal{D}$. The cumulative effect of feedback loops controlling the inner dynamics can be summarized as follows. The disturbance, introduced when the shock velocity $\mathcal{D}$ varies, propagates downstream (in the reference frame attached to the shock) towards the burnt gas with two modes, a downstream-running acoustic mode and an entropy wave. The resulting modification of heat release in turn perturbs the flow and thereby affects the shock velocity after a time delay associated with the upstream-running acoustic mode and thus depending on the place of emission. When approaching the CJ regime, the flow near the end of heat release becomes quasi-transonic and the delay of the upstream-running mode is larger than

those associated with the downstream-running modes, including the entropy wave whose transit time is of order $l/\mathcal{D}$. At the leading order of a multiple timescales analysis the downstream-running modes can be considered as quasi-instantaneous and the dynamics is mainly controlled by the upstream running mode. The key unsteady mechanism of direct initiation when the CJ regime is approached is the time delay for transferring the rarefaction-wave-induced deceleration to the lead shock. Because of the transonic flow at the exit of the inner detonation structure, the delay increases and diverges at the CJ velocity producing a drastic unsteady effect upon the dynamics. This difficult topic has not yet been addressed in the context of the direct initiation process. The present work is an attempt to fill this gap by an asymptotic analysis reducing the problem to solve a single nonlinear hyperbolic equation. Only the end of the detonation decay during a successful initiation is analyzed in detail here. The study of the dynamics is more difficult near criticality and requires a different theoretical approach left to future studies.

The multiple timescale nature of the dynamics is stressed and enlightened in the limit of small heat release ($M-1 \ll 1$) since the flow becomes quasi-transonic throughout the inner structure of the detonation. Combined with the Newtonian approximation in the reaction zone and a large activation energy, a small heat release is a convenient limit for the analytical study of the unsteady inner structure of detonation since the interplay of pressure waves, entropy wave and chemical kinetics at work in real detonations is fully taken into account. Moreover, purely technical difficulties (such as variation of the sound speed with the temperature and compressional heating in the reaction zone) are suppressed without modifying the order of magnitude of the result. Then, despite the difference of Mach numbers (M close to unity while $M \in [4, 8]$ in ordinary gaseous detonations), the dynamics is relevant for real detonations, at least qualitatively, provided that the inert shock wave at the leading edge of the ZND structure is still considered as a discontinuity satisfying the Rankine-Hugoniot conditions, as discussed earlier. Such asymptotic analyses have been performed in planar geometry by Clavin & Williams (2002) for the stability analysis of slightly overdriven detonations against planar disturbances, extended later to multidimensional disturbances in Clavin & Williams (2009). The numerical study of weakly nonlinear regimes performed by Faria *et al.* (2015) in this limit shows cellular patterns similar to those observed in ordinary detonations.

In the present paper a similar asymptotic analysis is carried out for the direct initiation process in spherical geometry. The attention is focused onto the trajectories close to the CJ velocity. The primary result is to show that the dynamics is controlled by a single hyperbolic equation for a scalar field representative of the flow inside the inner structure of the detonation. The problem of the dynamics of the inner structure is closed because the deceleration of the burnt at the downstream boundary condition is related to the curvature of the detonation wave. This relation is similar to that obtained by Liñan *et al.* (2012) with the discontinuous model in the opposite limit $M \gg 1$. Unfortunately essential features of the direct initiation process are lost by the rarefaction wave behind a detonation wave in the limit $M-1 \ll 1$. Therefore, a small heat release is used here only for the response of the detonation to the rarefaction-wave-induced deceleration, not for the rarefaction wave itself. As in the study of Clavin & Denet (2018) concerning the decay of plane detonations when the supporting piston is suddenly arrested, the analysis is not limited to a particular chemical kinetics scheme. The basic inputs are the spatial distribution of heat release in the planar CJ detonation (in steady state) and the thermal sensitivity of the detonation thickness. In order to overcome the current technical difficulty in spherical geometry for matching the reaction zone with the external flow

through a quasi-transonic zone, the rate of heat release is assumed to drop sharply to zero at the end of the reaction zone. For successful initiation the time-dependent propagation velocity $\mathcal{D}(t)$ is solution of an integral equation. Marginally stable and/or unstable detonations are investigated for a parameter controlling the thermal sensitivity of the planar dynamics smaller than that controlling the curvature effect. Unsteadiness is highlighted in the phase space *propagation velocity vs shock radius* by comparison with the quasi-steady trajectories. By the way a new and intriguing phenomenon at work during pulsations of unstable detonations is described.

The general formulation is recalled in § 2. Extending previous analyses to spherical geometry, the double limit of small heat release and large activation energy is presented in § 3. The peninsula of steady spherical CJ detonations representative of a curvature-induced quenching is revisited in § 4, extending the result of He & Clavin (1994) to a smooth distribution of reaction rate. The inner structure of the spherical CJ wave is presented in § 5 with a discussion on the sonic point. The closure relation and the hyperbolic equation controlling the initiation process are derived in § 6. The quasi-steady trajectories showing a transition between success and failure of the initiation process are presented in § 7. The limitation of the quasi-steady approximation is discussed in this section. The integral equation for $\mathcal{D}(t)$ is derived in § 8. The results and the complexity of the nonlinear dynamics are discussed in § 9 where unsteady trajectories "velocity-radius" are presented, pointing out the unsteady effect of the increase of the time delay near the CJ regime. Also a new dynamical phenomenon is identified in this section. Conclusion and perspectives are presented in § 10. In view of a self-contained paper, five appendices supplement the main text. The rarefaction wave behind a detonation whose propagation velocity is close to the sound speed is computed in Appendix A. Technical calculations are developed in Appendix B. The method of solution of a hyperbolic equation with a moving boundary is presented in Appendix C. The dynamics of planar detonations is recalled in Appendix D where the cold boundary difficulty of the CJ regime is also discussed. An analytical expression of the time delay along a straight trajectory ending up abruptly on the CJ regime is presented in Appendix E for a simple model.

2. General formulation

2.1. *Constitutive equations*

In spherical geometry, $\nabla.\mathbf{u} = \partial u/\partial r + 2u/r$, Euler's equations take the form

$$\frac{1}{\rho}\left(\frac{\partial}{\partial t} + u\frac{\partial}{\partial r}\right)\rho + \frac{\partial u}{\partial r} + 2\frac{u}{r} = 0, \qquad \rho\left(\frac{\partial}{\partial t} + u\frac{\partial}{\partial r}\right)u = -\frac{\partial p}{\partial r}, \tag{2.1}$$

$$\left(\frac{\partial}{\partial t} + u\frac{\partial}{\partial r}\right)\left[\ln T - \frac{(\gamma-1)}{\gamma}\ln p\right] = \frac{q_m}{c_p T}\frac{\dot{w}(T,Y)}{t_r}, \quad \left(\frac{\partial}{\partial t} + u\frac{\partial}{\partial r}\right)Y = \frac{\dot{w}(T,Y)}{t_r}, \tag{2.2}$$

where ρ, p and u are respectively the density, the pressure and the radial velocity in the laboratory frame and γ, q_m, T, Y, t_r and $\dot{w}$ are respectively the ratio of specific heat $\gamma \equiv c_p/c_v = \text{cst.}$, the chemical heat release per unit mass of mixture, the temperature, the progress variable ($Y = 0$ in the initial mixture and $Y = 1$ in the burned gas, $1 - Y$ is the reduced mass fraction of the limiting component in a one-step reaction), the reaction time at the Neuman state of the planar CJ detonation and the non dimensional heat-release rate. The second equation in (2.2) is a short notation for a complex chemical kinetics of combustion, the analysis being not limited to a one-step scheme. Assuming

the ideal gas law, pressure p and the sound speed a are

$$p = \frac{\gamma - 1}{\gamma} c_p \rho T, \qquad a = \sqrt{\gamma \frac{p}{\rho}}. \tag{2.3}$$

Attention is focused on an irreversible exothermal reaction whose rate $\dot{w}(Y,T) \geqslant 0$ is depending on the temperature T and the progress variable Y, the pressure dependence being neglected for simplicity by comparison with the thermal sensitivity. An alternative form of the energy equation in (2.2) is expressed in terms of p and u by using the ideal gas law (2.3) when ρ is eliminated by using the mass conservation (2.1),

$$\frac{1}{\gamma p}\left(\frac{\partial}{\partial t} + u\frac{\partial}{\partial r}\right) p + \frac{\partial u}{\partial r} + 2\frac{u}{r} = \frac{q_m}{c_p T}\frac{\dot{w}(T,Y)}{t_r}. \tag{2.4}$$

Equations for the conservation of mass and momentum in (2.1) can be put in the form of two hyperbolic equations for u and p when the equation for conservation of momentum in (2.1) is multiplied by $a/(\gamma p) = 1/(\rho a)$ and added to and subtracted from (2.4)

$$\frac{1}{\gamma p}\left[\frac{\partial}{\partial t} + (u \pm a)\frac{\partial}{\partial r}\right] p \pm \frac{1}{a}\left[\frac{\partial}{\partial t} + (u \pm a)\frac{\partial}{\partial r}\right] u = \frac{q_m}{c_p T}\frac{\dot{w}}{t_r} - 2\frac{u}{r}. \tag{2.5}$$

These equations relating the propagation of the disturbances of pressure p and radial velocity u to the rate of heat release $\dot{w}/t_r$ and the divergence of the flow $2u/r$ are the extension of the usual characteristic equations (simple waves) to reacting gases in spherical geometry. When (2.3) is used and when the chemical kinetics $\dot{w}(T,Y)$ is known, the four equations in (2.2) and (2.5) form a closed set for p, u, T and Y.

2.2. *Formulation*

Considering the lead shock as a discontinuity in the flow of inert gas at initial temperature T_u (composition frozen far from chemical equilibrium, $Y = 0$, $\dot{w}(T_u, 0) = 0$), the boundary conditions in the compressed gas at the front of the lead shock (Neumann state denoted by the subscript N) are given by the Rankine-Hugoniot equations

$$\frac{p_N}{p_u} = 1 + \frac{2\gamma}{\gamma+1}(M^2 - 1), \quad \frac{\rho_N}{\rho_u} = \frac{1 + (M^2-1)}{1 + \frac{\gamma-1}{\gamma+1}(M^2-1)}, \quad \frac{u_N}{a_u} = \left(1 - \frac{\rho_u}{\rho_N}\right) M, \tag{2.6}$$

where the subscript u denotes the fresh mixture at rest and $M \equiv \mathcal{D}/a_u$ is the propagation Mach number, $\mathcal{D}$ being the propagation velocity of the lead shock velocity. Introducing the equation for the trajectory of the shock front, $r = r_f(t)$, $\mathrm{d}r_f/\mathrm{d}t = \mathcal{D}(t)$, it is convenient to use the coordinate attached to the lead shock

$$\mathrm{x} \equiv r - r_f(t) \quad \Rightarrow \quad \partial/\partial r \to \partial/\partial \mathrm{x}, \quad \partial/\partial t \to \partial/\partial t - \mathcal{D}(t)\partial/\partial \mathrm{x}. \tag{2.7}$$

Considering an expanding spherical detonation, $\dot{r}_f \equiv \mathrm{d}r_f/\mathrm{d}t > 0$, $u \geqslant 0$, the initial mixture and the compressed gas are located at $\mathrm{x} > 0$ and $\mathrm{x} \leqslant 0$ respectively. The boundary conditions at the Neumann state, takes the form

$$\mathrm{x} = 0: \quad Y = 0,\ \dot{w} = \dot{w}_N(T_N) > 0, \quad p = p_N(t), \quad T = T_N(t), \quad u = u_N(t) \tag{2.8}$$

where $p_N(t)$, $T_N(t)$, and $u_N(t)$ are given in term of the instantaneous propagation velocity $\mathcal{D}(t)$ in (2.6).

A rear boundary condition in the burned gas is required for solving the detonation dynamics $M(t)$. When the length scale of the external flow $u_{ext}(r,t)$ in the burnt gas is larger than the detonation thickness, $l_{ext} \gg a_u t_r$, $1/l_{ext} \equiv |(1/u_{ext})\partial u_{ext}/\partial r|_{r=r_f(t)}$, and when the attention is focused on weakly curved detonations, $r_f/a_N t_r \gg 1$, the solution

can be decomposed into two parts: the inner structure of the detonation wave and the external flow of burnt gas, $u_{ext}(r,t)$. Generally speaking, matching the end of the inner structure and the burnt gas flow is a delicate question especially near the CJ regime since the flow is transonic in the matching layer. The difficulty is overcome here by a detonation structure in which the distance between the end of the exothermal reaction and the lead shock is bounded. Introducing the non dimensional coordinate ξ attached to the moving front of the lead shock,

$$\xi \equiv \frac{r - r_f(t)}{a_u t_r}, \tag{2.9}$$

and denoting $\xi_b < 0$ the end of the inner structure where the external flow is prescribed, the rear boundary condition takes the form

$$|\xi_b| = O(1), \qquad \xi = \xi_b(\tau) < 0 : \ u = u_b(t), \quad u_b(t) = u_{ext}(r_f(t), t), \tag{2.10}$$

the flow field of burnt gas $u_{ext}(r,t)$ being solution to the external problem. It has been known for a long time that the sonic point inside the inner structure of a curved Chapman-Jouguet detonation in steady state is located at a point of incomplete reaction where the rate of heat release is balanced by the divergence of the flow, see Wood & Kirkwood (1954) and § 5 below. The sonic locus is a saddle point through which the steady solution satisfying the boundary condition at the Neumann state should go (determining the CJ velocity). More details and references can be found in Fickett & Davis (1979), Short & Bdzil (2003) and Stewart & Kasimov (2005). For a weak curvature, the distance between the sonic point and the end of the heat release is small if the thermal sensitivity of the detonation thickness is large, see § 5.1. This is the case in the analysis of weakly curved detonation in steady state by Yao & Stewart (1995) in the limit of a large activation energy of a one-step reaction governed by an Arrhenius law. In the present unsteady study, the external flow is prescribed near the end of the exothermal reaction,

$$\xi = \xi_b(\tau) : \ \dot{w}(Y,T) \approx 0, \qquad \xi_b < \xi \leqslant 0 : \ \dot{w}(Y,T) > 0, \tag{2.11}$$

anticipating that the precise definition of $\xi_b(\tau)$ introduces a negligible correction to the time-dependent velocity $\mathcal{D}(t)$ of the lead shock when the thermal sensitivity is large.

3. Governing equations in the limit of small heat release

Direct initiation of detonation is studied here by an asymptotic analysis in the double limit of small heat release $\epsilon^2 \equiv q_m/c_pT_u \ll 1$ and large thermal sensitivity, using the Newtonian approximation (ratio of specific heats $\gamma \equiv c_p/c_v > 1$ close to unity),

$$\epsilon \equiv \sqrt{q_m/c_pT_u} \approx (M_{o_{CJ}} - 1) \ll 1, \qquad (\gamma - 1)/\epsilon \ll 1, \tag{3.1}$$

where $M_{o_{CJ}} \equiv \mathcal{D}_{o_{CJ}}/a_u \approx 1 + \sqrt{q_m/c_pT_u}$ is the Mach number of the planar CJ wave in steady state propagating at the velocity $\mathcal{D}_{o_{CJ}}$. For the small difference (3.1) of specific heats, the compressional heating is negligible in the reaction zone by comparison with the chemical heat release. This is indeed an accurate approximation in real detonations. The limit of small heat release provides us with a systematic way for taking fully advantage of the two timescales of the dynamics.

3.1. *Two-timescale analysis of the transonic flow*

Considering a radius of the lead shock r_f larger than the detonation thickness,

$$\frac{a_u t_r}{r_f} = \epsilon\kappa, \tag{3.2}$$

where κ is a non-dimensional parameter for the curvature of the detonation wave, the simplification in the limit $\epsilon \to 0$ is similar to that in plane geometry. The flow is transonic throughout the inner structure of the detonation so that the problem is one of two timescales; the inner structure evolves slowly, on a time scale larger by a factor $1/\epsilon$ than the transit time of a fluid particle. Moreover the variation of the sound speed can be neglected $a_b/a_u = 1 + O(\epsilon^2)$. The modification of the sound speed across the inner structure of real detonations introduces small quantitative differences but no new qualitative effects.

For a propagation velocity close the CJ velocity of the planar detonation we introduce the same dimensionless quantities of order unity in the limit (3.1) as in Clavin & Denet (2018), $\mu(\xi,\tau)$, $\pi(\xi,\tau)$ and $\dot\alpha_\tau(\tau)$ for respectively the flow velocity in the laboratory frame, the pressure and the instantaneous propagation velocity of the lead shock $\mathcal{D}(t) = \mathrm{d}r_f/\mathrm{d}t$,

$$\frac{u - \mathcal{D}_{o_{CJ}}}{a_u} \equiv -1 + \epsilon\,\mu(\xi,\tau), \quad \frac{\mathcal{D} - \mathcal{D}_{o_{CJ}}}{a_u} \equiv \epsilon\,\dot\alpha_\tau(\tau), \quad \frac{1}{\gamma}\ln\left(\frac{p}{p_u}\right) \equiv \epsilon\pi(\xi,\tau). \tag{3.3}$$

Focusing attention onto the inner structure of the detonations, $\xi = O(1)$, the curvature term r_f/r is, according to (2.9) and (3.2), almost constant and equal to unity,

$$\frac{r_f}{r} = \frac{1}{1+\epsilon\kappa\xi} \quad \Rightarrow \quad \frac{1}{r} = \frac{1}{r_f}\left[1 + O(\epsilon)\right]. \tag{3.4}$$

When the terms smaller than ϵ^2 are neglected, equations (2.5), written in the reference frame attached to the lead shock (2.7), take the following non dimensional form

$$\epsilon\left[t_r\frac{\partial}{\partial t} + \left[-2 + \epsilon(\mu - \dot\alpha_\tau)\right]\frac{\partial}{\partial\xi}\right](\pi - \mu) = \epsilon^2\dot w - 2\epsilon^2(1+\mu)\kappa, \tag{3.5}$$

$$\epsilon\left[t_r\frac{\partial}{\partial t} + \epsilon(\mu - \dot\alpha_\tau)\frac{\partial}{\partial\xi}\right](\pi + \mu) = \epsilon^2\dot w - 2\epsilon^2(1+\mu)\kappa, \tag{3.6}$$

which are obtained from (2.5) and (2.7) by using (3.1)-(3.3) written in the form

$$\frac{u}{a_u} = \epsilon(1+\mu), \quad \frac{(u-\mathcal{D})}{a_u} = \epsilon(\mu - \dot\alpha_\tau) - 1, \quad \frac{u}{r} = \epsilon^2\kappa(1+\mu)\frac{r_f}{r} \tag{3.7}$$

u being the gas velocity in the laboratory frame. Notice the difference of notation with Clavin & Williams (2002) who used the notation μ for the flow velocity relative to the lead shock $(\mathcal{D} - u)/a_u$. The boundary conditions at the Neumann state (2.6) yield

$$\xi = 0 : \mu = \mu_N(\tau) = (1 + 2\dot\alpha_\tau) + O(\epsilon), \quad \pi = \pi_N(\tau) = 2(1 + \dot\alpha_\tau) + O(\epsilon). \tag{3.8}$$

The two-timescale nature of the dynamics in the limit (3.1) is seen from (3.5) and (3.6). The velocity of the simple wave (3.5), issued from the lead shock ($\xi = 0$) and propagating toward the exit of the reaction zone (in the negative ξ direction) is larger (by a factor $1/\epsilon$) than the velocity of the simple wave (3.6), issued from the reaction zone and propagating in the opposite direction for sending the signal back to the lead shock. Therefore, to leading order in the limit (3.1), the propagation mechanism in (3.5) is considered as instantaneous compared to the simple wave (3.6) which thus controls the dynamics of

the inner structure. The resulting dynamics of the inner structure is slow at the scale of the transit time t_r and the reduced timescale of order unity is

$$\tau \equiv \epsilon \frac{t}{t_r}, \qquad \frac{\partial}{\partial t} = \frac{\epsilon}{t_r}\frac{\partial}{\partial \tau}. \tag{3.9}$$

The leading order of (3.5), $\partial(\pi-\mu)/\partial\xi = 0$, shows that, according to (3.8), the quantity $\pi - \mu$ is constant, $(\pi - \mu) \approx 1$. Expressed in terms of the reduced time (3.9) the leading order of (3.6) in the limit (3.1) takes the form of a single nonlinear equation for the non-dimensional flow velocity $\mu(\xi, \tau)$ satisfying the boundary conditions (2.10) and (3.8)

$$\frac{\partial \mu}{\partial \tau} + [\mu - \dot\alpha_\tau(\tau)]\frac{\partial \mu}{\partial \xi} = \frac{\dot w(T,Y)}{2} - (1+\mu)\kappa(\tau), \tag{3.10}$$

$$\xi = 0 : \mu = 1 + 2\dot\alpha_\tau(\tau), \qquad \xi = \xi_b(\tau) : \mu = \mu_b(\tau), \tag{3.11}$$

where, skipping the matching difficulty mentioned in § 2.2, the function $\mu_b(\tau)$ is given by the external solution, except for the CJ regime for which the dynamics of the inner structure is decoupled from the flow of burnt gas by the sonic condition,

$$\text{CJ wave:} \qquad \xi = \xi_b(\tau) : \ \mu = \dot\alpha_\tau(\tau) \tag{3.12}$$

($\dot\alpha_\tau = 0$ in the planar CJ wave, $\kappa = 0$). If the flow of shocked gas is kept subsonic relatively to the lead shock, as is the case in the steady state, the term in the bracket on the left-hand side of (3.10) is positive everywhere across the inner structure and represents the absolute value of the propagation velocity of the upward running mode (simple wave) propagating in the shocked gas toward the lead shock

$$\xi_b < \xi \leqslant 0 : \quad (\mu - \dot\alpha_\tau) = \left[a_u - (\mathcal{D} - u)\right]/\epsilon a_u \geqslant 0, \tag{3.13}$$

where the second relation in (3.7) has been used. The condition $(\mu - \dot\alpha_\tau) > 0$ means that the flow is subsonic (relatively to the lead shock) everywhere in the inner structure.

3.2. *Unsteady distribution of the heat release rate*

The compressional heating which is a key mechanism across the (inert) lead shock for the dynamics of detonation wave, is negligible in the compressed gas and the instantaneous distribution of heat release rate $\dot w(T,Y) = \omega(\xi, \dot\alpha_\tau(\tau))$ can be expressed in terms of the shock velocity $\dot\alpha_\tau(\tau)$. This is because the system of equations (2.2) for the entropy wave forms a closed set for $T(\xi,\tau)$ and $Y(\xi,\tau)$ in the Newtonian limit (3.1). Moreover, according to the two-timescale nature of the dynamics (3.9), the unsteady terms are negligible in (2.2) so that, the solutions $T(\xi,\tau)$ and $Y(\xi,\tau)$ are the same as in the steady states, $\overline{T}(\xi, \overline{T}_N)$, $\overline{Y}(\xi, \overline{T}_N)$, but with $\overline{T}_N$ replaced by the instantaneous value $T_N(\tau)$ which is expressed in terms of the unsteady shock velocity $\dot\alpha_\tau(\tau)$ by (2.3) and (2.6),

$$(M^2-1) \ll 1 : \qquad \frac{T_N}{T_u} \approx 1 + 2\frac{\gamma-1}{\gamma+1}(M^2-1), \qquad \frac{\delta T_N(\tau)}{T_u} \approx 4\frac{(\gamma-1)}{\gamma+1}\delta M. \tag{3.14}$$

Introducing the activation energy $\mathcal{E}$ controlling the variation of the induction length with the Neumann temperature $\delta l/l = (\mathcal{E}/k_b T_N)\delta T_N/T_N$,

$$\frac{\delta l}{l} = -b\,\dot\alpha_\tau \quad \text{where} \quad b \equiv \frac{4}{\gamma+1}(\gamma-1)\epsilon\frac{\mathcal{E}}{k_B T_u}, \tag{3.15}$$

and, assuming for simplicity that the thermal sensitivity of the induction length is dominant, the shape of $\omega(\xi, \dot\alpha_\tau(\tau))$, solution of (2.2) in the limit (3.1) corresponds simply to

a rescaling of the length scale by the time-dependent induction length,

$$\omega(\xi, b\dot{\alpha}_\tau) = \mathrm{e}^{b\dot{\alpha}_\tau}\omega_{o_{CJ}}(\xi\,\mathrm{e}^{b\dot{\alpha}_\tau}), \qquad \int_{-\infty}^{0}\omega(\xi, b\dot{\alpha}_\tau)\mathrm{d}\xi = 1, \tag{3.16}$$

where $\omega_{o_{CJ}}(\xi)$ is the steady distribution of the planar CJ detonation, $\int_{-\infty}^{0}\omega_{o_{CJ}}(\xi)\mathrm{d}\xi = 1$. The scaling law (3.16) was shown to be satisfactory for H_2-O_2 detonations, see Clavin & He (1996). Since the curvature is not involved explicitly in (2.2), the expression of $\omega(\xi, \dot{\alpha}_\tau(\tau))$ is the same as in the planar geometry considered previously. Equations (3.10)-(3.11) and (3.16) are the extension of the detonation model of Clavin & Williams (2002) to spherical geometry ($\kappa \neq 0$). In order to overcome the technical difficulty for matching the inner structure with the external flow, a bounded reaction zone of the CJ wave is assumed,

$$\xi \leqslant -1 : \omega_{o_{CJ}} = 0 \quad \text{and} \quad \xi = -1 : \mathrm{d}\omega_{o_{CJ}}/\mathrm{d}\xi|_{\xi+1=0^+} = h_\omega > 0, \quad h_\omega = O(1). \tag{3.17}$$

The length scales of the inner structure and of the external flow (rarefaction wave) being clearly separated, the approximation (3.17) does not produce relevant modifications since the heat release in the tail of the distribution of heat release is negligible. Equation (3.17) will be used in the following except in § 4.2 where the square-wave model is used.

The instantaneous distribution of heat release (3.16) depends on the time through $\mathrm{e}^{b\dot{\alpha}_\tau(\tau)}$ and on the space through $\xi\mathrm{e}^{b\dot{\alpha}_\tau(\tau)}$ so that the instantaneous thickness of the inner structure follows the same Arrhenius law as the induction length, $\xi_b = \mathrm{e}^{-b\dot{\alpha}_\tau}\xi_{bo_{CJ}}$. The reference time scale t_r in (2.2)-(2.9) being the reaction time at the Neumann state of the planar CJ solution in steady state, $\xi_{bo_{CJ}} = -1$, the instantaneous position (relative to the shock) of the exit of the inner structure zone is $\xi = -\mathrm{e}^{-b\dot{\alpha}_\tau(\tau)}$

$$\xi_{bo_{CJ}} = -1 \quad \Rightarrow \quad \xi_b(\tau) \approx -\mathrm{e}^{-b\dot{\alpha}_\tau(\tau)}. \tag{3.18}$$

The instantaneous reaction rate (3.16) has a bell-shaped form similar to that of $\omega_{o_{CJ}}(\xi)$

$$\xi = \xi_b(\tau) \approx -\mathrm{e}^{-b\dot{\alpha}_\tau(\tau)} : \omega(\xi, \dot{\alpha}_\tau) \approx 0, \qquad \mathrm{e}^{-b\dot{\alpha}_\tau(\tau)} < \xi \leqslant 0 : \omega(\xi, \dot{\alpha}_\tau) > 0, \tag{3.19}$$

with a maximum of order unity at $\xi = \xi_m$, $\xi_m \in [-\mathrm{e}^{-b\dot{\alpha}_\tau(\tau)}, 0]$ such that the reduced distance $|\xi_m + \mathrm{e}^{-b\dot{\alpha}_\tau(\tau)}| < 1$ is not small ($\lim_{1/b\to 0}|\xi_m - \xi_b| \neq 0$) as is typically the case in real detonations. This difference with the one-step reaction model in the limit of large activation energy (leading to the square-wave model $\lim_{1/b\to 0}|\xi_m - \xi_b| = 0$) is essential for a well-posed problem of detonation dynamics.

4. Peninsula of quasi-steady CJ waves in spherical geometry.

A preliminary step before studying the dynamics in the phase space *velocity-radius* $\mathcal{D} - r_f$ consists in determining the nonlinear relation between the propagation velocity $\mathcal{D}_{_{CJ}}$ of spherical CJ detonation and the radius of the lead shock r_f, $\mathcal{D}_{_{CJ}}(\kappa)$ assuming a steady-state approximation. This was performed by He & Clavin (1994) for large heat release and for a highly thermal-sensitive square-wave model of the inner structure and also by Yao & Stewart (1995) for a one-step reaction rate in the limit of large activation energy. The analysis of the curvature-induced quenching is presented below in the limit of small heat release.

4.1. *Steady-state approximation of curved CJ detonations*

Usually, the steady-state approximation is accurate if the characteristic time of evolution of the propagation velocity is larger than the response time of the inner detonation structure, which is possible for stable detonations. Even though the condition is satisfied, the

steady-state approximation is problematic for spherical CJ waves because the unsteady correction is of same order of magnitude as the curvature effect, as shown below, see (4.19) and the discussion in § 7.3. Nevertheless the steady-state approximation is worth considering since it sheds light on the initiation process. The steady-state approximation of the inner structure in the limit (3.1) corresponds to the solution of (3.10) when the unsteady term $\partial\mu/\partial t$ is neglected. Denoting the reduced flow velocity and the propagation velocity of the curved CJ detonation in steady-state $\overline{\mu}_{_{CJ}}(\xi)$ and $\overline{\dot{\alpha}}_{\tau_{CJ}}$ respectively, equation (3.10) yields

$$\left[\overline{\mu}_{_{CJ}}(\xi)-\overline{\dot{\alpha}}_{\tau_{CJ}}\right]\frac{\mathrm{d}\overline{\mu}_{_{CJ}}}{\mathrm{d}\xi}=\frac{1}{2}\mathrm{e}^{b\overline{\dot{\alpha}}_{\tau_{CJ}}}\omega_{o_{CJ}}(\xi\mathrm{e}^{b\overline{\dot{\alpha}}_{\tau_{CJ}}})-[1+\overline{\mu}_{_{CJ}}(\xi)]\kappa, \tag{4.1}$$

$$\xi=0:\quad \overline{\mu}_{_{CJ}}=1+2\overline{\dot{\alpha}}_{\tau_{CJ}}. \tag{4.2}$$

As recalled in § 2.2, the reaction rate of CJ waves is not exactly zero at the sonic point,

$$\xi=\overline{\xi}_{s_{CJ}}:\overline{\mu}_{_{CJ}}=\overline{\dot{\alpha}}_{\tau_{CJ}}\ \Rightarrow\ \mathrm{e}^{b\overline{\dot{\alpha}}_{\tau_{CJ}}}\omega_{o_{CJ}}(\xi\mathrm{e}^{b\overline{\dot{\alpha}}_{\tau_{CJ}}})=2[1+\overline{\mu}_{_{CJ}}(\overline{\xi}_{s_{CJ}})]\kappa\neq 0. \tag{4.3}$$

According to (3.17), the end of the reaction zone corresponds to $\xi=-\mathrm{e}^{-b\,\overline{\dot{\alpha}}_{\tau_{CJ}}}$ so that $\overline{\xi}_{s_{CJ}}>-\mathrm{e}^{-b\,\overline{\dot{\alpha}}_{\tau_{CJ}}}$. When the reduced curvature κ is small, the reaction rate at the sonic point is also small, of order κ according to (4.3). The difference between $\overline{\xi}_{s_{CJ}}$ and $-\mathrm{e}^{-b\,\overline{\dot{\alpha}}_{\tau_{CJ}}}$ introduces negligibly a small correction in the limit $\kappa\ll 1$, and the sonic condition can be considered to hold at the end of the reaction

$$\xi\approx-\mathrm{e}^{-b\,\overline{\dot{\alpha}}_{\tau_{CJ}}}:\quad \overline{\mu}_{_{CJ}}=\overline{\dot{\alpha}}_{\tau_{CJ}}(\kappa)\equiv\frac{[\mathcal{D}_{_{CJ}}(\kappa)-\mathcal{D}_{o_{CJ}}]}{\epsilon a_u}, \tag{4.4}$$

see § 5.1 for a detailed proof. Integration of (4.1) from $\xi=-\mathrm{e}^{-b\,\overline{\dot{\alpha}}_{\tau_{CJ}}}$ to $\xi=0$, using the normalization condition (3.16), then yields

$$(1+\overline{\dot{\alpha}}_{\tau_{CJ}})^2=1-2\kappa\int_{-\mathrm{e}^{-b\,\overline{\dot{\alpha}}_{\tau_{CJ}}}}^{0}(1+\overline{\mu}_{_{CJ}})\mathrm{d}\xi, \tag{4.5}$$

showing that the reduced CJ velocity $\overline{\dot{\alpha}}_{\tau_{CJ}}$ is as small as κ, $\overline{\dot{\alpha}}_{\tau_{CJ}}\propto\kappa$. When the thermal sensitivity is large, $b\gg 1$, the inner structure of the detonation is a strongly nonlinear function of the detonation velocity. As a result, the nonlinear expression of the propagation velocity in term of the curvature $\overline{\dot{\alpha}}_{\tau_{CJ}}(\kappa)$ involves a turning point in *the phase space "velocity-radius"*, as shown now.

4.2. *Curvature-induced quenching predicted by the square-wave model*

The square-wave model (which is well known to generate a singular dynamics) is useful for enlightening the quasi-steady mechanisms that are associated with a high thermal sensitivity. This model helps understanding the physical origin of the C-shaped form of the curve $\overline{\dot{\alpha}}_{\tau_{CJ}}(\kappa)$. The square-wave approximation of the inner structure consists in a uniform profile $\overline{\mu}(\xi,\tau)$, equal to its value at the Neumann state in (4.1), $\overline{\mu}_{_{CJ}}(0,\tau)=1+2\overline{\dot{\alpha}}_{\tau_{CJ}}$. Equation (4.5) then takes the form of the non-linear equation (4.7) for $\overline{\dot{\alpha}}_{\tau_{CJ}}$

$$\int_{-\mathrm{e}^{-b\,\overline{\dot{\alpha}}_{\tau_{CJ}}}}^{0}\left[1+\overline{\mu}_{_{CJ}}(\xi)\right]\mathrm{d}\xi=\left[1+\overline{\mu}_{_{CJ}}(0)\right]\mathrm{e}^{-b\,\overline{\dot{\alpha}}_{\tau_{CJ}}}=2(1+\overline{\dot{\alpha}}_{\tau_{CJ}})\mathrm{e}^{-b\,\overline{\dot{\alpha}}_{\tau_{CJ}}}, \tag{4.6}$$

$$(1+\overline{\dot{\alpha}}_{\tau_{CJ}})^2=1-4\kappa\,(1+\overline{\dot{\alpha}}_{\tau_{CJ}})\mathrm{e}^{-b\,\overline{\dot{\alpha}}_{\tau_{CJ}}}. \tag{4.7}$$

For expanding spherical detonations ($\kappa>0$) the branch of physical solutions $\overline{\dot{\alpha}}_{\tau_{CJ}}(\kappa)$ of (4.7) corresponds to values of $\overline{\dot{\alpha}}_{\tau_{CJ}}$ in the range $\overline{\dot{\alpha}}_{\tau_{CJ}}\in[-1,0]$ for $\kappa\in[0,+\infty]$,

$\lim_{\kappa\to\infty}\overline{\dot\alpha}_{\tau_{CJ}}=-1$, $\lim_{\kappa\to 0}\overline{\dot\alpha}_{\tau_{CJ}}=0$. The detonation velocity of curved CJ detonations is smaller than the velocity of the planar CJ detonation,

$$\kappa>0:\ \overline{\dot\alpha}_{\tau_{CJ}}<0\ \Rightarrow\ \overline{\mathcal{D}}_{_{CJ}}(\kappa)<\mathcal{D}_{o_{CJ}},\qquad \kappa=0:\ \overline{\dot\alpha}_{\tau_{CJ}}=0\ \Rightarrow\ \overline{\mathcal{D}}_{_{CJ}}=\mathcal{D}_{o_{CJ}}. \quad (4.8)$$

For a thermal sensitivity sufficiently small, the function $\kappa(\overline{\dot\alpha}_{\tau_{CJ}})=-(\overline{\dot\alpha}_{\tau_{CJ}}/4)(2+\overline{\dot\alpha}_{\tau_{CJ}})\mathrm{e}^{b\overline{\dot\alpha}_{\tau_{CJ}}}/(1+\overline{\dot\alpha}_{\tau_{CJ}})$ in (4.7) is decreasing monotonously from infinity to zero when $\overline{\dot\alpha}_{\tau_{CJ}}$ increases from -1 to 0, $\mathrm{d}\kappa/\mathrm{d}\overline{\dot\alpha}_{\tau_{CJ}}<0$ so that the detonation velocity decreases monotonously when the curvature increases from 0 to $+\infty$ (radius decreases from ∞ to 0). The situation is different for a thermal sensitivity sufficiently large; the function $\kappa(\overline{\dot\alpha}_{\tau_{CJ}})$ presents two local extrema in the range $\overline{\dot\alpha}_{\tau_{CJ}}\in[-1,0]$ so that the curve $\overline{\dot\alpha}_{\tau_{CJ}}(\kappa)$ has a S-shaped form. This is already the case for $b=3.2$. For a large thermal sensitivity $b\gg 1$ the situation is the same as in He & Clavin (1994), see figure 1 below. The graph "*propagation velocity of the spherical CJ detonation versus the curvature*" $\overline{\mathcal{D}}_{_{CJ}}(\kappa)$ presents a turning point at a critical radius $r=r^*$ corresponding to a small curvature $\kappa^*=O(1/b)$. The difference $(\mathcal{D}_{o_{CJ}}-\overline{\mathcal{D}}_{_{CJ}})/(\epsilon\mathcal{D}_{o_{CJ}})>0$ is small, of order $1/b$, in the upper branch of solutions (the one going to $\mathcal{D}_{o_{CJ}}$ at large radius, see figure 1) while it is of order unity in the third branch of solution (not represented in figure 1) which is non physical because it corresponds to a too small Neumann temperature. In other words there is no physical solution for $r<r^*$. Focusing the attention to radii of the same order of magnitude as the critical radius,

$$1/b\ll 1:\qquad \kappa=O(1/b),\qquad |\overline{\dot\alpha}_{\tau_{CJ}}|=O(1/b)\quad\Rightarrow\quad \mathrm{e}^{-b\,\overline{\dot\alpha}_{\tau_{CJ}}}=O(1), \quad (4.9)$$

the terms smaller than $1/b$ can be neglected in (4.7),

$$1/b\ll 1:\qquad -\overline{\dot\alpha}_{\tau_{CJ}}=2\kappa\mathrm{e}^{-b\,\overline{\dot\alpha}_{\tau_{CJ}}}>0. \quad (4.10)$$

In the limit $b\gg 1$ the quantities of order unity for the propagation velocity and the radius in the upper branch of detonations are respectively,

$$\overline{y}_{_{CJ}}\equiv b\,\overline{\dot\alpha}_{\tau_{CJ}}=\frac{b}{\epsilon}\left(\frac{\overline{\mathcal{D}}_{_{CJ}}-\mathcal{D}_{o_{CJ}}}{a_u}\right),\qquad \frac{1}{x}\equiv 2\,b\,\kappa=2\frac{b}{\epsilon}\left(\frac{l_{o_{CJ}}}{r_f}\right)>0, \quad (4.11)$$

where $l_{o_{CJ}}=a_u t_r$ denotes the thickness of the planar CJ detonation, t_r being the reaction time at the Neumann state (reference time) and, according to (3.15), $b/\epsilon=2(\gamma-1)\mathcal{E}/k_BT_u$. The propagation velocity of quasi-steady spherical CJ waves $\overline{y}_{_{CJ}}(x)$ in term of its radius x is, according to (4.10), solution to

$$1/b\ll 1:\qquad -\overline{y}_{_{CJ}}\mathrm{e}^{\overline{y}_{CJ}}=1/x\quad\Leftrightarrow\quad \overline{y}_{_{CJ}}+\frac{1}{x}\mathrm{e}^{-\overline{y}_{CJ}}=0, \quad (4.12)$$

$$\frac{\mathrm{d}\overline{y}_{_{CJ}}}{\mathrm{d}x}=\frac{\mathrm{e}^{-\overline{y}_{CJ}}}{x^2}\frac{1}{1+\overline{y}_{_{CJ}}}. \quad (4.13)$$

Because the terms of order ϵ have been neglected in (4.1), equations (4.10) and (4.12) are valid in the limit of small heat release ($\epsilon\ll 1$) for intermediate values of $1/b$,

$$\epsilon\ll 1/b\ll 1. \quad (4.14)$$

The solution (4.12), $\overline{y}_{_{CJ}}(x)$, is plotted in blue in figure 1 where the arrows indicate the direction of propagation ($\overline{y}_{_{CJ}}>-1:\mathrm{d}\overline{y}_{_{CJ}}/\mathrm{d}x>0$; $\overline{y}_{_{CJ}}<-1:\mathrm{d}\overline{y}_{_{CJ}}/\mathrm{d}x<0$). The critical value r_f^* is larger than the detonation thickness of the planar CJ wave, $r_f^*\gg l_{o_{CJ}}$,

$$\overline{y}^*_{_{CJ}}=-1,\quad x^*=\mathrm{e},\quad r_f^*/l_{o_{CJ}}=2\,\mathrm{e}\,b/\epsilon\gg 1,\quad (\mathcal{D}_{o_{CJ}}-\mathcal{D}^*)/a_u=\epsilon/b\ll 1, \quad (4.15)$$

corresponding effectively to the orders of magnitude anticipated in (4.9),

$$b \gg 1 : \qquad \kappa^* = (2\,\mathrm{e})^{-1}/b, \quad \overline{\dot{\alpha}}^*_{\tau_{CJ}} = -1/b. \tag{4.16}$$

Close to the critical radius, the CJ velocity $\overline{y}_{_{CJ}}$ varies as the square root of the radius x

$$0 < (x-\mathrm{e})/\mathrm{e} \ll 1 : \quad \overline{y}_{_{CJ}} \approx -1 + \sqrt{2}\sqrt{(x-\mathrm{e})/\mathrm{e}}. \tag{4.17}$$

According to (4.12), the two branches of solutions $0 > \overline{y}_{_{CJ+}}(x) > \overline{y}_{_{CJ-}}(x)$ for $x > x^*$ ($r_f > r_f^*$) merge at the critical radius $r_f = r_f^*$; $x = x^*$: $\overline{y}_{_{CJ+}} = \overline{y}_{_{CJ-}} = y^* = -1$. Both branches correspond to detonation velocities smaller than the velocity of the planar CJ wave, $\overline{y}_{_{CJ\pm}} < 0$, $\mathcal{D} < \mathcal{D}_{o_{CJ}}$. According to (4.13), the upper (lower) branch of solutions $\overline{y}_{_{CJ+}}(x) > -1$, ($\overline{y}_{_{CJ-}}(x) < -1$,) is an increasing (decreasing) function of x, $\lim_{x\to\infty} \overline{y}_{_{CJ+}} = 0$ ($\lim_{x\to\infty} \overline{y}_{_{CJ-}} = -\infty$), see figure1. The solution $\overline{\mathcal{D}}_{_{CJ}}(r_f)$ corresponding to $\overline{y}_{_{CJ+}}$ is an increasing function of the radius from $\mathcal{D}^*$ at $r_f = r_f^*$ up to the velocity of the planar CJ detonation for infinitely large radius, $\lim_{r_f/l_{o_{CJ}}\to\infty} \overline{\mathcal{D}}_{_{CJ}} = \mathcal{D}_{o_{CJ}}$. This branch of solutions is shown in § 7 to play the role of an attractor for the quasi-steady trajectories when the initiation process is successful. The physical mechanism of the curvature-induced quenching is clearly identified from (4.7) to be the thermal sensitivity, responsible for the nonlinear variation of the detonation thickness with the propagation velocity through the Neumann temperature and the Rankine-Hugoniot conditions.

In the opposite limit of a large propagation Mach number $M \gg 1$ used in He & Clavin (1994), the expression of the Rankine-Hugoniot condition

$$(\gamma-1)M^2 \gg 1 : \qquad \frac{\delta T_N}{T_N} \approx 2\frac{\delta M}{M} \tag{4.18}$$

differs quantitatively from (3.14). However the same phenomenology is described in the limit of small heat release (3.1) which is helpful for providing us with a qualitative description of the unsteady effects in the initiation process. The dynamics of a stable detonation on the upper branch of the CJ peninsula is effectively slow, except very close to the turning point. Unfortunately, according to (4.11), (4.13) and $\mathrm{d}r_f/\mathrm{d}t = \overline{\mathcal{D}}_{_{CJ}}$, the unsteady term is of same order of magnitude as the curvature term, $1/b$,

$$\frac{\mathrm{d}\overline{y}_{_{CJ}}}{\mathrm{d}\tau} = \frac{1}{2\,b}\frac{\mathrm{e}^{-\overline{y}_{CJ}}}{x^2}\frac{1}{1+\overline{y}_{_{CJ}}}. \tag{4.19}$$

4.3. *Critical conditions for a smooth distribution of the reaction rate in the limit (4.14).* To leading order in the limit $b \gg 1$, the results (4.12)-(4.13) obtained with the square-wave model are still valid for a smooth distribution of the reaction rate provided the factor 2 in the expression (4.11) of $1/x$ is replaced by $\lambda \in [1,\,2]$ where

$$b \gg 1 : \; 1/x = \lambda\, b\, \kappa, \; \lambda \equiv 1 + \int_{-1}^{0} \mu_{o_{CJ}}(\xi)\mathrm{d}\xi, \; x^* = \mathrm{e} \;\Rightarrow\; r_f^*/l_{o_{CJ}} = \lambda\,\mathrm{e}\,b/\epsilon, \tag{4.20}$$

$\mu_{o_{CJ}}(\xi)$ being the planar CJ solution obtained from (4.1) for $\kappa = 0$ and $\overline{\dot{\alpha}}_\tau = 0$

$$\mu_{o_{CJ}}(\xi) = \sqrt{\int_{-1}^{\xi} \omega_{o_{CJ}}(\xi')\mathrm{d}\xi'}, \; \int_{-1}^{0} \omega_{o_{CJ}}(\xi')\mathrm{d}\xi' = 1, \; 0 < \mu_{o_{CJ}}(\xi) < 1, \; 1 < \lambda < 2. \tag{4.21}$$

The proof is as follows. Consider a spherical CJ wave in the limit $1/b \ll 1$, $\overline{y}_{_{CJ}} \equiv b\overline{\dot{\alpha}}_{\tau_{CJ}} = O(1)$, $\kappa = O(1/b)$, $\overline{\mu}_{b_{CJ}} = \overline{\dot{\alpha}}_{\tau_{CJ}} = O(1/b)$. Neglecting terms smaller than $1/b$ in (4.1), the function $\overline{\mu}_{_{CJ}}(\xi)$ in the bracket on the right-hand side can be replaced by the steady

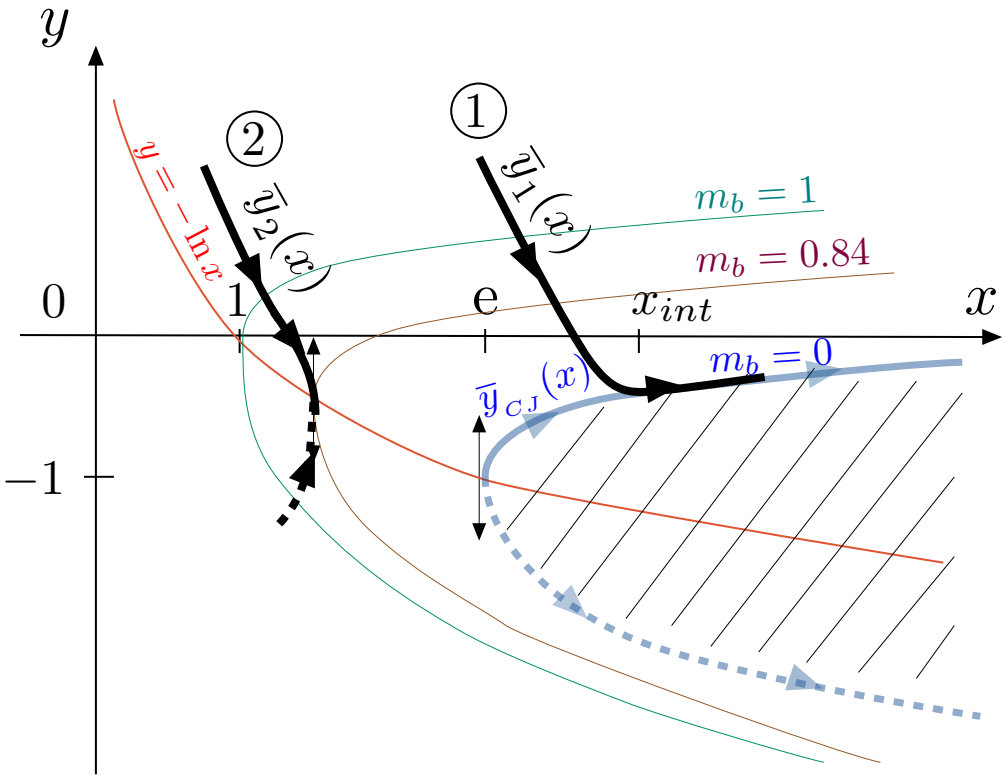

FIGURE 1. Phase space *"detonation velocity vs radius"* (y-x) in the non-dimensional form $y \equiv b\,\dot{\alpha}_\tau = (b/\epsilon)(\mathcal{D} - \mathcal{D}_{o_{CJ}})/a_u$, $x \equiv 1/(2b\kappa)$. The equation of the CJ peninsula $\overline{y}_{_{CJ}}(x)$ is (4.12) and the quasi-steady trajectories $\overline{y}(x)$ are given in (7.1). The trajectories $\overline{y}_1(x)$ and $\overline{y}_2(x)$ represent respectively success of detonation initiation and failure.

solution for $\kappa = 0$ but with $b\overline{\dot{\alpha}}_{\tau_{CJ}} \neq 0$. This is the zeroth-order solution $\overline{\mu}_{o_{CJ}}$ of the curved CJ wave $\overline{\mu}_{_{CJ}}(\xi)$ which can be expressed in terms of the velocity distribution of the planar CJ solution $\mu_{o_{CJ}}(\xi)$ in the form $\overline{\mu}_{o_{CJ}}(\xi) = \mu_{o_{CJ}}(\xi \mathrm{e}^{\overline{y}_{CJ}})$, as it is shown by (4.1), (4.2) and (4.4) in which the terms of order $1/b$ are neglected

$$\overline{\mu}_{o_{CJ}} \frac{\mathrm{d}\overline{\mu}_{o_{CJ}}}{\mathrm{d}\xi} = \frac{1}{2}\mathrm{e}^{\overline{y}_{CJ}} \omega_{o_{CJ}}(\xi\, \mathrm{e}^{\overline{y}_{CJ}}), \quad \xi = 0 : \overline{\mu}_{o_{CJ}} = 1, \quad \xi = -\mathrm{e}^{-\overline{y}_{CJ}} : \overline{\mu}_{o_{CJ}} = 0, \tag{4.22}$$

$$\overline{\mu}^2_{o_{CJ}}(\xi) = \int_{-\mathrm{e}^{-\overline{y}_{CJ}}}^{\xi} \mathrm{e}^{\overline{y}_{CJ}} \omega_{o_{CJ}}(\xi'\, \mathrm{e}^{\overline{y}_{CJ}})\mathrm{d}\xi', \qquad \overline{\mu}_{o_{CJ}}(\xi) = \mu_{o_{CJ}}(\xi \mathrm{e}^{\overline{y}_{CJ}}), \tag{4.23}$$

where $\mu_{o_{CJ}}(\xi)$ is the planar solution (4.21). Equation (4.23) means that the leading order of the distribution $\overline{\mu}_{_{CJ}}(\xi)$ in the limit $b \gg 1$ is obtained from the planar CJ solution by rescaling the length with the thickness of the spherical CJ detonation. Integration of $\overline{\mu}_{_{CJ}}(\xi)$ yields

$$\int_{-\mathrm{e}^{-\overline{y}_{CJ}}}^{0} \overline{\mu}_{_{CJ}} \mathrm{d}\xi \approx \mathrm{e}^{-\overline{y}_{CJ}} \int_{-1}^{0} \mu_{o_{CJ}}(z)\mathrm{d}z = \mathrm{e}^{-\overline{y}_{CJ}}(\lambda - 1). \tag{4.24}$$

valid at the leading order in the limit $b \gg 1$. Introducing (4.24) into (4.5) leads to (4.12) with the definition (4.20) of x, $x = 1/(b\lambda\kappa)$. The function $\mu_{o_{CJ}}(\xi) > 0$ varying monotonously from 0 at the exit of the reaction zone of the planar CJ detonation ($\xi_{ob_{CJ}} = -1$) to 1 at the Neumann state ($\xi = 0$), $0 < \int_{-1}^{0} \mu_{o_{CJ}}(\xi')\mathrm{d}\xi' < 1$, the parameter λ is in

between 1 and 2, $1 < \lambda < 2$. By comparison with (4.15), the critical radius for a smooth distribution in (4.20) is smaller than for the square-wave model by a factor $\lambda/2 < 1$.

5. Quasi-steady inner structure of spherical detonations

The analysis of the quasi-steady inner structure of spherical detonations helps to clarify the distance from the lead shock at which the velocity of the burnt gas flow is imposed in the limit (4.14). Let's begin with the CJ wave.

5.1. *Spherical CJ detonation in steady state. Sonic point*

Using the notation (4.20), equation (4.1) takes the form

$$2\left[\overline{\mu}_{_{CJ}}(\xi,\overline{y}_{_{CJ}})-\overline{y}_{_{CJ}}/b\right]\frac{\mathrm{d}\overline{\mu}_{_{CJ}}}{\mathrm{d}\xi}=e^{\overline{y}_{CJ}}\omega_{o_{CJ}}(\xi\mathrm{e}^{\overline{y}_{CJ}})-\frac{1}{b}\left[1+\mu_{o_{CJ}}(\xi\mathrm{e}^{\overline{y}_{CJ}})\right]\frac{2}{\lambda x} \quad (5.1)$$

where the $\overline{y}_{_{CJ}}$- dependence of the velocity distribution has been written explicitly in $\overline{\mu}_{_{CJ}}(\xi,\overline{y}_{_{CJ}})$. Integration of (5.1) from the Neumann state (4.2) yields

$$\left[\overline{\mu}_{_{CJ}}(\xi,\overline{y}_{_{CJ}})-\frac{\overline{y}_{CJ}}{b}\right]^2= \quad (5.2)$$
$$\left(1+\frac{\overline{y}_{CJ}}{b}\right)^2-\int_{\xi\mathrm{e}^{\overline{y}_{CJ}}}^{0}\omega_{o_{CJ}}(\xi')\mathrm{d}\xi'+\left[-\xi\mathrm{e}^{\overline{y}_{CJ}}+\int_{\xi\mathrm{e}^{\overline{y}_{CJ}}}^{0}\mu_{o_{CJ}}(\xi')\mathrm{d}\xi'\right]\frac{2}{b}\frac{\mathrm{e}^{-\overline{y}_{CJ}}}{\lambda\, x},$$

which takes the following form when using (3.16), (4.20) and (4.21), $\int_{-1}^{0}\omega_{o_{CJ}}(\xi')\mathrm{d}\xi'=1$, $\lambda\equiv 1+\int_{-1}^{0}\mu_{o_{CJ}}(\xi')\mathrm{d}\xi'$ and $\mu_{o_{CJ}}(\xi)=\int_{-1}^{\xi}\omega_{o_{CJ}}(\xi')\mathrm{d}\xi'$,

$$\left[\overline{\mu}_{_{CJ}}(\xi,\overline{y}_{_{CJ}})-\frac{\overline{y}_{CJ}}{b}\right]^2-\frac{\overline{y}_{CJ}^2}{b^2}=\mu_{o_{CJ}}^2(\xi\mathrm{e}^{\overline{y}_{CJ}})$$
$$+\frac{2}{b}\left\{\left[\overline{y}_{_{CJ}}+\frac{\mathrm{e}^{-\overline{y}_{CJ}}}{x}\right]-\frac{\mathrm{e}^{-\overline{y}_{CJ}}}{\lambda\, x}\left[(\mathrm{e}^{\overline{y}_{CJ}}\xi+1)+\int_{-1}^{\xi\mathrm{e}^{\overline{y}_{CJ}}}\mu_{o_{CJ}}(\xi')\mathrm{d}\xi'\right]\right\}. \quad (5.3)$$

In the limit (4.14), equation (5.3) shows that the difference $\overline{\mu}_{_{CJ}}(\xi,\overline{y}_{_{CJ}})-\mu_{o_{CJ}}(\xi\mathrm{e}^{\overline{y}_{CJ}})$ is smaller than unity. Neglecting terms of order $1/b^2$, equations (4.12) with (4.20) are recovered from (5.3) if the sonic condition $\left(\overline{\mu}_{_{CJ}}-\overline{y}_{_{CJ}}/b\right)=0$ is assumed to hold at the end of the heat release, $\overline{\xi}_{_{CJ}}\mathrm{e}^{\overline{y}_{CJ}}=-1$ where $\xi=-1$ is the reduced position of the exit of the reaction zone in the planar CJ wave, $\omega_{o_{CJ}}(-1)=0$; $\xi\leqslant-\mathrm{e}^{-\overline{y}_{CJ}}:\omega_{o_{CJ}}(\xi\mathrm{e}^{\overline{y}_{CJ}})=0$ and $\mu_{o_{CJ}}(\xi\mathrm{e}^{\overline{y}_{CJ}})=0$, see (4.21). In fact, the sonic condition holds inside the detonation thickness just before the end of the exothermal reaction. Denoting $\overline{\xi}_{s_{CJ}}$ its position,

$$\xi=\overline{\xi}_{s_{CJ}}:\quad \left(\overline{\mu}_{_{CJ}}-\overline{y}_{_{CJ}}/b\right)=0, \quad (5.4)$$

a first relation linking $\overline{y}_{_{CJ}}$ and $\overline{\xi}_{s_{CJ}}$ is given by (5.2)-(5.3)

$$\mu_{o_{CJ}}^2(\overline{\xi}_{s_{CJ}}\mathrm{e}^{\overline{y}_{CJ}})+\frac{2}{b}\left[\overline{y}_{_{CJ}}+\frac{\mathrm{e}^{-\overline{y}_{CJ}}}{\lambda\, x}\int_{\overline{\xi}_{s_{CJ}}\mathrm{e}^{\overline{y}_{CJ}}}^{0}[1+\mu_{o_{CJ}}(\xi')]\mathrm{d}\xi'\right]+\frac{\overline{y}_{CJ}^2}{b^2}=0. \quad (5.5)$$

The second relation necessary to determine $\overline{y}_{_{CJ}}$ and $\overline{\xi}_{s_{CJ}}$ is obtained from (5.1) if the derivative $\mathrm{d}\overline{\mu}_{_{CJ}}(\xi,\overline{y}_{_{CJ}})/\mathrm{d}\xi|_{\xi=-1}$ is bounded

$$\mathrm{e}^{\overline{y}_{CJ}}\omega_{o_{CJ}}(\overline{\xi}_{s_{CJ}}\mathrm{e}^{\overline{y}_{CJ}})=\frac{1}{b}\left[1+\mu_{o_{CJ}}(\overline{\xi}_{s_{CJ}}\mathrm{e}^{\overline{y}_{CJ}})\right]\frac{2}{\lambda x}\ \Rightarrow\ \omega_{o_{CJ}}(\overline{\xi}_{s_{CJ}}\mathrm{e}^{\overline{y}_{CJ}})=O(1/b) \quad (5.6)$$

showing that the reaction is not completed at the sonic point $\omega_{o_{CJ}}(\overline{\xi}_{s_{CJ}}\mathrm{e}^{\overline{y}_{CJ}}) > 0$, $\overline{\xi}_{s_{CJ}} > -\mathrm{e}^{-\overline{y}_{CJ}}$, the reaction rate being however small, of order $1/b$. Subtracting (5.5) from (5.3) yields

$$\xi \geqslant \overline{\xi}_{s_{CJ}} > -\mathrm{e}^{-\overline{y}_{CJ}} : \quad \left[\overline{\mu}_{_{CJ}}(\xi,\overline{y}_{_{CJ}}) - \frac{\overline{y}_{CJ}}{b}\right]^2 = \tag{5.7}$$
$$\int_{\overline{\xi}_{s_{CJ}}\mathrm{e}^{\overline{y}_{CJ}}}^{\xi\mathrm{e}^{\overline{y}_{CJ}}} \omega_{o_{CJ}}(\xi')\mathrm{d}\xi' - \frac{1}{b}\left[(\xi-\overline{\xi}_{s_{CJ}})\mathrm{e}^{\overline{y}_{CJ}} + \int_{\overline{\xi}_{s_{CJ}}\mathrm{e}^{\overline{y}_{CJ}}}^{\xi\mathrm{e}^{\overline{y}_{CJ}}} \mu_{o_{CJ}}(\xi')\mathrm{d}\xi'\right]\frac{2\mathrm{e}^{-\overline{y}_{CJ}}}{\lambda x},$$

so that the right-hand side should be positive

$$\int_{\overline{\xi}_{s_{CJ}}\mathrm{e}^{\overline{y}_{CJ}}}^{\xi\mathrm{e}^{\overline{y}_{CJ}}} \omega_{o_{CJ}}(\xi')\mathrm{d}\xi' \geqslant \frac{1}{b}\left[(\xi-\overline{\xi}_{s_{CJ}})\mathrm{e}^{\overline{y}_{CJ}} + \int_{\overline{\xi}_{s_{CJ}}\mathrm{e}^{\overline{y}_{CJ}}}^{\xi\mathrm{e}^{\overline{y}_{CJ}}} \mu_{o_{CJ}}(\xi')\mathrm{d}\xi'\right]\frac{2\mathrm{e}^{-\overline{y}_{CJ}}}{\lambda x}. \tag{5.8}$$

The inequality is automatically satisfied in the range $0 < (\xi-\overline{\xi}_{s_{CJ}}) = O(1)$ for $b \gg 1$ and $|\overline{y}_{_{CJ}}| = O(1)$ because the functions $\omega_{o_{CJ}}(\xi)$ and $\mu_{o_{CJ}}(\xi)$ are of order unity and positive for $\xi > -1$. Both sides of (5.8) are increasing functions of ξ from 0 at $\xi = \overline{\xi}_{s_{CJ}}$. The case $0 < (\xi-\overline{\xi}_{s_{CJ}}) \ll 1$ is easily investigated within the model (3.17) which will be used from now on. According to (3.17), the distribution of the reaction rate in the planar CJ wave is linear close to $\xi = -1$, $0 < \xi+1 \ll 1$: $\omega_{o_{CJ}} \approx h_\omega(\xi+1)$, $h_\omega > 0$ and, according to (4.21), the slope of the velocity profile in the plane CJ wave is also positive and of order unity at the end of the reaction zone

$$\xi \leqslant -1 : \mu_{o_{CJ}} = 0 \quad \text{but} \quad \mathrm{d}\mu_{o_{CJ}}/\mathrm{d}\xi|_{\xi+1=0^+} = h_\mu > 0, \tag{5.9}$$
$$0 < (\xi+1) \ll 1 : \mu_{o_{CJ}}(\xi) \approx h_\mu(\xi+1), \quad h_\mu > 0,\ h_\mu \equiv \sqrt{h_\omega/2} = O(1). \tag{5.10}$$

Then, according to (5.6), $0 < \left(\overline{\xi}_{s_{CJ}} + \mathrm{e}^{-\overline{y}_{CJ}}\right) = \mathrm{O}(1/b)$, the sonic condition can be safely applied at the exit of the reaction zone $\xi = -\mathrm{e}^{-\overline{y}_{CJ}}$ and the heThe first term of a Taylor expansion around $\xi = \overline{\xi}_{s_{CJ}}$ is the same on both sides of (5.8), and the second-order term satisfies the inequality (5.8) in the limit $b \gg 1$ when the second derivative $\mathrm{d}^2\omega_{o_{CJ}}/\mathrm{d}\xi^2|_{\xi+1=0^+}$ is of order unity (smaller than b). A Taylor expansion of (5.3) around the sonic point using (5.5)-(5.6) then yields

$$0 \leqslant (\xi-\overline{\xi}_{s_{CJ}}) \ll 1 : \quad \overline{\mu}_{_{CJ}}(\xi,\overline{y}_{_{CJ}}) - \frac{\overline{y}_{CJ}}{b} \approx h_\mu\,\mathrm{e}^{\overline{y}_{CJ}}(\xi-\overline{\xi}_{s_{CJ}})\left[1+O\left(1/b\right)\right] \tag{5.11}$$
$$\xi < \overline{\xi}_{s_{CJ}} : \quad \overline{\mu}_{_{CJ}}(\xi,\overline{y}_{_{CJ}}) - \overline{y}_{_{CJ}}/b = 0, \tag{5.12}$$

and, more generally, one has

$$x \geqslant \mathrm{e} : \quad \overline{\mu}_{_{CJ}}(\xi,\overline{y}_{_{CJ}}(x)) = \mu_{o_{CJ}}(\xi\mathrm{e}^{\overline{y}_{CJ}(x)})\left[1+O\left(1/b\right)\right], \tag{5.13}$$

valid everywhere inside the inner structure of the detonations on the upper branch of the CJ peninsula, even near the turning point $x = \mathrm{e}$ where, to leading order, $\overline{y}_{_{CJ}} \approx -1$. The correction to (4.12)-(4.13) then takes the form

$$\overline{y}_{_{CJ}} + \frac{1}{x}\mathrm{e}^{-\overline{y}_{CJ}} = O(\overline{y}_{_{CJ}}^2/b), \quad \frac{\mathrm{d}\overline{y}_{CJ}}{\mathrm{d}x} = \frac{\mathrm{e}^{-\overline{y}_{CJ}}}{x^2}\frac{1}{1+\overline{y}_{_{CJ}}\left[1+O(1/b)\right]}. \tag{5.14}$$

5.2. *Matching the quasi-steady inner structure with the rarefaction flow*

The steady state approximation of an overdriven detonation is governed by (3.10) when the unsteady term is neglected $\partial\mu/\partial\tau \approx 0$. For a small curvature (4.9), to leading order

in the limit (4.14), the term μ on the right-hand can be replaced by $\mu_{o_{CJ}}(\xi \mathrm{e}^{b\overline{\dot\alpha}_\tau})$ as in (5.1). Denoting the steady-state approximation by an overbar, the equation for $\overline{\mu}(\xi)$

$$[\overline{\mu}(\xi)-\overline{\dot\alpha}_\tau]\frac{\mathrm{d}\overline{\mu}}{\mathrm{d}\xi}=\frac{1}{2}\mathrm{e}^{b\overline{\dot\alpha}_\tau}\omega_{o_{CJ}}(\xi\,\mathrm{e}^{b\overline{\dot\alpha}_\tau})-[1+\mu_{o_{CJ}}(\xi\mathrm{e}^{b\overline{\dot\alpha}_\tau})]\kappa,\qquad \xi=0:\overline{\mu}=1+2\overline{\dot\alpha}_\tau, \tag{5.15}$$

completed by the boundary condition at the exit of the inner structure, $\xi=\xi_b$, where the flow is subsonic

$$\xi=\xi_b:\ \overline{\mu}\approx\mu_b,\qquad 0<(\mu_b-\overline{\dot\alpha}_\tau)\ll 1, \tag{5.16}$$

the last inequality holding for slightly overdriven regimes. When considering the direct initiation, the boundary condition taken at the end of the reaction $\xi=-\mathrm{e}^{-b\overline{\dot\alpha}_\tau}$ would lead to a negative slope at the end of the inner structure, $\mathrm{d}\overline{\mu}/\mathrm{d}\xi\approx-\kappa<0$. This is not quite satisfactory since the flow in the rarefaction wave is an increasing function of the radius. There is a weakly reactive and unsteady transition layer between the quasi-steady inner structure and the inert rarefaction wave (unsteady flow of burnt gas). Anticipating that the term on the left-hand side of (5.15) is smaller than the curvature $\kappa=O(1/b)$ inside the transition layer,

$$[\mu-\dot\alpha_\tau]\mathrm{d}\mu/\mathrm{d}\xi=o(1/b), \tag{5.17}$$

the balance of the two terms on the right-hand side of (5.15) determines ξ_b as in (4.3)

$$\mathrm{e}^{b\dot\alpha_\tau}\omega_{o_{CJ}}(\xi_b\,\mathrm{e}^{b\dot\alpha_\tau})=2/(b\,\lambda\,x). \tag{5.18}$$

In that respect, the situation is similar to the CJ case. The ordering (5.17) is easily verified for the rarefaction flow where the order of magnitude of the slope is typically $\partial u/\partial r|_{r=r_f}\approx u_{r=r_f}/r_f$. By using (3.2) and (4.9), $l/r_f=O(\epsilon/b)$, the matching condition $\mathrm{d}\overline{u}/\mathrm{d}\xi=l\,\partial u/\partial r|_{r=r_f}\approx l\,u_b/r_f$ leads to the order of magnitude of the reduced slope in the transition layer $\mathrm{d}\mu/\mathrm{d}\xi=O(\epsilon/b)$, the link between u and μ being in (3.7). At the scale of the detonation thickness, the flow is quasi-uniform inside the transition layer, $\xi=O(1)$, $\xi\leqslant\xi_b$. Then, according to (3.17) and (5.18) in the limit (4.14), the place where the external condition (5.16) $\overline{\mu}=\mu_b$ is applied inside the inner structure is fairly close to the end of the reaction

$$b\gg 1:\qquad \xi_b=-\mathrm{e}^{-b\dot\alpha_\tau}[1+O(1/b)]. \tag{5.19}$$

The calculation of the propagation velocity for a given flow velocity of burnt gas $\overline{\mu}_b$ proceeds as in § 5.1. Focusing the attention onto propagation velocities and radii close to their critical value $\mathcal{D}^*$ and r_f^* introduced in §§ 4.2-4.3, it is convenient to introduce the dimensionless variables y and x of order unity, similar to (4.11),

$$y\equiv b\dot\alpha_\tau=\frac{b}{\epsilon}\left(\frac{\mathcal{D}-\mathcal{D}_{o_{CJ}}}{a_u}\right)=O(1),\qquad\qquad \frac{1}{x}\equiv\lambda b\kappa=O(1), \tag{5.20}$$

the parameters $\epsilon\ll 1$, $b\gg 1$ and $\lambda\in[1,2]$ being defined in (3.1), (3.15) and (4.20) respectively. Integration of (5.15) from the Neumann state at $\xi=0$ leads to an expression similar to (5.3)

$$\begin{aligned}\left[\overline{\mu}(\xi)-\frac{\overline{y}}{b}\right]^2&=\frac{\overline{y}^2}{b^2}+\mu_{o_{CJ}}^2(\xi\mathrm{e}^{\overline{y}})\\&\quad+\frac{2}{b}\left\{\left[\overline{y}+\frac{\mathrm{e}^{-\overline{y}}}{x}\right]-\frac{\mathrm{e}^{-\overline{y}}}{\lambda\,x}\left[(\mathrm{e}^{\overline{y}}\xi+1)+\int_{-1}^{\xi\mathrm{e}^{\overline{y}}}\mu_{o_{CJ}}(\xi')\mathrm{d}\xi'\right]\right\}.\end{aligned} \tag{5.21}$$

The boundary condition in the burnt gas (5.16) using (5.19) and $\mu_{o_{CJ}}(\xi_b\mathrm{e}^{\overline{y}})=O(1/b)$,

leads to the relation between the propagation velocity $\overline{y}$ and the burnt gas velocity μ_b

$$b\mu_b^2/2 - \overline{y}\mu_b = \overline{y} + \mathrm{e}^{-\overline{y}}/x + O(1/b)$$
$$\mu_b = O(1/\sqrt{b}): \qquad b\mu_b^2/2 = \overline{y} + \mathrm{e}^{-\overline{y}}/x + O(1/\sqrt{b}), \tag{5.22}$$

where the last term on the right-hand side of (5.21) gives a negligible contribution of order $1/b$. The ordering $\mu_b(\tau) = O(1/\sqrt{b})$ corresponds to a propagation velocity and a radius of same order of magnitude as at the turning point, $\overline{y} = O(1)$ and $x = O(1)$. For slightly overdriven detonations in planar geometry $\kappa = 0$, equations (5.21)-(5.22) reduce to (D 5)-(D 8) in appendix and the classical square root relation is recovered between the flow velocity in the burned gas (overdrive factor) and the departure of the detonation velocity from its CJ value , $\kappa = 0,\ 0 < \overline{\dot{\alpha}}_\tau \ll 1 \ \Rightarrow\ \mu_b \approx \sqrt{2\overline{\dot{\alpha}}_\tau}$. According to (5.21), the ξ-variation of $\overline{\mu}(\xi)$ is through the grouping $\xi \mathrm{e}^{\overline{y}}$ like in $\mu_{o_{CJ}}(\xi \mathrm{e}^{\overline{y}})$. The difference $\overline{\mu}(\xi) - \mu_{o_{CJ}}(\xi \mathrm{e}^{b\overline{\dot{\alpha}}_\tau})$ is of order $1/\sqrt{b}$ near the end of the reaction where $\mu_{o_{CJ}}(\xi \mathrm{e}^{\overline{y}})$ is of order $1/\sqrt{b}$ while the difference is smaller, of order $1/b$, elsewhere inside the inner structure of the detonation. Moreover, at the scale of the detonation thickness, the slope of the external flow at the exit of the steady inner structure is negligible at the leading order in the limit (4.14). The quasi-steady trajectories (5.22) are analyzed in § 7.1.

6. Hyperbolic quation for the decay of spherical detonations

Using the discontinuous model and starting with the Sedov (1946)-Taylor (1950*b*) self-similar solution of a strong blast wave in cylindrical and/or spherical geometry, the numerical simulations of direct initiation of detonations propagating with a Mach number M substantially larger than unity $M \gg 1$ show that the CJ velocity is reached at finite time and finite radius with an abrupt transition analyzed by Liñan *et al.* (2012). In the limit of small heat release (3.1), the propagation velocity of a weakly overdriven detonation is close to the sound speed $0 < (M-1) \ll 1$ and the flow velocity is small in the laboratory frame. Then, the rarefaction wave behind the detonation front (discontinuous model) computed in Appendix A shows that the CJ regime is reached with a power law similar to the planar geometry discussed in Clavin & Denet (2018). In order to describe the unsteady effects in a real initiation process, the limit of small heat release will be considered here only for the response of the inner detonation-structure to the external flow, not for the rarefaction wave. The decrease rate of the flow of burnt gas near the end of the reaction zone is then the same as in Liñan *et al.* (2012), leading to a local closure assumption near the CJ regime discussed now.

6.1. *Flow of burnt gas near the detonation. Closure relation*

In the analysis of Liñan *et al.* (2012) (discontinuous model and $M \gg 1$), near the CJ regime, the quasi-transonic flow (relative to the detonation front) is described by a Burgers-like equation. The same equation is derived in the limit (3.1), $0 < M - 1 \ll 1$ from (3.10) for the flow of burnt gas close to the end of the reaction zone ($\dot{w} = 0$)

$$\xi \leqslant \xi_b,\ |\xi| = O(1): \quad \partial\mu/\partial\tau + (\mu - \dot{\alpha}_\tau)\partial\mu/\partial\xi = -\kappa(\tau)\,[1+\mu]\,, \tag{6.1}$$

leading to the Burgers-like equation obtained by Liñan *et al.* (2012)

$$\dot{\alpha}_\tau < \mu < 1: \qquad \partial\mu/\partial\tau + \mu\partial\mu/\partial\xi = -\kappa. \tag{6.2}$$

The curvature on the right-hand is quasi-constant when the radius gets close to the CJ condition. Back to the dimensional form by using (3.2), (3.4), (3.7) and (3.9), equation

(6.1) takes the more explicit form

$$\frac{\partial u}{\partial t}+[a-(\mathcal{D}-u)]\frac{\partial u}{\partial r}=-\frac{a}{r}u, \tag{6.3}$$

describing the propagation of the upstream running mode in the rarefaction wave near the detonation where the flow is quasi-transonic, $a \gg a-(\mathcal{D}-u) \geqslant 0$. In the laboratory frame, the flow behind an expending detonation ($\mathrm{d}r_f/\mathrm{d}t > 0$, $\xi \leqslant \xi_b < 0$) decreases when the distance from the detonation front increases; the flow is an increasing function of the radius, $\partial\mu/\partial\xi > 0$. The burnt-gas flow of the rarefaction wave varies in space on a length scale $l_{ext} \equiv [(1/u)\partial u/\partial r]^{-1}$ typically of order of magnitude of the shock radius r_f. When the radius is larger than the detonation thickness, $r_f \gg l$, the length scale of the external flow is larger than the detonation thickness $l_{ext} \gg l$, see however the comment at the end of this section. According to the quasi-transonic flow of burnt gas when approaching the CJ regime, $0 \leqslant a-(\mathcal{D}-u) \ll a$, the second term in the left-hand side of (6.1) and (6.3) (the one involving the derivative with respect to space) is smaller than the right-hand side and can be neglected. Therefore, near the end of the reaction zone, the time dependent flow $u_b(t)$ or $\mu_b(\tau)$ is simply a function of the flow curvature

$$\frac{\mathrm{d}\mu_b}{\mathrm{d}\tau}=-\kappa(\tau)[1+\mu_b], \quad \frac{1}{u_b}\frac{\mathrm{d}u_b}{\mathrm{d}t}=-\frac{a}{r_f}, \quad \mu_b(\tau)=[1+\mu_{bi}]\mathrm{e}^{-\int_0^\tau \kappa(\tau')\mathrm{d}\tau'}-1, \tag{6.4}$$

where the subscript i denotes the initial condition at $\tau = 0$. Introducing the reduced radius of the shock front (4.20), $x = 1/(\lambda\, b\, \kappa)$, and the definition (3.3) of $\dot{\alpha}_\tau$, the relations $\mathcal{D} \equiv \mathrm{d}r_f/\mathrm{d}t$, $\mathrm{d}/\mathrm{d}\tau = (t_r/\epsilon)\mathrm{d}/\mathrm{d}t$ and $l_{o_{CJ}} \equiv a_u t_r$, lead to

$$\frac{\mathrm{d}x}{\mathrm{d}\tau}=\frac{1}{\lambda b}\left[1+\epsilon(1+\dot{\alpha}_\tau)\right] \approx \frac{1}{\lambda b}, \quad x(\tau)-x_i \approx \frac{\tau}{b\lambda}, \quad \mu_b(\tau) \approx \mu_{bi}-\ln(x/x_i), \tag{6.5}$$

where the last relation is obtained from the first relation in (6.4) for $\mu_b \ll 1$.

According to Liñan *et al.* (2012), within the framework of the discontinuous model, the scale separation insuring the validity of (6.4)-(6.5) breaks down abruptly as soon as the CJ regime is reached. Moreover this occurs at a finite radius. Therefore the transition to the Chapman-Jouguet regime is abrupt, producing quasi-instantaneously a jump of flow gradient (not of the flow velocity) inside the rarefaction wave. The key point is that the velocity $\mathcal{D}(\tau)$ of an overdriven detonation whose inner structure is in steady state cannot decrease below the CJ velocity $\mathcal{D}_{o_{CJ}}$ so that the strong deceleration of the detonation ($\mathrm{d}\mathcal{D}/\mathrm{d}\tau < 0$) which is induced by the rarefaction wave is stopped suddenly ($\mathrm{d}\mathcal{D}/\mathrm{d}\tau \approx 0$) when $\mathcal{D}(t)$ reaches $\mathcal{D}_{o_{CJ}}$. Then, the velocity gradient of the external flow at the detonation front jumps to infinity and keeps on to be infinite subsequently. Just after the transition, the unsteady term $\partial\mu/\partial\tau$ in (6.1)-(6.2) drops off and, in contrast to (6.4), the curvature term κ is now balanced by the nonlinear term leading to the well known singularity of the flow gradient in the Taylor-Zeldovich self-similar solution behind the front of a spherical CJ detonation considered as a discontinuity, $(\mu-\dot{\alpha}_\tau)\partial\mu/\partial\xi = -\kappa$, $\Rightarrow\ (\mu-\dot{\alpha}_\tau)|_{\xi=0^-} = -\sqrt{-2\,\kappa\,\xi}$, see Zeldovich (1942), Taylor (1950*a*) and Zeldovich & Kompaneets (1960). The singular disturbance (jump of the velocity gradient) which is generated instantaneously at the sonic point moves away from the detonation front in the form of a weak discontinuity, see Liñan *et al.* (2012). As noticed first by Taylor (1950*a*), the compatibility of a discontinuous model and an infinite slope of the burnt gas velocity at the detonation front is questionable. This point is clarified when the response of the inner detonation structure is taken into account since the transition will be softened.

6.2. *Formulation in the double limit "small heat release and large activation energy"*

Solving the characteristic equation (3.10) for the upward-running mode for the flow field $\mu(\xi,\tau)$ satisfying the two boundary conditions (3.11), the detonation velocity $\dot\alpha_\tau(\tau)$ is an eigenfunction of the problem. Using (3.16), (3.18) and the notation (4.20) $x\equiv 1/(\lambda\, b\,\kappa)$, equations (3.10)-(3.11) take the form

$$\frac{\partial\mu}{\partial\tau}+[\mu-\dot\alpha_\tau(\tau)]\,\frac{\partial\mu}{\partial\xi}=\frac{1}{2}\mathrm{e}^{b\dot\alpha_\tau}\omega_{o_{CJ}}(\xi\,\mathrm{e}^{b\dot\alpha_\tau})-\frac{1}{b}\,(1+\mu)\,\frac{1}{\lambda\,x(\tau)}, \tag{6.6}$$

$$\xi=0:\ \mu=1+2\dot\alpha_\tau(\tau),\qquad\qquad \xi=\xi_b(\tau):\ \mu=\mu_b(\tau), \tag{6.7}$$

where $\mu_b(\tau)$ is the flow of the rarefaction wave at the detonation wave. For the same reason as in § 5.2, to leading order in the limit of large activation energy (4.14), the external flow $\mu_b(\tau)$ is imposed to the detonation wave at the end of the reaction rate, $\xi_b(\tau)\approx-\mathrm{e}^{-b\dot\alpha(\tau)}$. According to (6.5), $\mu_b(\tau)$ is a decreasing function ($\mathrm{d}\mu_b/\mathrm{d}\tau<0$ and $\mathrm{d}\dot\alpha_\tau/\mathrm{d}\tau<0$) down to the CJ regime $\mu_b=\dot\alpha_\tau$ which is reached at $x=x_{i_{CJ}}$ and $\tau=\tau_{i_{CJ}}$

$$\tau_{i_{CJ}}=b\,(x_{i_{CJ}}-x_i)\lambda,\qquad \ln(x_{i_{CJ}}/x_i)=\mu_{bi}-\dot\alpha_\tau(\tau_{i_{CJ}}), \tag{6.8}$$

and the sonic condition keeps on verified afterwards $\tau\geqslant\tau_{i_{CJ}}$,

$$\tau<\tau_{i_{CJ}}:\quad \mu_b(\tau)=\mu_{bi}-\ln(x/x_i)\quad\text{where}\quad x(\tau)-x_i\approx\tau/(b\lambda) \tag{6.9}$$

$$\tau\geqslant\tau_{i_{CJ}}:\quad \mu_b(\tau)=\dot\alpha_\tau(\tau). \tag{6.10}$$

Focusing the attention onto propagation velocities and radii of same order of magnitude as their critical values $\mathcal{D}^*$ and r_f^*, $|\dot\alpha_\tau|=O(1/b)$ and $\kappa=O(1/b)$, it is convenient to introduce the *phase space "velocity - radius"* $y-x$ involving the dimensionless variables (5.20) of order unity. Anticipating that the flow of burnt gas is then of same order of magnitude as in the slightly overdriven regimes (5.22), $\mu_b=O(1/\sqrt{b})$, $\dot\alpha_\tau\ll\mu_b$, equation (6.8) yields $\ln(x_{i_{CJ}}/x_i)\approx\mu_{bi}=O(1/\sqrt{b})\Rightarrow(x_{i_{CJ}}-x_i)/x_i\approx\mu_{bi}=O(1/\sqrt{b})$,

$$\mu_{bi}=O(1/\sqrt{b})\quad\Rightarrow\quad\tau_{i_{CJ}}\approx(b\mu_{bi})\lambda x_i=O(\sqrt{b}), \tag{6.11}$$

and the boundary condition at the exit of the inner structure $\xi_b\approx-\mathrm{e}^{-y}$ reduces to

$$0\leqslant\tau<\tau_{i_{CJ}}:\ \mu_b\approx\mu_{bi}(1-\tau/\tau_{i_{CJ}}).\qquad\qquad \tau>\tau_{i_{CJ}}:\ \mu_b\approx0. \tag{6.12}$$

The first equation in (6.12) is obtained from (6.9) for τ of the same order of magnitude as $\tau_{i_{CJ}}$, $\tau=O(\sqrt{b})$ and the second equation holds since the order of magnitude of $|\dot\alpha_\tau|=O(1/b)$ is smaller than $\mu_b=O(1/\sqrt{b})$ leading to the acceleration of the flow of burned gas in agreement with (6.4) $\mathrm{d}\mu_b/\mathrm{d}\tau=O(1/b)$. Introducing the radius $x_{i_{CJ}}\equiv x(\tau_{i_{CJ}})$ at which the CJ condition is reached and the functions of order unity $\mathrm{m}_b(\tau)$ and/or $\mathrm{m}_b(x)$ (x being a linear function of τ),

$$\mathrm{m}_b\equiv\sqrt{b/2}\,\mu_b=O(1),\quad \mathrm{m}_{bi}\equiv\sqrt{b/2}\,\mu_{bi}=O(1),\quad (x_{i_{CJ}}-x_i)/x_i\approx\sqrt{2/b}\,\mathrm{m}_{bi} \tag{6.13}$$

equations (6.12) take the form

$$x<x_{i_{CJ}}:\ \mathrm{m}_b(x)=\mathrm{m}_{bi}-\sqrt{b/2}\ln(x/x_i)\Leftrightarrow\tau<\tau_{i_{CJ}}:\ \mathrm{m}_b(\tau)/\mathrm{m}_{bi}\approx1-\tau/\tau_{i_{CJ}} \tag{6.14}$$

$$x>x_{i_{CJ}}:\ \mathrm{m}_b(x)=0\quad\Leftrightarrow\quad\tau>\tau_{i_{CJ}}:\ \mathrm{m}_b(\tau)=0. \tag{6.15}$$

To leading order in the double limit (4.14), equations (6.6)-(6.7), written in the notations (5.20), take the form

$$\frac{\partial\mu}{\partial\tau}+\left(\mu-\frac{y}{b}\right)\frac{\partial\mu}{\partial\xi}=\frac{1}{2}\mathrm{e}^{y(\tau)}\omega_{o_{CJ}}(\xi\,\mathrm{e}^{y(\tau)})-\frac{1}{b}\,(1+\mu)\,\frac{1}{\lambda\,x(\tau)}, \tag{6.16}$$

$$\xi=0:\ \mu=1+2y(\tau)/b,\qquad\qquad \xi=-\mathrm{e}^{-y(\tau)}:\ \mu=\sqrt{2/b}\,\mathrm{m}_b(\tau), \tag{6.17}$$

where $\mathrm{m}_b(\tau) = O(1)$ is given in (6.14)-(6.15). Except a negligible slope of order $1/b$ in the induction layer, the flow field $\mu(\xi,\tau)$ is an increasing function of ξ, so that no singularity of the wave breaking type is produced by the nonlinear term on the left-hand side of (6.16). The trajectories approaching the CJ regime are parametrized by an initial condition $\tau = 0 : x = x_i$ and $\mathrm{m}_b = \mathrm{m}_{bi}$ where x_i and m_{bi} are non dimensional parameters of order unity. If the trajectory is in quasi-steady state at the initial state ($\tau = 0$), then, according to (5.22), the initial velocity y_i is expressed in terms of m_{bi} and x_i

$$y_i + \mathrm{e}^{-\overline{y}_i}/x_i = \mathrm{m}_{bi}^2 + O(1/\sqrt{b}). \tag{6.18}$$

There is however no reason for this condition to be verified by unsteady trajectories.

A first rough comment on the initiation criterion can be made right now. If the initial condition is such that the radius $x_{i_{CJ}}$ was smaller than the critical radius, $x_{i_{CJ}} < x^*$ ($x^* = \mathrm{e}$, see (4.20)), then the peninsula of the quasi-steady CJ waves in § 4 cannot be reached and no success of initiation is expected like for the quasi-steady trajectories in figure 1 discussed in the next section. However this criterion of failure assumes implicitly that the critical radius is not strongly modified by unsteady effects. This remains to be proved by further studies of the hyperbolic equation (6.16)-(6.17) in the limit $b \gg 1$. In the following the attention is focused on the unsteady effects for $x_{i_{CJ}}$ larger than x^*. In this case the dynamical problem reduces to an integral equation presented in § 8 for the propagation velocity $y(\tau)$. Before analyzing the fully unsteady solution, it is worth discussing briefly the detonation decay in the quasi-steady state approximation.

7. Quasi-steady trajectories

In this section the trajectories $\overline{y}(x)$ in the phase space *"velocity-radius"* are analyzed in the double limit (4.14) when the unsteady term is neglected in (6.16), the term $\mu(\xi,\tau)$ in the last term on the right-hand side (curvature term) being replaced by the zeroth order solution $\mu_{o_{CJ}}(\xi \mathrm{e}^{\overline{y}(x)})$. This leads to solve (5.15) with the boundary condition $\xi = -\mathrm{e}^{-\overline{y}(x)} : \mu = \sqrt{2/b}\,\mathrm{m}_b$ and $\mathrm{m}_b(x)$ given in (6.14). According to (5.22) the result is

$$\overline{y}(x) + \frac{\mathrm{e}^{-\overline{y}(x)}}{x} = \mathrm{m}_b^2(x), \qquad \sqrt{\overline{y}(x) + \mathrm{e}^{-\overline{y}(x)}/x} = \mathrm{m}_{bi} - \sqrt{b/2}\ln(x/x_i). \tag{7.1}$$

Usually, the quasi-steady approximation is accurate for stable detonations whose characteristic time of evolution is larger than the response time of the inner structure. According to (6.11)-(6.12), the driving mechanism of the rarefaction wave evolves effectively on a timescale larger than the response time of the inner structure of a stable detonation, $\partial/\partial\tau = O(1)$ since $(1/\mu_b)\mathrm{d}\mu_b/\mathrm{d}\tau = O(1/\sqrt{b})$. Unfortunately, such a slow forcing term $\mu_b(\tau)$ introduces unsteady effects that are not smaller than the geometrical effect responsible of the S-shaped curve $\overline{y}_{_{CJ}}(x)$. Therefore, as shown in more details in § 7.3, despite the separation of timescale between the fast response of the inner structure and the slow dynamics of the burnt gas, the quasi-steady approximation is not accurate when the CJ condition is approached. However the *"quasi-steady trajectories"* are worth investigating first for two reasons; firstly to enlighten the effect of the curvature of the detonation front by comparison with the work of Liñan *et al.* (2012) in which the curvature is ignored and secondly to exhibit the role of unsteadiness by comparison with the results when the unsteady term is included.

7.1. *Quasi-steady trajectory for failure of the initiation process*

Two examples of C-shaped curves $\overline{y}(x)$, $\sqrt{\overline{y}(x)+\mathrm{e}^{-\overline{y}(x)}/x}=\overline{m}_b$, corresponding to a constant value $\overline{m}_b$, are plotted in figure 1 for $\overline{m}_b=0.71$ and $\overline{m}_b=1$, in comparison with the CJ solution $\overline{y}_{_{CJ}}(x)$, $\overline{m}_b=0$: $\overline{y}_{_{CJ}}+x^{-1}\mathrm{e}^{-\overline{y}_{CJ}}=0$. Inside the CJ peninsula, $\overline{y}+x^{-1}\mathrm{e}^{-\overline{y}}<0$, (dashed domain) there is no solution. The turning point of the iso-$\overline{m}$ lines $y=\overline{y}(x)$ is located at the intersection with the curve $y=-\ln x$ plotted in red in figure 1, $\mathrm{d}\overline{y}/\mathrm{d}x|_{\overline{m}^2=\mathrm{cst.}}=\mathrm{e}^{-\overline{y}}/[x(x-e^{-\overline{y}})]$. Consider first a trajectory (7.1) which does not intersect the upper branch of the CJ peninsula $\overline{y}_{_{CJ}}(x)$, $x_{i_{CJ}}<x^*=\mathrm{e}$. The derivative $\mathrm{d}\overline{y}/\mathrm{d}x$ becomes infinite at the intersection point with the curve $y=-\ln x$, $x=\mathrm{e}^{-\overline{y}}<x^*$, $\overline{y}>y^*=-1$, $\mathrm{d}\overline{y}/\mathrm{d}x|_{x=\mathrm{e}^{-\overline{y}}}=\infty$, where the derivative changes of sign, see (B 5) in appendix, $\mathrm{d}\overline{y}/\mathrm{d}x<0$ for $x>\mathrm{e}^{-\overline{y}}$ and $\mathrm{d}\overline{y}/\mathrm{d}x>0$ for $x<\mathrm{e}^{-\overline{y}}$. The situation is different at the critical point, $x=\mathrm{e}$, $\overline{y}=-1$ where the derivative is discontinuous, $\mathrm{d}\overline{y}/\mathrm{d}x|_{\overline{y}+1=0^+}\neq\mathrm{d}\overline{y}/\mathrm{d}x|_{\overline{y}+1=0^-}$, see (B 8). In any case, such singularities of the derivative $\mathrm{d}\overline{y}/\mathrm{d}x$ indicate that the quasi-steady approximation cannot be valid when approaching the curve $y=-\ln x$. The part of the trajectory $\overline{y}(x)$ below the curve $y=-\ln x$ ($\overline{y}<-\ln x$, $x<\mathrm{e}^{-\overline{y}}$, dashed part of $y_2(x)$ in Fig. 1) is not meaningful and cannot the extension of the trajectory because, according to (6.5), the radius should increase with the time, $\mathrm{d}x/\mathrm{d}\tau>0$. Even though the quasi-steady state approximation is no longer valid near the curve $y=-\ln x$, the quasi-steady trajectories suggest a curvature-induced failure mechanism.

7.2. *Quasi-steady trajectories for a successful initiation process*

Consider now a quasi-steady trajectory $\overline{y}(x)$ intersecting the upper branch of the CJ peninsula $\overline{y}_{_{CJ}}(x)$, $\overline{y}_{_{CJ}}+\mathrm{e}^{-\overline{y}_{CJ}}/x=0$ ($\overline{m}_b=0$), at a radius $x_{_{CJ}}>\mathrm{e}$ not too close to the critical radius, $\overline{y}(x_{_{CJ}})>-1$, see $y_1(x)$ in Fig. 1. A sharp transition occurs at $x=x_{_{CJ}}$, reminiscent of the transition described by Liñan *et al.* (2012) and the cases $x<x_{_{CJ}}$ and $x>x_{_{CJ}}$ have to be analyzed separately. After expressing $x_{_{CJ}}$ in term of the initial condition $x=x_i$, $\overline{y}=y_i$, $\overline{m}_b=m_{bi}>0$, equation (7.1) takes the form

$$x\leqslant x_{_{CJ}}:\quad \sqrt{\overline{y}(x)+\frac{1}{x}\mathrm{e}^{-\overline{y}(x)}}=\sqrt{\frac{b}{2}}\,\ln\Big(\frac{x_{_{CJ}}}{x}\Big)\,, \tag{7.2}$$

in agreement with (6.14), showing that the trajectory $\overline{y}(x)$ is tangent to the upper CJ branch $y_{_{CJ}}(x)$ from above in the form

$$\big[\overline{y}(x)-\overline{y}_{_{CJ}}(x)\big]=\frac{b/2}{x_{_{CJ}}^2\,\big[1+\overline{y}_{_{CJ}}(x_{_{CJ}})\big]}(x_{_{CJ}}-x)^2, \tag{7.3}$$

valid for a vicinity of $x_{_{CJ}}$ defined by the inequality $0<(x-x_{_{CJ}})\ll\big[1+\overline{y}_{_{CJ}}(x_{_{CJ}})\big]\,x_{_{CJ}}$, see (B 9)-(B 18). In that respect, the quasi-steady decay towards the upper branch of the CJ peninsula is similar to the decay towards the planar CJ velocity studied by Liñan *et al.* (2012) with the discontinuous model which is equivalent to a frozen inner structure of planar detonation (no curvature effect). However the convergence radius of (7.3) decreases to zero at the turning point ($x_{_{CJ}}=\mathrm{e}$, $y_{_{CJ}}+1=0$) stressing the critical nature of this point.

7.3. *Limitation of the steady-state approximation*

Integration of (6.16) across the inner structure when μ is replaced by $\mu_{o_{CJ}}(\xi\mathrm{e}^{b\overline{y}})$ in the curvature term, the unsteady term introduces an additional term into (7.1)

$$\left[y(\tau)+\frac{\mathrm{e}^{-y(\tau)}}{x(\tau)}\right]\approx \mathrm{m}_b^2(\tau)+b\int_{-\mathrm{e}^{-y(\tau)}}^{0}(\partial\mu/\partial\tau)\mathrm{d}\xi. \tag{7.4}$$

The validity of the quasi-steady assumption requires that the integral term on the right-hand side of (7.4) is smaller than $1/b$. This cannot be true for unstable detonations, $\partial\mu/\partial\tau = O(1)$, and attention is limited here onto stable waves. In the spirit of the multiple-time scale approximation, neglecting the fast relaxation of the inner structure toward its quasi-steady state, the unsteady term $(\partial\mu/\partial\tau)$ can be evaluated by using the zeroth-order of the solution of (5.21) in the limit $b \gg 1$, $\overline{\mu}_0(\xi,\overline{y}) = \mu_{o_{CJ}}(\xi \mathrm{e}^{\overline{y}})$,

$$\partial\overline{\mu}_0(\xi,\overline{y}(\tau))/\partial\tau = (\mathrm{d}\overline{y}/\mathrm{d}\tau)\xi \mathrm{e}^{\overline{y}} \mathrm{d}\mu_{o_{CJ}}(\xi')/\mathrm{d}\xi'|_{\xi'=\xi\,\mathrm{e}^{\overline{y}}} \tag{7.5}$$

where $\mathrm{d}\overline{y}(\tau)/\mathrm{d}\tau$ is obtained from (7.1) using (6.5), $\mathrm{d}x/\mathrm{d}\tau = 1/(\lambda b)$,

$$\left(1 - \frac{e^{-\overline{y}}}{\overline{x}}\right)\frac{\mathrm{d}\overline{y}}{\mathrm{d}\tau} = -\frac{1}{\sqrt{b}}\frac{\sqrt{2}\,\overline{\mathrm{m}}_b}{\lambda\,\overline{x}} + \frac{1}{b}\frac{e^{-\overline{y}}}{\lambda\,\overline{x}^2} \quad \Rightarrow \quad \overline{y} \neq -\ln\overline{x}: \ \frac{\mathrm{d}\overline{y}}{\mathrm{d}\tau} = O(1/\sqrt{b}). \tag{7.6}$$

This shows that the unsteady term $(\partial\mu/\partial\tau)$ is of order $1/\sqrt{b}$, larger than the curvature term on the right-hand side of (5.15) and (6.6). Then, the integral term in (7.4), evaluated from (7.5) by an integral by parts,

$$\int_{-\mathrm{e}^{-b\overline{\alpha}_\tau}}^{0} (\partial\overline{\mu}_0/\partial\tau)\mathrm{d}\xi = -(\lambda-1)\frac{\mathrm{d}\overline{y}}{\mathrm{d}\tau}e^{-\overline{y}}, \tag{7.7}$$

is of order $1/\sqrt{b}$, and cannot be neglected in (7.4). Near the curve $y = -\ln x$ the situation is even worth since the derivative $\mathrm{d}\overline{y}/\mathrm{d}\tau$ diverges.

To summarize, despite the separation of time scale, the steady-state assumption is not self-consistent near to the critical radius in the limit (4.14) since the unsteady effects are stronger than the geometrical effects. Concerning the evolution of a stable detonation on the upper branch of the CJ peninsula, the dynamics (4.19) is slow, $(1/\mathcal{D}_{_{CJ}})\mathrm{d}\mathcal{D}_{_{CJ}}/\mathrm{d}\tau = O(\epsilon/b^2)$ but the unsteady term in (6.16) is of the same order of magnitude as the curvature term, $\partial\mu_{_{CJ}}/\partial\tau = O(1/b)$.

8. Unsteadiness of the inner structure for successful initiation

Consider the trajectories for which $x_{i_{CJ}}$ is larger than x^*, $x_i > x^*/(1+\sqrt{2/b}\,\mathrm{m}_{bi})$, so that a successful initiation is expected.When approaching the CJ regime, we will now show that the solution of the hyperbolic problem (6.16)-(6.17) for the flow field $\mu(\xi,\tau)$ leads to an integral equation for the propagation velocity $y(\tau)$.

8.1. *Splitting*

Introducing the decomposition

$$\mu(\xi,\tau) = \mu_0(\xi,\tau) + \mu_1(\xi,\tau) \tag{8.1}$$

into (6.16)-(6.17) yields the following nonlinear equation for $\mu_1(\xi,\tau)$, the field $\mu_0(\xi,\tau)$ being assumed to be known,

$$\frac{\partial\mu_1}{\partial\tau} + \frac{\partial}{\partial\xi}\left[\mu_0\mu_1 + \frac{\mu_1^2}{2}\right] - \frac{y(\tau)}{b}\frac{\partial\mu_1}{\partial\xi} + \frac{1}{b}\frac{\mu_1}{\lambda x} = H(\xi,\tau) + W(\xi,\tau), \tag{8.2}$$

$$\text{where} \quad H(\xi,\tau) \equiv -\frac{\partial\mu_0(\xi,\tau)}{\partial\tau} - \frac{1}{b}\frac{1}{\lambda\,x(\tau)} - \frac{1}{b}\frac{\mu_0(\xi,\tau)}{\lambda\,x(\tau)} \tag{8.3}$$

$$\text{and} \quad W(\xi,\tau) \equiv \frac{1}{2}\left[\mathrm{e}^{y(\tau)}\omega_{o_{CJ}}(\xi\,\mathrm{e}^{y(\tau)})\right] - \left[\mu_0(\xi,\tau) - \frac{y(\tau)}{b}\right]\frac{\partial\mu_0(\xi,\tau)}{\partial\xi}. \tag{8.4}$$

with the boundary conditions (6.17) in the form

$$\xi=0:\ \mu_1=1+2\frac{y(\tau)}{b}-\mu_0(0,\tau),\qquad \xi=-\mathrm{e}^{-y(\tau)}:\ \mu_1=\mu_b(\tau)-\mu_0(-\mathrm{e}^{-y(\tau)},\tau). \quad (8.5)$$

The attention being focused onto the decay of detonations whose radius is above criticality $x(\tau)>x^*$, the choice of the first term μ_0 in (8.1) is the steady solution of the upper branch of the CJ peninsula $\overline{\mu}_{_{CJ}}(\xi,\overline{y}_{_{CJ}}(x))$, namely the solution (5.3) in which $\overline{y}_{_{CJ}}(x)$ is function of the time through (6.5), $x(\tau)=x_i+\tau/b\lambda$,

$$\mu_0(\xi,\tau)=\overline{\mu}_{_{CJ}}(\xi,\overline{y}_{_{CJ}}(x)),\quad \mu(\xi,\tau)=\overline{\mu}_{_{CJ}}(\xi,\overline{y}_{_{CJ}}(x))+\mu_1(\xi,\tau) \quad (8.6)$$

where, according to (4.12)-(4.13), (5.13) and (6.5),

$$\overline{\mu}_{_{CJ}}(\xi,\overline{y}_{_{CJ}}(x))=\mu_{o_{CJ}}(\xi\mathrm{e}^{\overline{y}_{_{CJ}}(x)})\left[1+O\left(\frac{1}{b}\right)\right],\quad \frac{\mathrm{d}\overline{y}_{_{CJ}}}{\mathrm{d}\tau}=\frac{1}{b}\frac{\mathrm{e}^{-\overline{y}_{_{CJ}}}}{\lambda\,x^2}\frac{1}{1+\overline{y}_{_{CJ}}}, \quad (8.7)$$

and $\mu_{o_{CJ}}(\xi)$ is the planar CJ solution (4.21). Sufficiently above the critical radius, the derivative of $\overline{\mu}_{_{CJ}}(\xi,\overline{y}_{_{CJ}}(x))$ with respect to time is small, of order $1/b$,

$$\frac{\partial\,\overline{\mu}_{_{CJ}}(\xi,\overline{y}_{_{CJ}}(x))}{\partial\tau}=\frac{\partial\,\mu_{o_{CJ}}(\xi\mathrm{e}^{\overline{y}_{_{CJ}}(x)})}{\partial\tau}\,[1+O(1/b)]\approx\frac{1}{\lambda\,b}\frac{\mathrm{d}\overline{y}_{_{CJ}}}{\mathrm{d}x}\mathrm{e}^{\overline{y}_{_{CJ}}}\xi\mu'_{o_{CJ}}(\xi\,\mathrm{e}^{\overline{y}_{_{CJ}}}) \quad (8.8)$$

where $\mu'_{o_{CJ}}(\xi)$ denotes $\mathrm{d}\mu_{o_{CJ}}(\xi)/\mathrm{d}\xi$. Expressing the last term in (8.4)

$$-\left[\mu_0-\frac{y}{b}\right]\frac{\partial\mu_0}{\partial\xi}=-\left[\overline{\mu}_{_{CJ}}-\frac{\overline{y}_{_{CJ}}}{b}\right]\frac{\partial\overline{\mu}_{_{CJ}}}{\partial\xi}+\frac{(y-\overline{y}_{_{CJ}})}{b}\frac{\partial\overline{\mu}_{_{CJ}}}{\partial\xi}$$

by using (5.1) and (8.7), the two last terms on the right-hand side of (8.3) are eliminated and the terms $H(\xi,\tau)$ and $W(\xi,\tau)$ are replaced by $\mathrm{h}(\xi,\tau)$ and $\mathrm{w}(\xi,\tau)$

$$\mathrm{h}(\xi,\tau)\equiv-b\frac{\partial\,\mu_{o_{CJ}}(\xi\mathrm{e}^{\overline{y}_{_{CJ}}(x)})}{\partial\tau}=-\frac{1}{\lambda}\frac{\mathrm{d}\overline{y}_{_{CJ}}}{\mathrm{d}x}\mathrm{e}^{\overline{y}_{_{CJ}}}\xi\mu'_{o_{CJ}}(\xi\,\mathrm{e}^{\overline{y}_{_{CJ}}})=-\frac{1}{\lambda x^2}\frac{\xi\mu'_{o_{CJ}}(\xi\,\mathrm{e}^{\overline{y}_{_{CJ}}})}{1+\overline{y}_{_{CJ}}} \quad (8.9)$$

$$\mathrm{w}(\xi,y,\overline{y}_{_{CJ}})\equiv\frac{b}{2}\left[\mathrm{e}^{y}\omega_{o_{CJ}}(\xi\,\mathrm{e}^{y})-\mathrm{e}^{\overline{y}_{_{CJ}}}\omega_{o_{CJ}}(\xi\,\mathrm{e}^{\overline{y}_{_{CJ}}})\right]+\mathrm{e}^{\overline{y}_{_{CJ}}}\mu'_{o_{CJ}}(\xi\,\mathrm{e}^{\overline{y}_{_{CJ}}})\,(y-\overline{y}_{_{CJ}}), \quad (8.10)$$

so that equations (8.2)-(8.4) take the form

$$\frac{\partial\mu_1}{\partial\tau}+\frac{\partial}{\partial\xi}\left[\overline{\mu}_{_{CJ}}(\xi,\overline{y}_{_{CJ}})\mu_1+\frac{\mu_1^2}{2}\right]-\frac{y(\tau)}{b}\frac{\partial\mu_1}{\partial\xi}+\frac{1}{b}\frac{\mu_1}{\lambda x}=\frac{1}{b}\left[\mathrm{h}(\xi,\tau)+\mathrm{w}(\xi,y,\overline{y}_{_{CJ}})\right] \quad (8.11)$$

in which y and $\overline{y}_{_{CJ}}$ are functions of τ. Notice the divergence of $\mathrm{h}(\xi,\tau)$ at the turning point $\overline{y}_{_{CJ}}=-1$ coming from (8.7). The eigenfunction $y(\tau)$ is determined by the two boundary conditions (8.5), written when (4.2) is used, $\overline{\mu}_{_{CJ}}(0,\overline{y}_{_{CJ}})=1+2\overline{y}_{_{CJ}}/b$

$$\xi=0:\ \mu_1=2[y(\tau)-\overline{y}_{_{CJ}}(x(\tau))]/b;\quad \xi=-\mathrm{e}^{-y(\tau)}:\ \mu_1=\mu_b(\tau)-\mu_{o_{CJ}}(-\mathrm{e}^{(\overline{y}_{_{CJ}}-y)}), \quad (8.12)$$

where, using (8.7), the term of order $1/b$ has been omitted on the right-hand side of the last equation in (8.12), the function $\mu_b(\tau)=O(1/\sqrt{b})$ being given in (6.11)-(6.12). The expression of the boundary condition at the exit of the reaction zone in (8.12) changes form depending wether $y>\overline{y}_{_{CJ}}$ or $y<\overline{y}_{_{CJ}}$ since $\mu_{o_{CJ}}(\xi)>0$ for $\xi>-1$ and $\mu_{o_{CJ}}(\xi)=0$ for $\xi<-1$. Above the CJ peninsula, $y(\tau)>\overline{y}_{_{CJ}}(x(\tau))$, $-\mathrm{e}^{(\overline{y}_{_{CJ}}-y)}>-1$, according to (5.10), the function $\mu_{o_{CJ}}(-\mathrm{e}^{(\overline{y}_{_{CJ}}-y)})$ is positive and of order unity when $h_\mu=O(1)$, so that the value of $|\mu_1|$ is of order unity at the exit of the reaction zone. Therefore, sufficiently far above the CJ peninsula, $y(\tau)>\overline{y}_{_{CJ}}(x(\tau))$, the velocity field $\mu(\xi,\tau)$ corresponds to the leading order of the velocity distribution of the quasi-steady solution (5.21) $\overline{\mu}(\xi,\overline{y})$ in which $\overline{y}$ is replaced by $y(\tau)$, $\mu\approx\mu_{o_{CJ}}(\xi\mathrm{e}^{y})$, see Appendix B.2.

8.2. *Integral equation.*

The decomposition (8.1) with (8.6) is suitable if the term μ_1 is smaller than $\mu_{o_{CJ}}$

$$\mu_1(\xi,\tau) < \mu_{o_{CJ}}(\xi \mathrm{e}^{\overline{y}_{CJ}}) \tag{8.13}$$

which is expected to be the case in the vicinity of the CJ peninsula, $0 < y(\tau) - \overline{y}_{CJ} \ll 1$, so that, $\mu_{o_{CJ}}(-\mathrm{e}^{(\overline{y}_{CJ}-y)})$ being small, the boundary conditions (8.12) are small,

$$0 < \big(y(\tau) - \overline{y}_{CJ}\big) \ll 1 \quad \Rightarrow \quad \mu_{o_{CJ}}(-\mathrm{e}^{(\overline{y}_{CJ}-y)}) \ll 1. \tag{8.14}$$

Neglecting the terms of order μ_1/b on the left-hand side, equation (8.11) yields

$$\frac{\partial \mu_1}{\partial \tau} + \frac{\partial}{\partial \xi}\left[\mu_{o_{CJ}}(\xi \mathrm{e}^{\overline{y}_{CJ}})\mu_1 + \frac{\mu_1^2}{2}\right] = \frac{1}{b}\left[\mathrm{h}(\xi) + \mathrm{w}(\xi,\tau)\right] \tag{8.15}$$

the functions $h(\xi)$ and $\mathrm{w}(\xi, y(\tau))$ being given respectively in (8.9) and (8.10). When the planar CJ detonation is stable or weakly unstable, the right-hand side of (8.15) is small. We will come back to this point later. Moreover, according to (8.7) and (8.9), $\mathrm{d}\overline{y}_{CJ}(x)/\mathrm{d}\tau = O(1/b)$, $\partial \mu_{o_{CJ}}(\xi \mathrm{e}^{\overline{y}_{CJ}})/\partial\tau = O(1/b)$, the time variation of $\mu_{o_{CJ}}(\xi \mathrm{e}^{\overline{y}_{CJ}})$ is negligible in the left-hand side of (8.15). In the steady state solution, the nonlinear term $\mu_1 \partial\mu_1/\partial\xi$ is essential, especially at the end of the reaction zone near the CJ regime, even when μ_1 is small. Then, according to (8.15), it is worth introducing the function

$$Z(\xi,\tau) \equiv b\left[\mu_{o_{CJ}}(\xi \mathrm{e}^{\overline{y}_{CJ}})\mu_1 + \mu_1^2/2\right]. \tag{8.16}$$

Assuming that the terms $\mu_1 \partial \mu_{o_{CJ}}(\xi \mathrm{e}^{\overline{y}_{CJ}})/\partial\tau = O(\mu_1/b)$ and $\mu_1 \partial\mu_1/\partial\tau$ are negligible,

$$\partial Z(\xi,\tau)/\partial\tau \approx b\mu_{o_{CJ}}(\xi \mathrm{e}^{\overline{y}_{CJ}})\partial\mu_1/\partial\tau, \tag{8.17}$$

equation (8.15) multiplied by $b\mu_{o_{CJ}}(\xi \mathrm{e}^{\overline{y}_{CJ}})$ takes the form

$$\left[\frac{\partial}{\partial\tau} + \mu_{o_{CJ}}(\xi \mathrm{e}^{\overline{y}_{CJ}})\frac{\partial}{\partial\xi}\right] Z(\xi,\tau) = \mu_{o_{CJ}}(\xi \mathrm{e}^{\overline{y}_{CJ}})\left[\mathrm{h}(\xi) + \mathrm{w}(\xi, y(\tau))\right], \tag{8.18}$$

with the boundary conditions (8.12)

$$\xi = 0: \ Z = Z_N(y(\tau)) = 2\big(y(\tau) - \overline{y}_{CJ}\big) \tag{8.19}$$

$$\xi = -\mathrm{e}^{-y(\tau)}: \ Z = Z_b(\tau) \equiv \frac{b}{2}\left[\mu_b^2(\tau) - \mu_{o_{CJ}}^2(-\mathrm{e}^{-[y(\tau)-\overline{y}_{CJ}]})\right] \tag{8.20}$$

where the term $b\mu_b^2(\tau)$ in $Z_b(\tau)$ is defined in (6.12), $b\mu_b^2(\tau) = O(1)$. Notice that the second term in $Z_b(\tau)$ is also of order unity if $(\overline{y}_{CJ} - y(\tau)) = O(1/\sqrt{b})$. Introducing the change of variable $\xi < 0 \to \zeta < 0$ and the time lag $|\zeta_b(\tau)|$, $\zeta_b(\tau) < 0$

$$\zeta(\xi) \equiv -\int_{\xi}^{0} \frac{\mathrm{d}\xi'}{\mu_{o_{CJ}}(\xi' \mathrm{e}^{\overline{y}_{CJ}})} < 0, \quad \zeta_b(\tau) \equiv \zeta(-\mathrm{e}^{-y(\tau)}) = -\int_{-\mathrm{e}^{-y(\tau)}}^{0} \frac{\mathrm{d}\xi'}{\mu_{o_{CJ}}(\xi' \mathrm{e}^{\overline{y}_{CJ}})} \tag{8.21}$$

and neglecting the time variation of $\mu_{o_{CJ}}(\xi \mathrm{e}^{\overline{y}_{CJ}})$, equations (8.18)-(8.20) yield

$$\left[\frac{\partial}{\partial\tau} + \frac{\partial}{\partial\zeta}\right] \tilde{Z}(\zeta,\tau) = \tilde{F}(\zeta,\tau), \quad \tilde{F} \equiv \mu_{o_{CJ}}\big(\xi(\zeta)\mathrm{e}^{\overline{y}_{CJ}}\big)\left[\mathrm{h}\big(\xi(\zeta)\big) + \mathrm{w}\big(\xi(\zeta), y(\tau)\big)\right] \tag{8.22}$$

$$\zeta = 0: \tilde{Z} = Z_N(y(\tau)), \qquad \zeta = \zeta_b(\tau): \tilde{Z} = Z_b(\tau) \tag{8.23}$$

where $\tilde{Z}(\zeta,\tau) \equiv Z(\xi(\zeta),\tau)$ and $\xi(\zeta)$ is the inverse function of $\zeta(\xi)$ which is well defined since $\mu_{o_{CJ}}(\xi \mathrm{e}^{\overline{y}_{CJ}})$ is an increasing function of ξ from 0 at $\xi = -1$ to 1 at $\xi = 0$. Using

the development recalled in Appendix D the solution of (8.22)-(8.23) takes the form

$$\tilde{Z}(\zeta,\tau)=\int_{\zeta_b(\tau_b)}^{\zeta}\tilde{F}(\zeta',\tau-\zeta+\zeta')\mathrm{d}\zeta'+Z_b(\tau-\zeta+\zeta_b(\tau_b)) \tag{8.24}$$

where τ_b is a function of $(\zeta-\tau)$ which is obtained by the intersection of the characteristic curve going through (ζ,τ) and the curve $\zeta=\zeta_b(\tau)$, so that τ_b is solution to the equation

$$\zeta_b(\tau_b)-\tau_b=\zeta-\tau, \tag{8.25}$$

see figure 7 in Appendix C. The boundary condition at the Neumann state $\zeta=0$ yields

$$Z_N(y(\tau))=\int_{\zeta_b(\tau_b)}^{0}\tilde{F}(\zeta',\tau+\zeta')\mathrm{d}\zeta'+Z_b(\tau+\zeta_b(\tau_b)) \text{ where } \zeta_b(\tau_b)\equiv\zeta(-\mathrm{e}^{-y(\tau_b)}). \tag{8.26}$$

Using the change of variable (8.21) $\mathrm{d}\zeta=\mathrm{d}\xi/\mu_{o_{CJ}}(\xi\mathrm{e}^{\overline{y}_{CJ}})$, the solution of (8.26) takes the form of an integral equation for $y(\tau)$

$$2\big(y(\tau)-\overline{y}_{CJ}\big)=\int_{-\mathrm{e}^{-y(\tau_b)}}^{0}\big[\mathrm{h}(\xi)+\mathrm{w}\big(\xi,y(\tau+\zeta(\xi))\big)\big]\,\mathrm{d}\xi+Z_b(\tau+\zeta_b(\tau_b)) \tag{8.27}$$

where, according to (8.25),

$$\zeta=0:\qquad \tau_b=\tau+\zeta_b(\tau_b)<\tau \tag{8.28}$$

see figure 7 in Appendix C, so that τ_b and $\zeta_b(\tau_b)$ are both function of the time τ.

The time delay at time τ, $z_b(\tau)\equiv-\zeta_b(\tau_b)>0$, $\tau_b=\tau-z_b<\tau$, is solution of a nonlinear equation obtained from (8.21)

$$z_b(\tau)\equiv-\zeta_b(\tau_b)=-\zeta(-\mathrm{e}^{-y(\tau_b)}),\quad z_b=\int_{-\mathrm{e}^{-y(\tau-z_b)}}^{0}\frac{\mathrm{d}\xi'}{\mu_{o_{CJ}}(\xi'\mathrm{e}^{\overline{y}_{CJ}})}>0 \tag{8.29}$$

$$z_b=\mathrm{e}^{-\overline{y}_{CJ}}\int_{-\mathrm{e}^{-\left[y(\tau-z_b)-\overline{y}_{CJ}\right]}}^{0}\frac{\mathrm{d}\xi}{\mu_{o_{CJ}}(\xi)}, \tag{8.30}$$

showing so that $z_b(\tau)$ is a functional of the time dependent velocity of the lead shock $y(\tau)$. Equation (8.30) is discussed in the next sections §§ 9.1-9.3. Introducing $\tau_b=\tau-z_b$ into (8.27) yields a nonlinear integral equation for the shock velocity $y(\tau)$ in the form

$$2\big(y(\tau)-\overline{y}_{CJ}\big)=\int_{-\mathrm{e}^{-y(\tau-z_b(\tau))}}^{0}\big[\mathrm{h}(\xi)+\mathrm{w}\big(\xi,y(\tau+\zeta(\xi))\big)\big]\,\mathrm{d}\xi+Z_b\big(\tau-z_b(\tau)\big), \tag{8.31}$$

illustrating the complexity of the dynamics, since, according to (8.28), the time delay $z_b(\tau)$ in the lower bound of the integral $-\mathrm{e}^{-y(\tau-z_b(\tau))}$ and in the last term on the right-hand side depends on the solution $y(\tau)$. Equation (8.31) takes a more convenient when the terms $Z_b(\tau-z_b)$ and the integral involving $\mathrm{w}(\xi,y)$ are rewrote by using equation (4.21) for the planar CJ solution $\mathrm{d}\mu_{o_{CJ}}^2(\xi)/\mathrm{d}\xi=\omega_{o_{CJ}}$, $\mu_{o_{CJ}}^2(0)=1$

$$-\frac{b}{2}\int_{-\mathrm{e}^{-y(\tau-z_b)}}^{0}\mathrm{e}^{\overline{y}_{CJ}}\omega_{o_{CJ}}(\mathrm{e}^{\overline{y}_{CJ}}\xi)\mathrm{d}\xi=-\frac{b}{2}+\frac{b}{2}\mu_{o_{CJ}}^2(-\mathrm{e}^{-[y(\tau-z_b)-\overline{y}_{CJ}]}). \tag{8.32}$$

so that the last term on the right-hand side of (8.32) balances the second term of $Z_b(\tau-z_b)$

in the expression (8.20) of $Z_b(\tau)$. Introducing three functionals of $y(\tau)$

$$G_1 \equiv \int_{-\mathrm{e}^{-y(\tau-z_b(\tau))}}^{0} \Big[\mathrm{e}^{y(\tau+\zeta(\xi))}\omega_{o_{CJ}}\big(\xi\,\mathrm{e}^{y(\tau+\zeta(\xi))}\big)\Big]\,\mathrm{d}\xi - 1, \tag{8.33}$$

$$G_2 \equiv \int_{-\mathrm{e}^{-y(\tau-z_b(\tau))}}^{0} \mathrm{e}^{\overline{y}_{CJ}}\,\mu'_{o_{CJ}}(\xi\,\mathrm{e}^{\overline{y}_{CJ}})\,\big[y\big(\tau+\zeta(\xi)\big)-\overline{y}_{CJ}\big]\,\mathrm{d}\xi, \tag{8.34}$$

$$I_{\mathrm{h}} \equiv \int_{-\mathrm{e}^{-y(\tau-z_b(\tau))}}^{0} \mathrm{h}(\xi)\mathrm{d}\xi \quad \text{where} \quad \mathrm{h}(\xi) \text{ is defined in (8.9)}, \tag{8.35}$$

the integral equation (8.31) for $y(\tau)$ takes the form

$$2\big(y(\tau)-\overline{y}_{CJ}\big) = \frac{b}{2}G_1 + G_2 + I_{\mathrm{h}} + \mathrm{m}_b^2(\tau - z_b), \tag{8.36}$$

where $z_b(\tau) = O(1)$ is a functional of $y(\tau)$ given in (8.30) and the function $\mathrm{m}_b(\tau) = O(1)$ is defined in (6.14)-(6.15),

$$\tau < \tau_{i_{CJ}} : \mathrm{m}_b(\tau)/\mathrm{m}_{bi} = 1 - \tau/\tau_{i_{CJ}}, \qquad \tau \geqslant \tau_{i_{CJ}} : \mathrm{m}_b(\tau) = 0. \tag{8.37}$$

According to (6.11), the time $\tau_{i_{CJ}} = \sqrt{2b}\,\lambda\,x_i\,\mathrm{m}_{bi}$ at which the CJ condition is reached can be expressed in terms of the initial condition ($\tau = 0$: $x = x_i$, $\mathrm{m}_b = \mathrm{m}_{bi}$), so that $\mathrm{dm}_b/\mathrm{d}\tau = -1/(\sqrt{2b}\,\lambda\,x_i)$ is small, of order $1/\sqrt{b}$. The time delay z_b has to be kept in the forcing term $\mathrm{m}_b^2(\tau - z_b)$ since $z_b(\tau)$ becomes large near the CJ regime yielding a correction which is not so small, typically of order $\ln b/\sqrt{b}$, see (D 30) in appendix. The CJ velocity $\overline{y}_{CJ}(x)$ of the quasi-steady spherical detonation in (8.33)-(8.36) is a function of the radius. The trajectories in the phase space $y - x$ are obtained from the solution of (8.36)-(8.37) by using (6.5), $x = x_i + \tau/(b\lambda)$.

9. Discussion of the results

9.1. *Physical insights*

The nonlinear coupling of the physical mechanisms controlling the dynamics (8.36) can be summarized as follows. According to the Arrhenius law and the two fast downstream-propagating modes, the thickness of the inner structure $|\xi_b(\tau)| = \mathrm{e}^{-y}$ varies quasi-instantaneously with the shock velocity y, $\xi_b = -\mathrm{e}^{-y} < 0$ denoting the position (relative to the shock) of the downstream boundary on the burnt gas side. The time $\tau_b = \tau - z_b$ at which the upstream running mode leaves the downstream boundary to reach the lead shock at time τ depends on the transit time $z_b(\tau)$ of the upwards running mode to travel across the detonation thickness from $\xi = \xi_b(\tau_b) < 0$ to $\xi = 0$, explaining that the triggering term $\mathrm{m}_b^2(\tau - z_b)$ in (8.36) is shifted by the time delay z_b. The complexity of the dynamics comes from the variation of the time delay $z_b(\tau)$ which depends on the position of the downstream boundary at an earlier time shifted itself by $z_b(\tau)$, $\xi_b(\tau - z_b) = -\mathrm{e}^{-y(\tau-z_b)}$. Therefore, under the approximation of a frozen field $\mu_{o_{CJ}}(\xi \mathrm{e}^{\overline{y}_{CJ}})$, z_b is solution of the nonlinear equation (8.30). Notice right now that equation (8.30) is meaningful if and only if $y(\tau - z_b) > \overline{y}_{CJ}$ since $\mu_{o_{CJ}}(\xi)$ is zero for $\xi \leqslant -1$. We will come back to this point in § 9.3 after discussing another important point concerning causality.

The integral equation (8.36) for $y(\tau)$ involves the past ranging from $\tau_b = \tau - z_b(\tau)$ to τ in order to integrate the cumulative effects upon the lead shock velocity produced by the modification of the reaction rate at different distance from the shock $|\xi|$. These modifications at ξ that are generated quasi-instantaneously at time τ by the variation of the shock velocity $y(\tau)$, produce a retarded effect on the shock velocity at a time delayed by the transit time (8.21) $-\zeta(\xi) > 0$ of the upstream-running mode travelling from ξ to

0. According to (8.18), the transit time is computed under the approximation of a frozen flow $\mu_{o_{CJ}}(\xi \mathrm{e}^{\overline{y}_{CJ}})$. The memory effects in the integral equation (8.36) are represented by the term $(b/2)G_1 + G_2$ which governs the stability of the planar detonation recalled in § 9.4. The dependence on the past is not only through the integration in the expressions (8.33) and (8.34) of G_1 and G_2 but also through the delay $z_b(\tau)$ in the lower bound of the integrals. The complexity of the dynamics is illustrated by (8.30) showing that $z_b(\tau)$ is a functional of $y(\tau)$.

9.2. *Causality*

When the detonation velocity $y(\tau)$ evolves under a time-dependent flow of burnt gas at $\xi = \xi_b(\tau)$ which is represented by the forcing term $\mathrm{m}_b^2(\tau - z_b(\tau))$ on the right-hand side of (8.36), the time dependent delay $z_b(\tau)$ should satisfy a causal link between $\mathrm{m}_b^2(\tau - z_b(\tau))$ (the cause) and $y(\tau)$ (the consequence). Consider a prescribed unsteady forcing term, namely a known function $\mathrm{m}_b(\tau)$ ($\mathrm{d}\mathrm{m}_b/\mathrm{d}\tau \neq 0$). The retarded responses $y(\tau_1)$ and $y(\tau_2)$ at two consecutive times ($\tau_1 < \tau_2$) correspond to the forcing term at time $\tau_b(\tau_1) = \tau_1 - z_b(\tau_1)$ and $\tau_b(\tau_2) = \tau_1 - z_b(\tau_2)$ respectively. Causality then requires that the inequality $\tau_b(\tau_1) < \tau_b(\tau_2)$ should holds if $\tau_1 < \tau_2$. Otherwise the latest response $y(\tau_2)$ would be produced by the earliest forcing $\mathrm{m}_b^2(\tau_b(\tau_2))$. This means that the function $\tau_b(\tau) \equiv \tau - z_b(\tau)$ should be an increasing function of time $\mathrm{d}\tau_b/\mathrm{d}\tau > 0$ so that the derivative of the delay should be bounded, $\mathrm{d}z_b/\mathrm{d}\tau \leqslant 1$. Since, according to (8.30),

$$\frac{\mathrm{d}z_b}{\mathrm{d}\tau} = \mathcal{A}(\tau - z_b)\left[1 - \frac{\mathrm{d}z_b}{\mathrm{d}\tau}\right] \quad \Rightarrow \quad \frac{\mathrm{d}z_b}{\mathrm{d}\tau} = \frac{1}{[1 + 1/\mathcal{A}(\tau - z_b)]} \tag{9.1}$$

$$\text{where} \qquad \mathcal{A}(\tau) \equiv -\frac{\mathrm{d}y(\tau)}{\mathrm{d}\tau}\frac{\mathrm{e}^{-[y(\tau)-\overline{y}_{CJ}]}}{\mu_{o_{CJ}}(-\mathrm{e}^{-[y(\tau)-\overline{y}_{CJ}]})}, \tag{9.2}$$

the causal relation $\mathrm{d}z_b(\tau)/\mathrm{d}\tau \leqslant 1$ is satisfied if $\mathcal{A} \geqslant -1$

$$\mathrm{d}y/\mathrm{d}\tau \leqslant \mathrm{e}^{[y(\tau)-\overline{y}_{CJ}]}\mu_{o_{CJ}}(-\mathrm{e}^{-[y(\tau)-\overline{y}_{CJ}]}). \tag{9.3}$$

This is always the case if the shock velocity decreases monotonously $y(\tau) > \overline{y}_{CJ}$, $\mathrm{d}y(\tau)/\mathrm{d}\tau < 0$. In this case the nonlinear equation (8.30) has a single solution for $z_b(\tau)$. For a reactive blast wave impinging the CJ peninsula with a moderately small deceleration of same order of magnitude as in the quasi-steady decay (7.6) $|\mathrm{d}y/\mathrm{d}\tau| = O(1/\sqrt{b})$, the delay z_b becomes moderately large when the CJ velocity is reached, $z_b = O(\sqrt{b})$ see Appendix E. Moreover, according to (9.3), the causal relation (9.3) is verified when the shock velocity increases $\dot{y}_\tau > 0$ if and only if the acceleration is not too large.

9.3. *An intriguing phenomenon: the jump of time delay*

In unsteady regimes, the solution of (8.36) can describe a velocity of the lead shock $y(\tau)$ decreasing below the CJ velocity (intermittently and for a short period of time). Oscillation of the detonation velocity at the CJ regime or when approaching the CJ regime requires a particular attention. The understanding of unstable detonations is somewhat difficult since $y(\tau)$ oscillates around $\overline{y}_{CJ}$ while the integral in (8.30) diverges for $y(\tau - z_b) < \overline{y}_{CJ}$. For an oscillatory shock velocity around its CJ value, the nonlinear equation (8.30) for z_b is meaningful at any time τ indeed, but is multivalued with a discrete spectrum of roots none of which involving a shock velocity corresponding to a forbidden band $y(\tau - z_b) < \overline{y}_{CJ}$. Keeping in mind the response of the shock velocity to variations in the burnt gas, causality implies that the time delay $z_b(\tau)$ is properly defined as the smallest root. The latter is a continuous function of time except for periodic discontinuity of first order (jump). More precisely, the delay $z_b(\tau)$ increases when

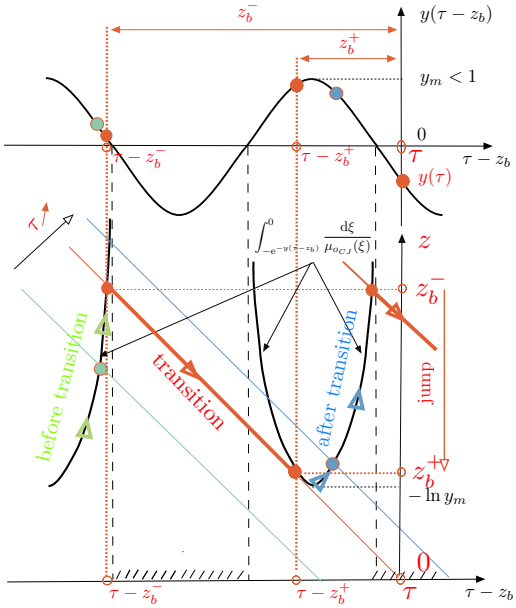

FIGURE 2. Sketch of the geometrical construction of the time delay $z_b(\tau)$ for an oscillatory shock velocity $y(\tau) = y_m \cos(2\pi\,\tau/\tau_p)$ around the planar CJ regime $\overline{y}_{_{CJ}} = 0$ plotted on top of the figure. The delay z_b at time τ is defined as the smallest roots of equation (8.30). The roots are represented on a plan (z_b, z) by the intersection of the straight line $z = z_b$ and the array of periodic curves $z(z_b) = \int_{-e^{-y(\tau-z_b)}}^{0} d\xi/\mu_{o_{CJ}}(\xi)$ defined in the z_b-bands corresponding to $y(\tau - z_b) > 0$. The forbidden bands are the shaded parts of the horizontal axis. The picture is drawn for the model (9.4) $z(z_b) = -\ln[y_m \cos(2\pi\,(\tau - z_b)/\tau_p)]$ with $\tau - z_b$ (instead of z_b) on the horizontal axis and z on the vertical axis so that the straight line $(z = z_b)$ intersects the horizontal axis at the point $\tau - z_b = \tau$ which is also the position of the vertical z-axis and y-axis. The red straight line corresponds to the transition time τ at which the smallest root, namely the delay $z_b(\tau)$, jumps from z_b^- to z_b^+, $z_b^- > z_b^+$. These values are associated with the intersection points represented by the red dots on the array of curves at the bottom of the figure. The corresponding values of the shock velocity $y(\tau - z_b^-)$, $y(\tau - z_b^+)$ and $y(\tau)$ are represented by the red dots on the harmonic function on top of the figure. According to the picture, $y(\tau) < 0 < y(\tau - z_b^-) < y(\tau - z_b^+)$, the detonation thickness, namely the distance between the lead shock and the end of the reaction zone, $l(\tau) \equiv e^{-y(\tau)} \approx 1 - y(\tau) > 0$ (approximated for $y_m < 1$), taken at the retarded time at which the upstream running mode leaves the burnt gas to reach the lead shock at the time τ, is larger just before the jump than after, the detonation thickness at the transition time τ being the largest one, $l(\tau - z_b^+) < l(\tau - z_b^-) < l(\tau)$. The time delay before and after the transition corresponds to the dots in green and blue respectively.

$y(\tau - z_b)$ approaches 0 from above and decreases suddenly by a jump to a smaller value corresponding to a larger shock velocity $y(\tau - z_b)$. The problem is more easily understood by the geometrical construction in figure 2. Consider a simplified example $\mu_{oCJ} = \xi + 1$ of the model (5.9)-(5.10) and the case $\overline{y}_{_{CJ}} = 0$ (planar geometry) for simplicity, equation (8.30) then takes the form written for $|y| \ll 1$

$$y(\tau - z_b) > 0 : z_b = -\ln y(\tau - z_b), \qquad y(\tau - z_b) < 0 : \text{ no solution.} \tag{9.4}$$

Consider a harmonic pulsation of period τ_p, $y(\tau) = y_m \cos(2\pi\,\tau/\tau_p)$ with $y_m < 1$. Equation (8.30) for $z_b(\tau)$ $z_b = -\ln[y_m \cos(2\pi\,(\tau - z_b)/\tau_p)]$ has a countable (infinite) set of roots which is bounded from below, none of the roots being smaller than $-\ln y_m > 0$. As shown in figure 2 the smallest root, namely the time delay, jumps at time τ from a value z_b^- well above the absolute minimum $-\ln y_m$ to z_b^+ slightly larger than $-\ln y_m$,

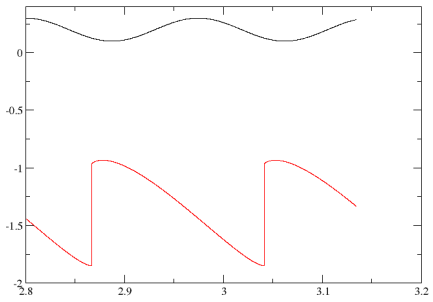

FIGURE 3. Numerical solution of (8.30) for $\overline{y}_{_{CJ}} = 0$ and $y(\tau) = 0.2 + 0.1\cos 3\,\tau$ plotted on top and for the reaction rate $\omega_{o_{CJ}}(\xi)$ used in Clavin & Denet (2018). The function $-z_b(\tau)$, $z_b(\tau) > 0$ being the smallest root of (8.30), is plotted in red. The time on the horizontal axis has been rescaled. The jump of z_b is slightly smaller than unity and the maximum of $z_b(\tau)$ is approximately 1.8.

$z_b^- > z_b^+$. In other words a new lower bound z_b^+ smaller than z_b^- appears suddenly at τ when the time increases. Few time before τ, the smallest root (in green in figure 2) increases continuously up to z_b^- while, few time after τ, the new smallest root z_b^+ begins to decrease for a while, crosses the minimum $-\ln y_m$ and then increases continuously again (in blue) up to reach z_b^- for experiencing the same jump as before, and so on... The same scenario is observed for an oscillation of $y(\tau)$ around a positive mean value $\overline{y} > 0$ even if the amplitude is sufficiently small for $y(\tau) > 0\ \forall\tau$, so that the number of roots is finite without forbidden band, see the numerical solution of (8.30) in figure 3. The function $z_b(\tau)$ corresponding to the case investigated in figure 2 has a shape similar to the red curve in figure 3.

Causality is satisfied when the delay z_b increases during the deceleration range $\mathrm{d}y/\mathrm{d}\tau < 0$ since the calculation of $\mathrm{d}z_b/\mathrm{d}\tau$ leads to (9.1) with $\mathcal{A} = -y^{-1}\mathrm{d}y/\mathrm{d}\tau > 0$. During the short laps of time (after the jump) during which z_b is decreasing smoothly after the jump down to the minimum $-\ln y_m > 0$, the causality condition $\mathrm{d}z_b/\mathrm{d}\tau < 1$ is also verified since the acceleration $\mathrm{d}y/\mathrm{d}\tau > 0$ is small. It is worth noticing that the jumps of $z_b(\tau)$ not only avoid the forbidden band when they exist ($y(\tau - z_b) < 0$) but also eliminate the eventual non causal variation of $z_b(\tau)$ which would result from a sufficiently large acceleration of the lead shock $\mathrm{d}y(\tau - z_b)/\mathrm{d}\tau > 0$. The jump of the time delay $z_b(\tau)$ corresponds to two different values of the detonation thicknesses at two different moment in the past $\mathrm{e}^{-y(\tau - z_b^+)}$ and $\mathrm{e}^{-y(\tau - z_b^-)}$ while the detonation thickness $\mathrm{e}^{-y(\tau)}$ is a continuous function of time if the propagation velocity $y(\tau)$ is continuous. Moreover the time delay z_b increases but its jump becomes negligible when the amplitude of oscillation of $y(\tau)$ becomes small $-\ln y_m \gg \tau_p$, since, according to the geometrical construction, the order of magnitude of the time delay z_b and of its jump Δz_b is $-\ln y_m$ and τ_p respectively, $z_b = O(-\ln y_m)$, $\Delta z_b = O(\tau_p)$, $\Delta z_b \approx 3\tau_p/4$ in figure 2, $\lim_{y_m \to 0} \Delta z_p/z_b = 0$.

9.4. *Intrinsic dynamics of the inner structure and detonation decay*

The quasi-steady state approximation of (8.36) is obtained when the time delays $\zeta(\xi)$ and z_b of the upward-running mode are neglected, $G_1 = 0$ and $G_2 = y - \overline{y}_{_{CJ}}$. Neglecting also the unsteady term I_{h} coming from (7.7), the quasi-steady solution $y_{qs}(\tau) - \overline{y}_{_{CJ}} \approx \overline{m}_b^2(\tau)$,

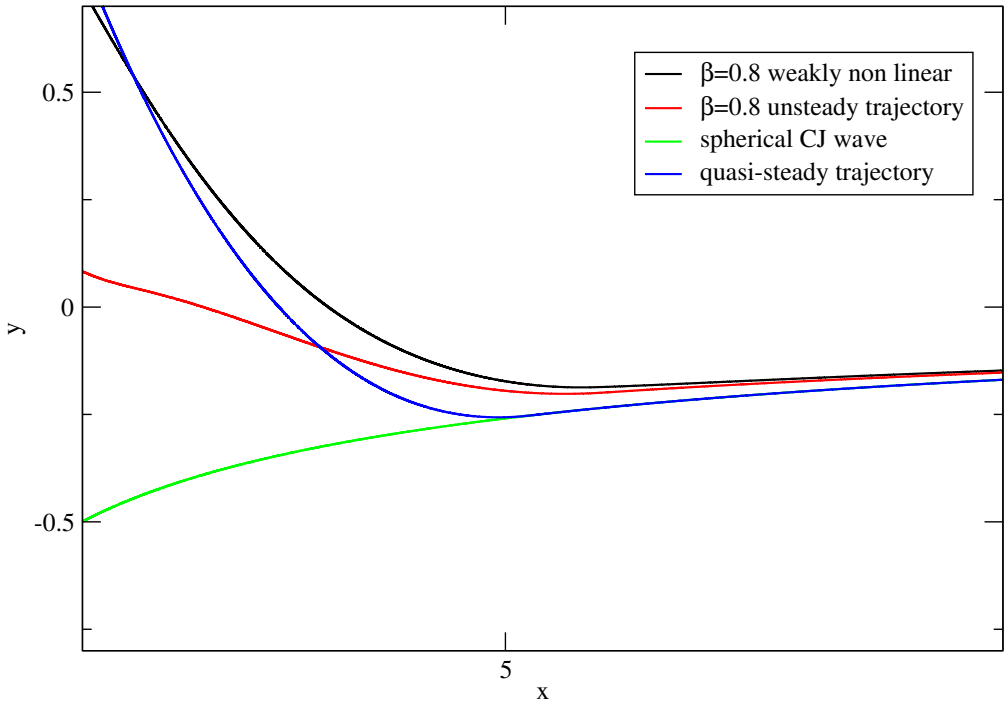

FIGURE 4. Decay in spherical geometry of a stable detonation. The trajectory corresponding to the solution of (9.6) with (8.37) is plotted in red for $\beta = 0.8$ with the reaction rate used in Clavin & Denet (2018), $\beta_c \approx 1.27$, and for $x_{i_{CJ}} = 5.1$ ($x_i = 2.8$, $\mu_{bi} = 0.6$), the trajectory being computed by using $\mathrm{d}x/\mathrm{d}\tau = 0.08$ ($b\lambda = 12$). The quasi-steady trajectory is plotted in blue and the trajectory of the weakly nonlinear version of (9.6) is plotted in black. In green is the peninsula of the quasi-steady CJ detonation

yields a trajectory tangent to the upper branch of the peninsula of the steady spherical solution $\overline{y}_{_{CJ}}(x)$.

The time delays $\zeta(\xi)$ in G_1 and G_2 control the intrinsic dynamics of the inner structure of the detonation wave. When $\overline{y}_{_{CJ}}(x)$ in $(b/2)G_1 + G_2$ is replaced by the unperturbed planar solution $\overline{y}_o$ corresponding to a constant flow of burnt gas $\mathrm{m}_b = \mathrm{cst} > 0$ and when the unsteady curvature term I_h is neglected, equation (8.36) describes the dynamic of a slightly overdriven detonation in planar geometry. Following the same method as in the text, the corresponding equation is obtained whatever b from the constitutive equations in § 2 (written in planar geometry) in the limit of small heat release (3.1). The total time delay $|z_b|$ (from the exit of the inner structure to the lead shock) is defined in a way similar to (8.30)

$$z_b = \mathrm{e}^{-\overline{y}_o} \int_{-\mathrm{e}^{-[y(\tau - z_b) - \overline{y}_o]}}^{0} \frac{\mathrm{d}\xi}{\overline{\mu}_o(\xi)} \tag{9.5}$$

where $\overline{\mu}_o(\xi)$ is the the flow (D 5) inside the inner structure of a overdriven detonation satisfying the condition in the burnt gas $\xi \leqslant -\mathrm{e}^{-\overline{y}_o} : \overline{\mu}_o = \sqrt{2/b}\,\mathrm{m}_b$. The steady state solution is $\overline{y}_o = \mathrm{m}_b^2 > 0$ and there is no divergence of the delay $\overline{z}_b$. For unstable detonations against longitudinal disturbances, equation (9.5) becomes multivalued introducing jumps of $z_b(\tau)$ if the acceleration $\mathrm{d}y/\mathrm{d}\tau > 0$ becomes sufficiently large during an oscillatory period of the propagation velocity $y(\tau)$, see figures 2 and 3.

Stability for a constant flow of burnt gas, $\mathrm{m}_b = \mathrm{cst} > 0$, is analyzed with the linear

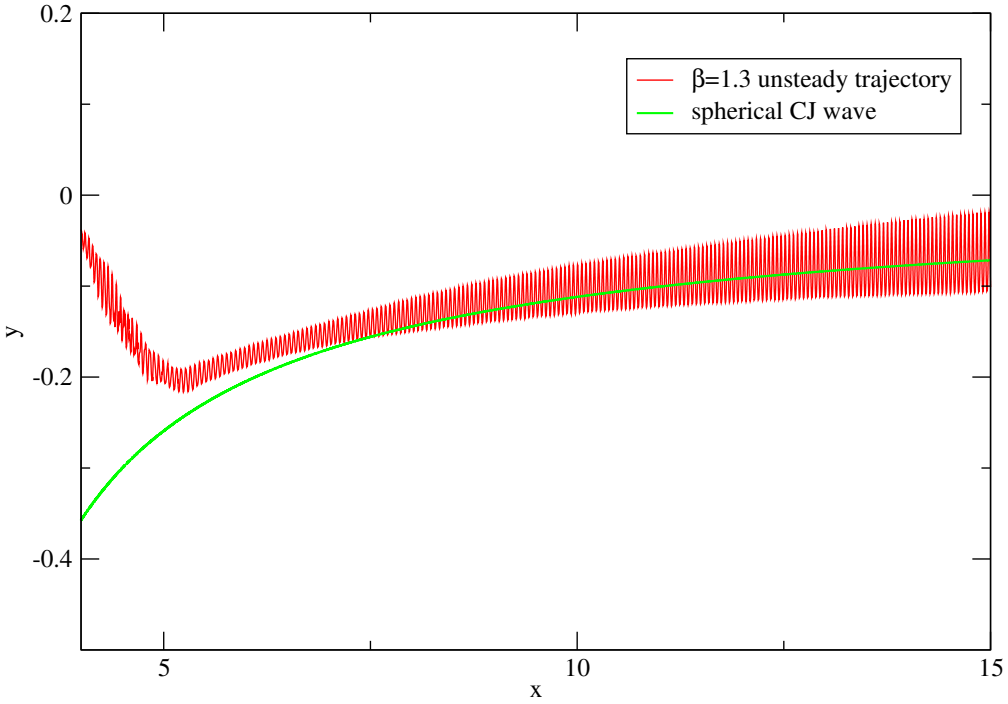

FIGURE 5. Decay in spherical geometry of a marginally unstable detonation. The pulsating solution of (9.6) with (8.37) is plotted in red for the same condition as in figure 4, except for $\beta = 1.3$, just above the instability threshold $\beta_c \approx 1.27$.

version of $(b/2)G_1 + G_2$ around $\overline{y}_o$. This leads to the integral equation (D 24) obtained by Clavin & Williams (2002) and recalled in appendix D.2. The disturbance of the lower bound of the integrals (8.33)-(8.34) yields a nonlinear contribution which is neglected in the linear approximation so that $-\mathrm{e}^{-y(\tau-z_b)}$ is replaced by $-\mathrm{e}^{-\overline{y}_o}$ which in turn can be replaced by $-\infty$ in (D 24) because the linear version (D 22) of the integrant is zero for $\xi \leqslant -\mathrm{e}^{-\overline{y}_o}$: $g_o(\xi) = 0$, see the text below (D 20) in appendix D.2. Notice also that the linear integral equation thus written is valid for a CJ wave with a reaction rate $\omega_{o_{CJ}}(\xi)$ decreasing smoothly to zero in the burnt gas, free from the assumption (3.17). Usually, the threshold of instability against longitudinal disturbances corresponds to a critical value b_c of b which is not large. For example, $b_c \approx 1.27$ for a CJ wave sustained by the same reaction rate as in Clavin & Denet (2018).

The above simplification of the lower bound of the integrals in G_1 and G_2 can also be used for the nonlinear dynamics of a weakly unstable detonation wave because the pulsations with small amplitude are mainly governed by the deformation of the distribution of heat release at distance from the lead shock significantly shorter than the detonation thickness. This is a good approximation when the variations of the distance of the maximum of heat release from the lead shock produce larger modifications of the integral than the variations near the end of the reaction where the reaction rate is small. Putting $-\infty$ in the lower bound of the integrals (8.33) and (8.34) (like in the linear analysis) leads to equations (D 25)-(D 26) that describe the intrinsic dynamics of weakly unstable detonations. In the unstable domain, the corresponding solution $y(\tau)$ becomes chaotic when b is increased beyond the instability threshold. What is a good approximation for the intrinsic dynamics of weakly unstable detonation is relevant neither for strongly unstable detonation nor for the unsteady response of the detonation wave to modifications of the

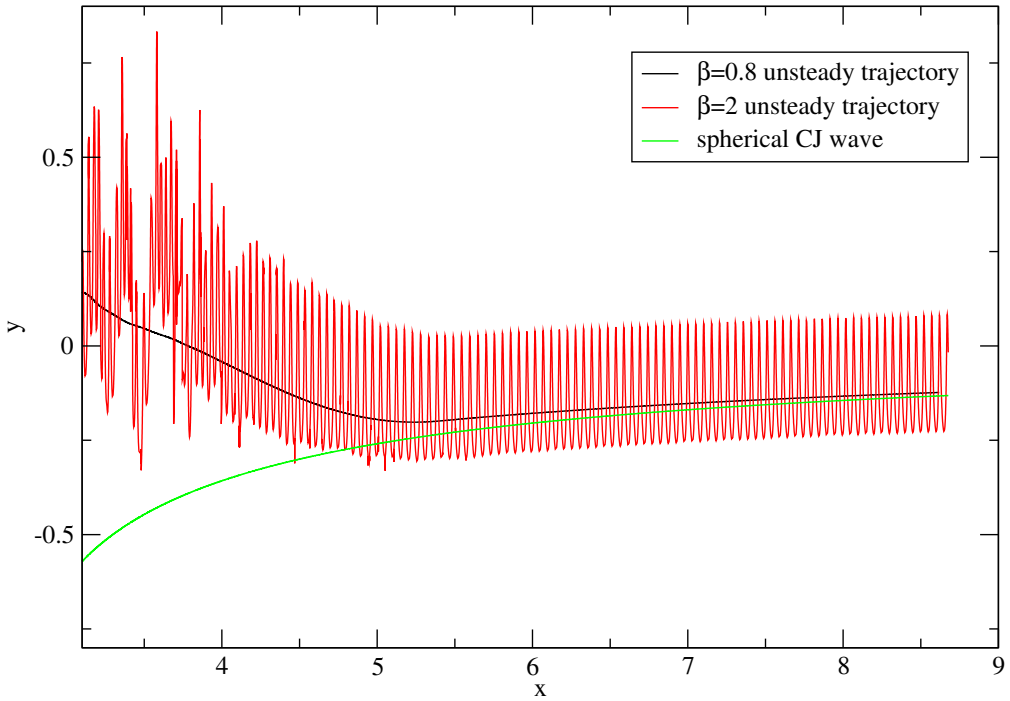

FIGURE 6. Decay in spherical geometry of a strongly unstable detonation. The pulsating solution of the weakly nonlinear version of (9.6) with (8.37) is plotted in red for the same condition as in figure 4, except for $\beta = 2$, above the instability threshold $\beta_c \approx 1.27$.

flow in the burnt gas. The total time delay $z_b(\tau)$ from the exit of the inner structure to the lead shock is a key mechanism in the rarefaction-wave-driven detonation decay. Not only z_b is non negligible in the forcing term $\mathrm{m}_b^2(\tau - z_b)$ when z_b is not sufficiently smaller than the time scale of the external flow but, also, the lower bound $-\mathrm{e}^{-y(\tau - z_b(\tau))}$ should be kept in the integrals (8.33)-(8.35), as shown by the comparison of the solutions of (8.36)-(8.37) with and without the lower bound replaced by $-\infty$, see figure 4.

9.5. *Extension to marginally stable or unstable CJ regimes*

For usual reaction rates, the double limit (4.14) $\epsilon \ll 1$ and $b \gg 1$ (small heat release and large activation energy) correspond to unstable detonations $b > b_c$ since b_c is not a large number for a typical reaction rate $\omega_{oCJ}(\xi)$. CJ detonations of usual gaseous mixtures are effectively unstable against longitudinal perturbations. However, the decay of a spherical detonation to a marginally stable (or unstable) CJ regime is instructive in many ways, for example by comparison with the existing direct numerical simulations and also with the steady-state approximation, including the discontinuous model used by Liñan *et al.* (2012). Also the erratic dynamics of strongly unstable detonations are avoided with marginally stable and unstable detonations. Working near the CJ regime, the asymptotic analysis in the limit (4.14) introduces the same non dimensional parameter of thermal sensitivity b for the quasi-steady curvature-induced quenching and for the intrinsic dynamics of the inner structure controlling the stability (and the response) of the detonation wave. For real detonations with a propagation Mach number sufficiently large (typically $\sqrt{q_m/c_pT_u} \approx 2$ and $M_{CJ}^2 \approx 16$), the two parameters are different even though the same physical mechanism, namely the thermal sensitivity of the reaction rate, is at the root of the two phenomena. In fact, the only parameter b left in (8.36) is the

one controlling the dynamics of the inner structure discussed in § 9.4. Then, equation (8.36) can be formally extended to the decay toward a marginally stable or unstable CJ wave by considering values of the parameter b in front of G_1 close to its marginal value b_c at the instability threshold, keeping the expression (4.12) with (4.20) for $\overline{y}_{_{CJ}}(x)$. Since typically b_c is not a large number while equations (4.12) and (4.20) are valid when corrections of order $1/b$ are neglected, the extended expression of (8.36) is not relevant near the critical radius x^* of curvature-induced quenching. Anyway, this region where the term $I_{\rm h}$ is large was already outside the validity domain of (8.36). Equation (8.36) thus modified yields relevant results away from the curvature quenching, namely for a radius sufficiently large compare to x^* in the intermediate range of CJ velocity where the curvature effect is non negligible but not strong enough for quenching $-1 < \overline{y}_{_{CJ}} < 0$. It is then convenient to re-write equation (8.36) by using a notation for the parameter of thermal sensitivity controlling the inner dynamics different from that involved in the curvature-induced quenching

$$2\big(y(\tau) - \overline{y}_{_{CJ}}\big) = \frac{\beta}{2} G_1 + G_2 + I_{\rm h} + {\rm m}_b^2(\tau - z_b), \tag{9.6}$$

where the functionals z_b, G_1, G_2, $I_{\rm h}$ are given in (8.30), (8.33)-(8.35) respectively and the function ${\rm m}_b(\tau)$ is defined in (8.37). The critical value of the parameter β at the instability threshold is called β_c in the following. The trajectory in the phase space (x - y) is obtained from the solution $y(\tau)$ of (9.6) by using the linear relation between x and τ in (6.11). For β close to β_c equation (9.6) constitutes a model for successful initiation of spherical detonations that are stable or marginally unstable against radial disturbances. The strongly unstable detonations in the asymptotic limit (4.14) are recovered for values of β sufficiently larger than β_c. A weakly nonlinear version of (9.6) is obtained when the lower bond of the integral in G_1, G_2 and $I_{\rm h}$ is replaced by $-\infty$, as discussed in § 9.4. This is an accurate approximation only at the very end of the decay of a stable or marginally unstable CJ detonation when $y(\tau)$ becomes very small. Comparison of the full solution of (9.6) with the solution of the weakly non linear version helps to clarify the importance of the different physical phenomena at work during the detonation decay.

9.6. *Numerical solutions of the integral equation. Unsteadiness*

A difficulty in the numerical analysis of integral equations comes from the fact that the past of the solution should be known. A relevant numerical solution is obtained if the memory effect of the initial condition is forgotten after a time lag relatively short. In the parameter space (x - y), initialization of the trajectories that are solution of (9.6) requires to proceed by iteration. For a given initial condition, $x_i > x^*$ and ${\rm m}_{bi}$ corresponding to a function ${\rm m}_b(\tau)$, namely for a given $\tau_{i_{CJ}}$ in (8.37), the initial value $y_i \equiv y(x_i)$ is part of the solution. The difficulty is overcome more easily for a stable detonation $\beta < \beta_c$ by using an iterative procedure. If the initial value of y is too far from $y(x_i)$, the numerical solution $y(x)$ of (9.6) shows large oscillations decreasing quickly to a quiet trajectory. The relevance of the solution is checked by extrapolating the quiet trajectory in the past for $x < x_i$ and staring again the numerical simulation. An example of the trajectory decaying to the upper branch of the CJ peninsula is presented in figure 4 where the solution of (9.6) with (8.37) is plotted in red for $\beta = 0.8$ with the reaction rate used in Clavin & Denet (2018), $\beta_c \approx 1.27$, and for $x_{i_{CJ}} = 5.1$ ($x_i = 2.8$, $\mu_{bi} = 0.6$), the trajectory being computed for ${\rm d}x/{\rm d}\tau = 0.08$ ($b\lambda = 12$). For comparison, the quasi-steady trajectory in blue in figure 4, obtained by neglecting the delays $\zeta(\xi)$ and z_b in (9.6), is effectively tangent to the CJ peninsula at $x = x_{i_{CJ}}$, as predicted in § 7.2. The comparison of the two trajectories enlightens the effect of unsteadiness produced by the time delays. Two main

informations are extracted from this comparison. Firstly, in contrast to the quasi-steady approximation, the transition to the CJ regime is not abrupt; a relatively long tail of the velocity decay is observed. However the trajectory is quite close to the CJ peninsula as soon as the radius is sufficiently large, for example et $x \approx 10$, while the difference with the planar CJ velocity is still consequent. This illustrates to what extend the quasi-steady CJ peninsula is an attractor of the trajectories. Secondly, far from the CJ peninsula in the early part of the decay, that is for $y(x)$ larger than $\overline{y}_{CJ}(x)$, the trajectory is never quasi-steady. The cause of this spectacular manifestation of unsteadiness is clearly shown by the comparison with the solution of the weakly nonlinear version of (9.6), namely when the lower bound of the integrals in G_1, G_2 and I_h are replaced by $-\infty$. The corresponding trajectory is plotted in black in figure 4, showing a quasi-steady behavior far away from the CJ peninsula, in contrast to the previous solution. This points out the drastic unsteady effect which is produced upon the detonation decay by the time delay from the exit of the inner structure to the lead shock (lower bound of the integrals) resulting from the upstream running mode.

Similar results illustrating unsteadiness during the decay of stable detonations are obtained when the curvature effect upon the inner structure is neglected, namely the solutions of (9.6) for $\overline{y}_{CJ} = 0$ and $I_\mathrm{h} = 0$.

The instantaneous trajectories of marginally unstable detonations characterized by a small amplitude of pulsation are obtained in a similar way. The result is plotted in figure 5 for the same conditions as in figure 4, except for $\beta = 1.3$ slightly large than $\beta_c = 1.27$. The frequency of pulsation is that predicted by the stability analysis at bifurcation, $\omega_c = 4.5$. The mean trajectory, averaged over a time window larger than the period of pulsation, is quite similar to the trajectory of the stable detonation shown by the red curve in figure 4 for $\beta = 0.8$.

Numerical solution of (9.6) is much more difficult for strongly unstable detonations. The solution becomes quickly chaotic above the instability threshold. Then it is practically impossible to guess a reasonably accurate past of the solution which is required to initiate a relevant calculation of the trajectory. Moreover the relative jumps of the time delay $\Delta z_b/z_b$ become sufficiently large to pollute the numerical solution of the trajectory from the beginning. This could also be the case in direct numerical simulation of the decay of strongly unstable detonations. Much work remains to be done on this topic. An illustration of the problem is shown in figure 6 for $\beta = 2$ when part of the difficulty is removed by using the weakly nonlinear version of (9.6). The initial trajectory is effectively chaotic but becomes regular some time later. Unfortunately, this is not the case when the lower bound $-\mathrm{e}^{-y(\tau - z_b)}$ is kept in the integrals G_1, G_2 and I_h in (9.6).

10. Conclusion and perspective

The theoretical analysis presented in this paper brought to light unsteadiness of the detonation decay during a successful direct initiation of a stable or weakly unstable detonation. The unsteady mechanism is clearly identified on the example of figure 4 as being the time delay z_b of the upstream running mode for propagating the rarefaction-wave-induced deceleration from the exit of the inner structure to the lead shock.

No definitive conclusion can be formulated for strongly unstable detonations. An intriguing new phenomenon associated with jumps of z_b during an oscillatory pulsation of the shock velocity is identified. This phenomenon which is related to causality has no noticeable effect on the dynamics of the lead shock for stable or marginally unstable detonations near to the instability threshold against longitudinal disturbances. However

it could play an important role in strongly unstable detonations. Much work remains to be done on this topic, including further direct numerical simulations.

The role of unsteadiness near criticality is an open question at the present stage of the analysis. Future works have to be devoted to answering the key question: to what extend unsteadiness modifies the quasi-steady curvature-induced quenching ? According to the existing direct numerical simulations, the order of magnitude of the critical radius is not modified from its quasi-steady value r^*. If this is the case, why and how ? In order to describe the dynamics of stable and marginally unstable detonations near the critical condition for initiation, the analysis should identify separately the parameters controlling the thermal sensibility of the curvature effect and of the intrinsic dynamics of the inner structure, and this right from the beginning. This parameter differentiation which has been done here on the integral equation for successful initiation (radius larger than r^*) cannot be made on the hyperbolic equation obtained in the double limit of small heat release and large activation energy. The basic idea of future analytical works is to keep the dynamics of the inner structure controlled by the upward running mode but with a heat release which is not small so that the propagation Mach number of the steady and planar detonation is not close to unity. The result thus obtained will be quantitatively accurate for real detonations since the dynamics of their inner structure is one of two timescales, more particularly close to the CJ regime.

Declaration of interests. The authors report no conflict of interest

Acknowledgements

Prof. Amable Liñan is acknowledged for stimulating and enlightening discussions. Partial financial support of *Agence National de la Recherche* (contract ANR-18-CE05-0030) is acknowledged.

Appendix A. Rarefaction wave behind a nearly sonic detonation

In this Appendix, the analysis of the rarefaction wave behind a spherical detonation treated as a discontinuity in the limit of small heat release is performed when the propagation velocity is just above the sound speed, $0 < M-1 \ll 1$, so that the flow velocity is small in the laboratory frame. The discontinuous model is valid if the radius is sufficiently large $r \gg at_r > at_{coll}/(M-1)$ so that the length scale of the burnt gas flow is still much larger than the detonation thickness, see the discussion in § 1.

The conditions behind a planar detonation in quasi-steady state takes the form

$$1-\frac{\rho_u}{\rho_b}=\frac{1}{\gamma+1}\frac{(M^2-1)}{M^2}\left[1+\sqrt{1-\left(\frac{M_{o_{CJ}}-M_{o_{CJ}}^{-1}}{M-M^{-1}}\right)^2}\right], \tag{A 1}$$

$$\frac{p_b}{p_u}-1=\gamma M^2\left(1-\frac{\rho_u}{\rho_b}\right), \qquad \frac{u_b}{a_u}=\left(1-\frac{\rho_u}{\rho_b}\right)M, \quad M_{o_{CJ}}-M_{o_{CJ}}^{-1}=2\sqrt{Q} \tag{A 2}$$

where $Q \propto q_m/c_pT_u$ see Clavin & Searby (2016). The square root is zero for the CJ regime corresponding to the sonic condition in the burnt gas $M=M_{o_{CJ}}$: $u_{bo_{CJ}}=\mathcal{D}_{o_{CJ}}-a_{bo_{CJ}}$ with $a_{bo_{CJ}}=\sqrt{\gamma p_{bo_{CJ}}/\rho_{bo_{CJ}}}$ and, according to the last equation in (A 2), the CJ Mach number is close to unity in the limit of small heat release, $0<(M_{o_{CJ}}-1)\ll 1$. For weakly overdriven regimes $0<(M-M_{o_{CJ}})/M_{o_{CJ}}\ll 1$ the square root in (A 1) is small and the propagation Mach number is also close to unity $0<(M-1)\ll 1$ so that the

flow velocity in the laboratory frame is small $u_b/a_u = O(M-1)$. Considering sufficiently small variations of the detonation velocity so that the variation of entropy in the burnt gas is negligible, the rarefaction wave in the burnt gas can be described by the linear version of the Euler equations

$$\frac{\partial(\rho-\overline{\rho}_b)/\overline{\rho}_b}{\partial t}+\nabla.\ \mathbf{u}=0, \qquad \frac{\partial\ \mathbf{u}}{\partial t}=-\frac{a^2}{\overline{\rho}_b}\nabla\rho, \tag{A 3}$$

where $(\rho-\overline{\rho}_b)/\overline{\rho}_b \ll 1$ with $\overline{\rho}_b$ and $a=a_b\approx a_u$ constant, the difference $(a_b-a_u)/a_u$ being of order $\epsilon^2\equiv(M-1)^2$. The linear approximation (A 3) is valid in the laboratory frame despite the sonic condition of the burnt gas flow relative to the detonation front in the CJ regime $(\mathcal{D}_{o_{CJ}}-u_{bo_{CJ}})=a$. In the limit of small heat release the rarefaction wave behind a weakly overdriven detonation-front is a spherical acoustic wave.

A.1. *Spherical acoustic wave*

Introducing the potential φ, equations (A 3) yield

$$\frac{(\rho-\overline{\rho}_b)}{\overline{\rho}_b}=\frac{\partial\varphi}{\partial t}, \qquad \mathbf{u}=-a^2\nabla\varphi, \qquad \frac{\partial^2\varphi}{\partial t^2}-a^2\Delta\varphi=0, \tag{A 4}$$

where $\Delta\varphi=\frac{1}{r^2}\frac{\partial}{\partial r}\left(r^2\frac{\partial\varphi}{\partial r}\right)$ in spherical geometry. Introducing the function $f(r,t)$, and looking for the solution in the form $\varphi=f/r$,

$$\frac{\partial^2 f}{\partial t^2}-a^2\frac{\partial^2 f}{\partial r^2}=0, \tag{A 5}$$

the flow expressed in terms of the non-dimensional the transit time $\mathrm{r}\equiv r/a$ is

$$\varphi=\frac{f_1(t-\mathrm{r})+f_2(t+\mathrm{r})}{\mathrm{r}} \quad\Rightarrow\quad \frac{(\rho-\overline{\rho}_b)}{\overline{\rho}_b}=\frac{f_1'(t-\mathrm{r})+f_2'(t+\mathrm{r})}{\mathrm{r}} \tag{A 6}$$

$$\frac{u(\mathrm{r},t)}{a}=\frac{f_1'(t-\mathrm{r})-f_2'(t+\mathrm{r})}{\mathrm{r}}+\frac{f_1(t-\mathrm{r})+f_2(t+\mathrm{r})}{\mathrm{r}^2}, \tag{A 7}$$

where $f_1'(\eta)$ and $f_2'(\eta)$ denote the derivative of $f_1(\eta)$ and $f_2(\eta)$, $f_1'(\eta)\equiv \mathrm{d}f_1(\eta)/\mathrm{d}\eta$, $f_2'(\eta)\equiv \mathrm{d}f_2(\eta)/\mathrm{d}\eta$, the unknown functions $f_1(\eta)$ and $f_2(\eta)$ being determined by the boundary conditions.

Denoting $u_b(t)$ and $\rho_b(t)$ the flow velocity and the density at the lead front $r=r_f(t)$ propagating with the velocity $\mathcal{D}(t)=\mathrm{d}r_f/\mathrm{d}t$, $M(t)=\mathcal{D}(t)/a$, and introducing the notations $\mathrm{r}_f(t)=r_f(t)/a$, $\mathrm{d}r_f/\mathrm{d}t=M(t)$ and

$$F_1(t)\equiv f_1\big(t-\mathrm{r}_f(t)\big), \qquad \dot{F}_1(t)\equiv \mathrm{d}F_1/\mathrm{d}t=[1-M(t)]\,f_1'\big(t-\mathrm{r}_f(t)\big), \tag{A 8}$$

$$F_2(t)\equiv f_2\big(t+\mathrm{r}_f(t)\big), \qquad \dot{F}_2(t)\equiv \mathrm{d}F_2/\mathrm{d}t=[1+M(t)]\,f_2'\big(t+\mathrm{r}_f(t)\big), \tag{A 9}$$

the boundary conditions at the front take the form

$$\frac{1}{\mathrm{r}_f(t)}\left[\frac{\dot{F}_1(t)}{1-M(t)}+\frac{\dot{F}_2(t)}{1+M(t)}\right]=\frac{\delta\rho_b(t)}{\overline{\rho}_b}\equiv\frac{\big(\rho_b(t)-\overline{\rho}_b\big)}{\overline{\rho}_b} \tag{A 10}$$

$$\frac{1}{\mathrm{r}_f(t)}\left[\frac{\dot{F}_1(t)}{1-M(t)}-\frac{\dot{F}_2(t)}{1+M(t)}\right]+\frac{F_1(t)+F_2(t)}{\mathrm{r}_f^2(t)}=\frac{u_b(t)}{a} \tag{A 11}$$

where ρ_b and u_b/a are expressed in terms of the propagation Mach number $M(t)$ through (A 1)-(A 2). In a rarefaction wave the radial velocity $u(r,t)>0$ is an increasing function of the radius r and there is a spherical core of gas at rest spreading behind the detonation

front with a radius $r_0(t)$ increasing with the time at the local sound speed $\mathrm{d}r_0/\mathrm{d}t = a < \mathcal{D}$ ($\mathrm{d}r_o/\mathrm{d}t = 1$). In other words the point at which the flow vanishes $u\big(r_0(t),t\big) = 0$ is a weak discontinuity,

$$r \leqslant r_0(t) < r_f(t) : u(r,t) = 0, \quad r > r_0(t) : u(r,t) > 0, \qquad \mathrm{d}r_0/\mathrm{d}t = a. \tag{A 12}$$

A.2. *Rarefaction wave of spherical CJ detonation for small heat release*

Neglecting the modification of the inner structure (discontinuous model), a spherical CJ detonation propagates with the constant velocity of the planar wave in steady state $\mathcal{D} = \mathcal{D}_{oCJ}$ (constant Mach number $M = M_{o_{CJ}} \equiv \mathcal{D}_{o_{CJ}}/a > 1$),

$$r_{fo_{CJ}}(t) = \mathcal{D}_{o_{CJ}}\, t + r_{foi}, \quad \mathrm{r}_{fo_{CJ}}(t) = M_{o_{CJ}} t + \mathrm{r}_{fi}, \quad \mathrm{r}_{foi} = \mathrm{cst}, \tag{A 13}$$

where the constant r_{foi} is introduced for later purpose, the validity of the linear solution being limited to large radius, $\mathrm{r}_{foi} \gg 1$, and the time of order unity $t = O(1)$. The right-hand sides of (A 10) and (A 11) are constant with, according to (A 1)-(A 2),

$$1 - \frac{\rho_u}{\rho_{bo_{CJ}}} = \frac{1}{M_{o_{CJ}}}\frac{u_{bo_{CJ}}}{a}, \qquad \frac{u_{bo_{CJ}}}{a} = \frac{1}{\gamma+1}\frac{(M_{o_{CJ}}^2-1)}{M_{o_{CJ}}} > 0. \tag{A 14}$$

Taking $\overline{\rho}_b = \rho_{bo_{CJ}}$ the right-hand side of (A 10) is zero

$$\big(\rho_b(t) - \overline{\rho}_b\big)/\overline{\rho}_b = 0. \tag{A 15}$$

For small heat release $\epsilon \equiv (M_{o_{CJ}} - 1) \ll 1$, according to (A 14), $u_b/a_u \ll 1$, the flow field is small so that the linear approximation is accurate. The rarefaction wave of the CJ detonation is obtained from (A 7) by the solution of (A 10)-(A 11) for (A 14)-(A 15)

$$\frac{u(\mathrm{r},t)}{u_{bo_{CJ}}} = \left[1 - \frac{1}{M_{o_{CJ}}^2 - 1}\left(\frac{\mathrm{r}_{fo_{CJ}}^2(t)}{\mathrm{r}^2} - 1\right)\right], \quad \mathrm{r}_{fo_{CJ}} \equiv M_{o_{CJ}}\, t + \mathrm{r}_{foi} \tag{A 16}$$

$$\frac{\rho(\mathrm{r},t) - \rho_{bo_{CJ}}}{\rho_{bo_{CJ}}} = -2\frac{M_{o_{CJ}}}{M_{o_{CJ}}^2 - 1}\left[\frac{\mathrm{r}_{fo_{CJ}}(t)}{\mathrm{r}} - 1\right] \tag{A 17}$$

where, according to (A 14), $u_{bo_{CJ}}/a = \epsilon[1/(\gamma+1)](M_{o_{CJ}}+1)/M_{o_{CJ}} \approx \epsilon$. The solution (A 16)-(A 17) to the system of linear equations (A 10)-(A 11) is obtained without using explicitly the condition $\epsilon \ll 1$, see the details of the calculation at the end of the subsection. The sonic condition (A 12) is automatically satisfied by (A 16)

$$(M_{o_{CJ}}\, t + \mathrm{r}_{foi})/\mathrm{r}_0 = M_{o_{CJ}} \qquad \Rightarrow \qquad \mathrm{d}r_0/\mathrm{d}t = a. \tag{A 18}$$

This corresponds to a thickness of the rarefaction wave which is relatively small and increases linearly with the time,

$$\frac{r_{fo_{CJ}} - r_0}{r_{fo_{CJ}}} = O(\epsilon), \quad \frac{r_{fo_{CJ}} - r}{r_{fo_{CJ}}} = O(\epsilon), \quad \frac{1}{a}\frac{\mathrm{d}(r_{fo_{CJ}} - r_0)}{\mathrm{d}t} = O(\epsilon). \tag{A 19}$$

The rarefaction wave (A 16)-(A 17) is different from the self-similar solution of Zeldovich (1942)-Taylor (1950*a*) in the limit $M_{o_{CJ}} \gg 1$ for which the nonlinear terms are essential. According to (A 16) and $u_{bo_{CJ}}/a \approx \epsilon$, the condition for the validity of the linear analysis $u\partial u/\partial r \ll \partial u/\partial t$ is satisfied throughout the rarefaction wave in the limit $\epsilon \ll 1$,

$$\frac{1}{u_{bo_{CJ}}}\frac{\partial u}{\partial \mathrm{r}}\Big|_{\mathrm{r}=\mathrm{r}_{fo_{CJ}}} = -\frac{1}{u_{bo_{CJ}}}\frac{\partial u}{\partial t}\Big|_{\mathrm{r}=\mathrm{r}_{fo_{CJ}}} = \frac{1}{\epsilon}\frac{1}{\mathrm{r}_{fo_{CJ}}}\left[1 + O(\epsilon)\right] \tag{A 20}$$

and the gradient of the velocity profile at the detonation front is finite $\partial u/\partial r|_{\mathrm{r}=\mathrm{r}_{fo_{CJ}}} \approx 1/r_{fo_{CJ}}$ while it is infinite in the self-similar solution of Zeldovich (1942)-Taylor (1950*a*).

For consistency with the assumption of an unperturbed inner structure, the radius must be sufficiently larger than the detonation thickness. More precisely, according to (A 20), one must have $r_{fo_{CJ}}/(a_u t_r) \gg 1/\epsilon$. Moreover, according to (A 19), unlike the self-similar solution for $M_{o_{CJ}} \gg 1$, the relative thickness of the rarefaction wave is small for $M_{o_{CJ}} - 1 \ll 1$, while it is of order unity in Zeldovich (1942) and Taylor (1950*a*).

The calculation leading to (A 16)-(A 17) is straightforward and proceeds as follows. Using (A 12) and (A 15) equation (A 10) is easily integrated

$$\frac{F_1(t)}{1-M} + \frac{F_2(t)}{1+M} = A' \quad \Rightarrow \quad F_2 = -\frac{1+M}{1-M} F_1 + (1+M)A' \tag{A 21}$$

where A' is a constant. In order to save the notation the subscript o_{CJ} has been omitted in $M_{o_{CJ}}$ which is replaced by M in (A 21). Adding (A 10) and (A 11) yields a differential equation for $F_1(t)$ when $F_2(t)$ is eliminated by using (A 21)

$$(t + \mathrm{r}_{foi}/M)\,\dot{F}_1 - F_1 = -A + (t + \mathrm{r}_{foi}/M)^2\,(u_b/a)(1-M)M/2 \tag{A 22}$$

where $A = (1-M^2)A'/(2M)$ is constant. Equation (A 22) is easily integrated

$$F_1(t) = A + (t + \mathrm{r}_{fi}/M)\,B + (t + \mathrm{r}_{fi}/M)^2\,(u_b/a)(1-M)M/2, \tag{A 23}$$

where B is another constant and $F_2(t)$ is obtained from (A 21). According to (A 8)-(A 9), $f_1(t-\mathrm{r})$ and $f_2(t+\mathrm{r})$ are obtained from $F_1(t)$ and $F_2(t)$ by the substitution $t \to [(t-\mathrm{r}) + \mathrm{r}_{fi}]/(1-M)$ and $t \to [(t+\mathrm{r}) + \mathrm{r}_{fi}]/(1+M)$ respectively,

$$f_1(t-\mathrm{r}) = A + \frac{B}{1-M}\left[(t-\mathrm{r}) + \frac{\mathrm{r}_{fi}}{M}\right] + (u_b/a)\frac{M/2}{1-M}\left[(t-\mathrm{r}) + \frac{\mathrm{r}_{fi}}{M}\right]^2 \tag{A 24}$$

$$f_2(t+\mathrm{r}) = -A - \frac{B}{1-M}\left[(t+\mathrm{r}) + \frac{\mathrm{r}_{fi}}{M}\right] - (u_b/a)\frac{M/2}{1+M}\left[(t+\mathrm{r}) + \frac{\mathrm{r}_{fi}}{M}\right]^2 \tag{A 25}$$

The constants A and B disappear from (A 7) leading to (A 16).

A.3. *End of the decay*

The end of the decay of a spherical detonation considered as a discontinuity in the limit of small heat release is analyzed close to the CJ regime

$$\dot{\alpha}_\tau \equiv \frac{\mathcal{D}(t) - \mathcal{D}_{o_{CJ}}}{\epsilon\, a} \ll 1, \quad M = 1 + \epsilon(1 + \dot{\alpha}_\tau) \quad \text{where} \quad \epsilon \equiv M_{o_{CJ}} - 1 \ll 1. \tag{A 26}$$

According to (A 1)-(A 2), the leading order of the relative modifications of the flow at the detonation front is small of order $\sqrt{\dot{\alpha}_\tau}$

$$\frac{u_b}{a} \approx \frac{u_{bo_{CJ}}}{a}\left[1 + \sqrt{2\dot{\alpha}_\tau} + \dot{\alpha}_\tau + ..\right], \quad \frac{\rho_b - \rho_{bo_{CJ}}}{\rho_{bo_{CJ}}} \approx \frac{u_{bo_{CJ}}}{a}[\sqrt{2\dot{\alpha}_\tau} + \dot{\alpha}_\tau + ..], \tag{A 27}$$

so that, to leading order in the limit $\sqrt{\dot{\alpha}_\tau} \ll 1$, one has

$$\frac{(\rho_b - \rho_{bo_{CJ}})}{\rho_{bo_{CJ}}} \approx \frac{(u_b - u_{bo_{CJ}})}{u_{bo_{CJ}}} \approx \sqrt{2\dot{\alpha}_\tau}. \tag{A 28}$$

A perturbation analysis is then performed for $\sqrt{\dot{\alpha}_\tau}$ small. In order to insure that the terms of order ϵ^2 are still negligible in the expression of $u/a = O(\epsilon)$, the ordering $\sqrt{\dot{\alpha}_\tau} < \epsilon$ is assumed so that the variation of entropy is negligible to leading order in the limit $\sqrt{\dot{\alpha}_\tau} \ll 1$. In a way reminiscent of the planar case studied in Clavin & Denet (2018), the key simplification in the limit $\sqrt{\dot{\alpha}_\tau} \ll 1$ is that the leading order of the rarefaction

wave is the same as in the CJ wave, extrapolated to values of r larger than $r_{fo_{CJ}}$ but sufficiently close to $r_{fo_{CJ}}$ such that the following ordering is satisfied

$$\frac{(\rho(r,t)-\rho_{bo_{CJ}})}{\rho_{bo_{CJ}}} \approx \frac{(u(r,t)-u_{bo_{CJ}})}{u_{bo_{CJ}}} = O(\sqrt{2\dot{\alpha}_\tau}). \tag{A 29}$$

According to (A 16)-(A 17), the relations in (A 29) are valid on a distance from $\mathrm{r}_{fo_{CJ}}(t)$ smaller than the thickness of the rarefaction wave of the CJ detonation by a factor $\sqrt{2\dot{\alpha}_\tau}$,

$$r > r_{fo_{CJ}}(t), \qquad 1 - r_{fo_{CJ}}/r = O(\epsilon\sqrt{2\dot{\alpha}_\tau}). \tag{A 30}$$

Then, using (A 26) in the form $\mathrm{d}(\mathrm{r}_f - \mathrm{r}_{fo_{CJ}})/\mathrm{d}t = \epsilon\dot{\alpha}_\tau$, an ordinary differential equation for the front position $\mathrm{r}_f(t)$ is obtained by combining (A 28) with the expression (A 16) for the flow velocity at the front $(u_b/u_{bo_{CJ}} - 1) \approx (\mathrm{r}_f/\mathrm{r}_{fo_{CJ}} - 1)/\epsilon$

$$0 < (\mathrm{r}_f - \mathrm{r}_{fo_{CJ}})/\mathrm{r}_{fo_{CJ}} \ll 1 : \qquad \sqrt{2\frac{\mathrm{d}(\mathrm{r}_f - \mathrm{r}_{fo_{CJ}})}{\mathrm{d}t}} = \frac{1}{\sqrt{\epsilon}}\left(\frac{\mathrm{r}_f - \mathrm{r}_{fo_{CJ}}}{\mathrm{r}_{fo_{CJ}}}\right) \tag{A 31}$$

where the approximation $[1-(r_{fo_{CJ}}/\mathrm{r}_f)^2] \approx 2[(\mathrm{r}_f/\mathrm{r}_{fo_{CJ}}) - 1] \ll 1$ has been used. Using the expression (A 16) for $\mathrm{r}_{fo_{CJ}}(t)$, equation (A 31) is easily integrated for a given initial condition $r_f(0) \equiv r_{fi} > r_{foi}$,

$$t = 0 : r_f = r_{fi} > r_{foi} \Rightarrow \frac{1}{\mathrm{r}_f(t) - \mathrm{r}_{fo_{CJ}}(t)} = \frac{1}{\mathrm{r}_{fi} - \mathrm{r}_{foi}} - \frac{1}{2\epsilon\,\mathrm{r}_{foi}}\left[1 + \frac{\mathrm{r}_{foi}}{t}\right]^{-1} \tag{A 32}$$

where ϵ has been neglected in front of 1. In order to satisfy the condition $(\mathrm{r}_f - \mathrm{r}_{fo_{CJ}}) > 0$ $\forall t > 0$ as it should be in (A 31), equation (A 32) is valid for initial positions r_{fi} such that

$$(\mathrm{r}_{fi}/\mathrm{r}_{foi} - 1) < 2\epsilon \qquad \Leftrightarrow \qquad R_i \equiv [2\epsilon\,\mathrm{r}_{foi}/(\mathrm{r}_{fi} - \mathrm{r}_{foi}) - 1] > 0. \tag{A 33}$$

This corresponds to an initial distance of the detonation front from the stagnant core (gas at rest) samller than $r_0(0) = \mathrm{r}_{foi}/(1+\epsilon)$ by a factor 3ϵ, $(\mathrm{r}_{fi}/\mathrm{r}_0(0) - 1) < 3\epsilon$. The derivative with respect to time of (A 32) in the long time limit

$$(\mathrm{r}_{fi}/\mathrm{r}_{foi} - 1) < 2\epsilon, \qquad t \gg \mathrm{r}_{foi} : \quad M - M_{o_{CJ}} \approx \frac{2}{R_i^2}\epsilon\left(\frac{\mathrm{r}_{foi}}{t}\right)^2 \tag{A 34}$$

shows that the propagation velocity decreases toward the CJ velocity like the inverse of the time squared. Such an asymptotic behavior for small heat release $(M_{o_{CJ}} - 1) \ll 1$ is similar to the planar case, so that the curvature of the flow does not play a significant role in the long time limit of the linear solution, at least for an initial condition satisfying (A 32). Nothing can be said when the initial radius of the detonation front r_{fi} reaches its limiting value in (A 33) $(\mathrm{r}_{fi}/\mathrm{r}_{foi} - 1) = 2\epsilon$ because of the divergence of the coefficient $1/R_i^2$ in (A 34). The long-time behavior (A 34) is quite different from the direct initiation of ordinary detonations for which the CJ velocity is reached at finite time and finite radius with an abrupt transition to the self-sustained regime, see the discussion in the last paragraph of § 6.1.

Appendix B. Technical details

B.1. *Calculation in § 7*

Denoting $(x_o,\, y_o)$ the coordinates of the intersection of the steady-state trajector with the curve $y = -\ln x$, equation (7.1) yields

$$\sqrt{\overline{y}(x) + \mathrm{e}^{-\overline{y}(x)}/x} - \sqrt{y_o + \mathrm{e}^{-y_o}/x_o} = -\sqrt{b/2}\ln(x/x_o). \tag{B 1}$$

Expanding the first term in the left hand side around (x_o, y_o) yields

$$\overline{y} + \frac{\mathrm{e}^{-\overline{y}}}{x} = y_o + (\overline{y} - y_o) + \frac{\mathrm{e}^{-y_o}}{x_o}\left[1 - \frac{(x - x_o)}{x_o} + ..\right]\left[1 - (\overline{y} - y_o) + \frac{1}{2}(\overline{y} - y_o)^2 + ..\right] \quad (B\,2)$$

Using the relation $e^{-y_o}/x_o = 1$ the linear terms $(y - y_o)$ cancel and anticipating that the term $(x - x_o)(\overline{y} - y_o)$ is smaller than $(\overline{y} - y_o)^2$ one gets

$$\overline{y} + \frac{\mathrm{e}^{-\overline{y}}}{x} = y_o + \frac{e^{-y_o}}{x_o} + \left[-\frac{(x - x_o)}{x_o} + \frac{1}{2}(\overline{y} - y_o)^2 + ..\right]. \quad (B\,3)$$

Equation (B 1) then yields

$$y_o \neq -1,\ y_o + 1 > 0: \quad \frac{(\overline{y} - y_o)^2/2 - (x - x_o)/x_o}{2\sqrt{y_o + 1}} \approx -\sqrt{b/2}\frac{(x - x_o)}{x_o}, \quad (B\,4)$$

$$2(y_o + 1)\sqrt{b/2} \gg 1 \ \Rightarrow\ \frac{(x - x_o)}{x_o} \approx -\frac{(\overline{y} - y_o)^2}{4\sqrt{b/2}\sqrt{y_o + 1}} \quad (B\,5)$$

describing a turning point of the trajectory at $(x_o,\, y_o)$ as shown figure 1.

The expansion (B 3) is no longer valid at the critical point. For $x_o = \mathrm{e}$, $y_o + 1 = 0$, $\sqrt{y_o + \mathrm{e}^{-y_o}/x_o} = 0$, equation (B 1)

$$\sqrt{\overline{y} + \frac{\mathrm{e}^{-\overline{y}}}{x}} = \left[\frac{(\mathrm{e} - x)}{\mathrm{e}} - \frac{(\mathrm{e} - x)}{\mathrm{e}}(\overline{y} + 1) + \frac{1}{2}(\overline{y} + 1)^2 + ..\right]^{1/2} \approx \sqrt{b/2}\frac{(\mathrm{e} - x)}{\mathrm{e}}, \quad (B\,6)$$

$$\frac{(\mathrm{e} - x)}{\mathrm{e}} - \frac{(\mathrm{e} - x)}{\mathrm{e}}(y + 1) + \frac{1}{2}(y + 1)^2 + .. \approx \frac{b}{2}\left[\frac{(\mathrm{e} - x)}{\mathrm{e}}\right]^2, \quad (B\,7)$$

showing that there is a small neighborhood of the critical point for $x < \mathrm{e}$, $(\mathrm{e} - x)/\mathrm{e} = O(1/\sqrt{b})$, $(y+1)^2 \approx b[(\mathrm{e} - x)/\mathrm{e}]^2$ in which the trajectory $\overline{y}(x)$ is linear with a large slope

$$b \gg 1,\ (\mathrm{e} - x)/\mathrm{e} = O(1/\sqrt{b}): \quad \lim_{(x-\mathrm{e})\to 0^-} |\overline{y} + 1| = \sqrt{b}(\mathrm{e} - x)/\mathrm{e},\ \left[\frac{\mathrm{d}\overline{y}}{\mathrm{d}x}\right]_{\overline{y}+1=0^-}^{\overline{y}+1=0^+} = -\frac{2\sqrt{b}}{\mathrm{e}} \quad (B\,8)$$

Consider now a quasi-steady trajectory intersecting the upper branch of the CJ peninsula. According to (7.1) and $\mathrm{m}_{bi} = \sqrt{y_i + \mathrm{e}^{-y_i}/x_i}$ and

$$\sqrt{\overline{y}(x) + \mathrm{e}^{-\overline{y}(x)}/x} - \sqrt{y_i + \mathrm{e}^{-y_i}/x_i} = -\sqrt{b/2}\ln(x/x_i), \quad (B\,9)$$

$$\overline{y}_{_{CJ}}(x_{_{CJ}}) + \mathrm{e}^{-\overline{y}_{_{CJ}}(x_{_{CJ}})}/x_{_{CJ}} = 0 \quad \Rightarrow \quad -\sqrt{y_i + \mathrm{e}^{-y_i}/x_i} = -\sqrt{b/2}\ln(x_{_{CJ}}/x_i). \quad (B\,10)$$

This leads to (7.2) which can be written for $(x_{_{CJ}} - x)/x_{_{CJ}} \ll 1$ in the form

$$\sqrt{\overline{y}(x) + \mathrm{e}^{-\overline{y}(x)}/x} = \sqrt{b/2}(x_{_{CJ}} - x)/x_{_{CJ}}. \quad (B\,11)$$

According to the equation of the CJ peninsula, $\overline{y}_{_{CJ}}(x) + \mathrm{e}^{-\overline{y}_{_{CJ}}(x)}/x = 0$, equation (B 11) can be written in the form

$$\sqrt{\overline{y}(x) - \overline{y}_{_{CJ}}(x) + \mathrm{e}^{-\overline{y}(x)}/x - \mathrm{e}^{-\overline{y}_{_{CJ}}(x)}/x} = \sqrt{b/2}(x_{_{CJ}} - x)/x_{_{CJ}}, \quad (B\,12)$$

$$\overline{y}(x) - \overline{y}_{_{CJ}}(x) + \mathrm{e}^{-\overline{y}(x)}/x - \mathrm{e}^{-\overline{y}_{_{CJ}}(x)}/x = b/2(x_{_{CJ}} - x)^2/x_{_{CJ}}^2. \quad (B\,13)$$

Expanding $\mathrm{e}^{-\overline{y}(x)}$ around $\mathrm{e}^{-\overline{y}_{CJ}(x)}$ yields

$$\overline{y}-\overline{y}_{CJ}+\frac{\mathrm{e}^{-\overline{y}_{CJ}(x)}}{x}[1+(\overline{y}_{CJ}-\overline{y})]-\frac{\mathrm{e}^{-\overline{y}_{CJ}(x)}}{x}=b/2\frac{(x_{CJ}-x)^2}{x_{CJ}^2}, \tag{B 14}$$

$$\overline{y}(x)-\overline{y}_{CJ}(x)+\frac{\mathrm{e}^{-\overline{y}_{CJ}(x)}}{x}\left[\overline{y}_{CJ}(x)-\overline{y}(x)\right]=b/2\frac{(x_{CJ}-x)^2}{x_{CJ}^2}. \tag{B 15}$$

which can also be written, using again $\mathrm{e}^{-\overline{y}_{CJ}(x)}/x=-\overline{y}_{CJ}(x)$,

$$\overline{y}(x)-\overline{y}_{CJ}(x)-y_{CJ}(x)\left[\overline{y}_{CJ}(x)-\overline{y}(x)\right]=b/2\frac{(x_{CJ}-x)^2}{x_{CJ}^2}, \tag{B 16}$$

$$\left[\overline{y}(x)-\overline{y}_{CJ}(x)\right]\left[1+\overline{y}_{CJ}(x)\right]=b/2\frac{(x_{CJ}-x)^2}{x_{CJ}^2}. \tag{B 17}$$

For an intersection point sufficiently far from the critical point $x_{CJ}>\mathrm{e}$, $1+y_{CJ}(x_{CJ})>0$, the derivative $\mathrm{d}\overline{y}_{CJ}/\mathrm{d}x$ is finite, $\overline{y}_{CJ}(x)\approx\overline{y}_{CJ}(x_{CJ})+(x-x_{CJ})\mathrm{d}\overline{y}_{CJ}/\mathrm{d}x|_{x_{CJ}}$ and (B 17) leads to (7.3) valid for

$$0<(x-x_{CJ})\ll-\overline{y}_{CJ}(x_{CJ})[\mathrm{d}\overline{y}_{CJ}/\mathrm{d}x|_{x_{CJ}}]^{-1}=\left[1+\overline{y}_{CJ}(x_{CJ})\right]x_{CJ}. \tag{B 18}$$

B.2. *Calculation in § 8.1*

Sufficiently above the CJ peninsula such that $\mu_{oCJ}(-\mathrm{e}^{(\overline{y}_{CJ}-y)})=O(1)$, the zeroth-order of the steady version of (8.11)-(8.12) takes the form

$$\frac{\partial}{\partial\xi}\left[\mu_{oCJ}(\xi\mathrm{e}^{\overline{y}_{CJ}})\mu_{1,0}+\frac{\mu_{1,0}^2}{2}\right]=\frac{1}{2}\left[\mathrm{e}^{y}\omega_{oCJ}(\xi\,\mathrm{e}^{y})-\mathrm{e}^{\overline{y}_{CJ}}\omega_{oCJ}(\xi\,\mathrm{e}^{\overline{y}_{CJ}})\right], \tag{B 19}$$

$$\xi=0:\quad \mu_{1,0}=0;\qquad \xi=-\mathrm{e}^{-y}:\quad \mu_{1,0}=-\mu_{oCJ}(-\mathrm{e}^{(\overline{y}_{CJ}-y)}). \tag{B 20}$$

and the solution is

$$0<(y-\overline{y}_{CJ})=O(1)\quad\Rightarrow\quad \mu_{1,0}(\xi,\tau)=\mu_{oCJ}(\xi\mathrm{e}^{y(\tau)})-\mu_{oCJ}(\xi\,\mathrm{e}^{\overline{y}_{CJ}(x)}), \tag{B 21}$$

as it is verified by introducing (B 21) into the left-end side of (B 19) and by performing a spatial integration from $\xi=-\mathrm{e}^{-y}$ where $\mu_{1,0}=-\mu_{oCJ}(-\mathrm{e}^{-(y-\overline{y}_{CJ})})$ since $\mu_{oCJ}(\xi\mathrm{e}^{y})=0$

$$\mu_{oCJ}(\xi\mathrm{e}^{\overline{y}_{CJ}})\mu_{1,0}+\frac{\mu_{1,0}^2}{2}+\frac{\mu_{oCJ}^2(-\mathrm{e}^{-(y-\overline{y}_{CJ})})}{2}=$$
$$\frac{1}{2}\left[\int_{-\mathrm{e}^{-y}}^{\xi}\mathrm{e}^{y}\omega_{oCJ}(\xi'\,\mathrm{e}^{y})\mathrm{d}\xi'-\int_{-\mathrm{e}^{-y}}^{\xi}\mathrm{e}^{\overline{y}_{CJ}}\omega_{oCJ}(\xi'\,\mathrm{e}^{\overline{y}_{CJ}})\mathrm{d}\xi'\right] \tag{B 22}$$

which takes the form $[\mu_{1,0}+\mu_{oCJ}(\xi\,\mathrm{e}^{\overline{y}_{CJ}})]^2=\mu_{oCJ}^2(\xi\,\mathrm{e}^{y})$ since the first integral on the right-hand side of (B 22) corresponds to $\mu_{oCJ}^2(\xi\mathrm{e}^{y})/2$ and the second integral, decomposed into $-(1/2)\int_{-\mathrm{e}^{-y}}^{-\mathrm{e}^{-\overline{y}_{CJ}}}-(1/2)\int_{-\mathrm{e}^{-\overline{y}_{CJ}}}^{\xi}$, gives $\mu_{oCJ}^2(-\mathrm{e}^{-(y-\overline{y}_{CJ})})/2-\mu_{oCJ}^2(\xi\mathrm{e}^{\overline{y}_{CJ}})/2$, so that (B 21) is recovered. Equation (B 21) corresponds simply to the leading order of the velocity distribution of the quasi-steady solution (5.21) $\overline{\mu}(\xi,\overline{y})$ in which $\overline{y}$ is replaced by $y(\tau)$, $\mu\approx\mu_{oCJ}(\xi\mathrm{e}^{y})$.

Appendix C. Useful example of hyperbolic problems

Consider the following hyperbolic problem for the field $z(\zeta,\tau)$

$$0 \geqslant \zeta \geqslant \zeta_b, : \quad \frac{\partial z}{\partial \tau} + \frac{\partial z}{\partial \zeta} = f(\zeta,\tau) > 0, \quad \zeta = \overline{\zeta}_b : \ z(\overline{\zeta}_b,\tau) = z_b(\tau) > 0 \tag{C 1}$$

where $\overline{\zeta}_b$ is a fixed coordinate, the source term $f(\zeta,\tau) > 0$ and $z_b(\tau) > 0$ being given functions. The general solution $z(\zeta,\tau)$ is obtained by the method of characteristics, $\mathrm{d}\zeta(\tau')/\mathrm{d}\tau' = 1$, $\zeta(\tau') = \zeta - \tau + \tau'$

$$\forall \tau_b \quad z(\zeta,\tau) = \int_{\tau_b}^{\tau} f(\zeta - \tau + \tau',\, \tau')\mathrm{d}\tau' + z(\zeta - \tau + \tau_b, \tau_b). \tag{C 2}$$

Choosing for τ_b the time at which the characteristic curve goes through the position $\overline{\zeta}_b$, $\forall \tau' : \quad \zeta(\tau') - \tau' = \overline{\zeta}_b - \tau_b$, $\zeta(\tau) = \zeta$, $\zeta - \tau = \overline{\zeta}_b - \tau_b$, the solution of (C 1) takes the form

$$z(\zeta,\tau) = \int_{\tau_b}^{\tau} f(\zeta - \tau + \tau',\, \tau')\mathrm{d}\tau' + z(\overline{\zeta}_b, \tau - \zeta + \overline{\zeta}_b), \tag{C 3}$$

$$z(\zeta,\tau) = \int_{\tau_b}^{\tau} f(\zeta - \tau + \tau',\, \tau')\mathrm{d}\tau' + z_b(\tau - \zeta + \overline{\zeta}_b) \tag{C 4}$$

$$z(\zeta,\tau) = \int_{\tau_b}^{\tau} f(\zeta - \tau + \tau',\, \tau')\mathrm{d}\tau' + z_b(\tau_b). \tag{C 5}$$

A change of variable of integration $\tau' \to \zeta' = \zeta - \tau + \tau'$ leads to a self-explanatory form by eliminating the time τ_b (in the lower bound of the integral) in favor of $\overline{\zeta}_b$,

$$z(\zeta,\tau) = \int_{\zeta - \tau + \tau_b = \overline{\zeta}_b}^{\zeta} f\big(\zeta',\ \tau + \zeta' - \zeta\big)\mathrm{d}\zeta' + z_b(\tau - \zeta + \overline{\zeta}_b). \tag{C 6}$$

Taking $\zeta = 0$ leads to the self-explanatory form,

$$\zeta = 0, \quad \overline{\zeta}_b < 0 : \qquad z(0,\tau) = \int_{\overline{\zeta}_b}^{0} f\big(\zeta',\ \tau + \zeta'\big)\mathrm{d}\zeta' + z_b(\tau - |\overline{\zeta}_b|), \tag{C 7}$$

where $\tau + \overline{\zeta}_b = \tau_b$ since $\zeta = 0$, so that $z_b(\tau - |\overline{\zeta}_b|) = z_b(\tau_b)$, the function $z_b(\tau)$ in the boundary condition (C 1) being given.

Consider now the case of a moving boundary. If $\overline{\zeta}_b$ in (C 1) is replaced by a known function of the time $\zeta_b(\tau)$,

$$\zeta = \zeta_b(\tau) : \ z(\zeta_b(\tau),\tau) = z_b(\tau) > 0, \tag{C 8}$$

the solution is still given by (C 2) in which τ_b is a function of $\tau - \zeta$ obtained by the intersection of the curve $\zeta' = \zeta_b(\tau')$ and the characteristic curve going through the point $(\zeta,\, \tau)$ in the phase space $\zeta' = \tau' + (\zeta - \tau)$ so that τ_b is the root of the equation

$$\zeta_b(\tau_b) - \tau_b = \zeta - \tau \quad \Rightarrow \quad \tau_b(\tau - \zeta), \tag{C 9}$$

showing that τ_b and thus $\zeta_b(\tau_b)$ are functions of $\tau - \zeta$, see figure 7. Then the solution is obtained from (C 2) and/or (C 4) in which $\overline{\zeta}_b$ is replaced by $\zeta_b(\tau_b)$,

$$z(\zeta,\tau) = \int_{\tau_b}^{\tau} f(\zeta - \tau + \tau',\, \tau')\mathrm{d}\tau' + z_b\big(\tau - \zeta + \zeta_b(\tau_b)\big) \tag{C 10}$$

$$z(\zeta,\tau) = \int_{\zeta_b(\tau_b)}^{\zeta} f(\zeta',\, \zeta' + \tau - \zeta)\mathrm{d}\zeta' + z_b(\tau_b) \tag{C 11}$$

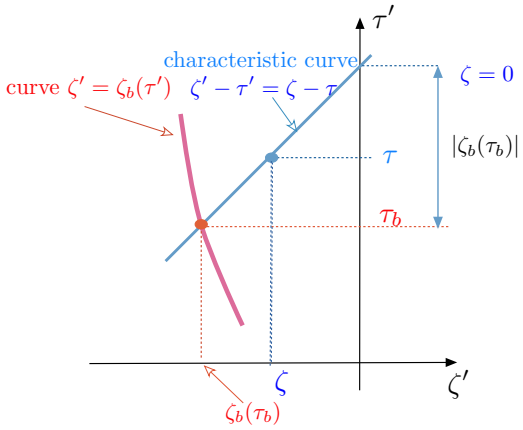

FIGURE 7. Determination of τ_b by the intersection of the characteristic curve in blue going through the point $(\zeta,\, \tau)$ $\zeta' - \tau' = \zeta - \tau$ with the curve $\zeta' = \zeta_b(\tau')$ in red.

where the relations $z_b\big(\tau - \zeta + \zeta_b(\tau_b)\big) = z\big(\zeta_b(\tau_b), \tau - \xi + \zeta_b(\tau_b)\big)$ and $\tau - \zeta + \zeta_b(\tau_b) = \tau_b$ have been used.

If the right-hand side of the first equation (C 1) depends on τ through an unknown function $y(\tau)$, $f(\zeta,\tau) = F\big(\zeta, y(\tau)\big) > 0$, an integral equation for $y(\tau)$ is obtained when an additional boundary condition is imposed to $z(\zeta,\tau)$, for example at $\zeta = 0$, $z(0,\tau) = z_N\big(y(\tau)\big)$ where $z_N(y)$ is a given function,

$$z_N\big(y(\tau)\big) = \int_{\zeta_b(\tau_b)}^{0} F\big(\zeta',\ y(\tau+\zeta')\big)\mathrm{d}\zeta' + z_b(\tau_b), \quad \tau_b = \tau + \zeta_b(\tau_b) < \tau \qquad \text{(C 12)}$$

where the expression of τ_b is valid for $\zeta = 0$.

Appendix D. Dynamics of planar detonations for small heat release

The dynamic of planar detonations is briefly revisited here in the small heat limit (4.14). The corresponding stability analysis against planar disturbances was first performed by Clavin & Williams (2002) for a smooth distribution of reaction rate. Here, the attention is focused onto the model (3.17)-(5.10) with (3.16) for which the reaction rate drops sharply to zero at the end of the reaction zone. Including the response to fluctuations of the flow of burnt gas, the flow field $\mu(\xi,\tau)$ is described by (3.10)-(3.11) with $\kappa = 0$, yielding with the notation $y/b \equiv \dot{\alpha}_\tau$

$$\xi_b \leqslant \xi \leqslant 0, : \quad \frac{\partial \mu}{\partial \tau} + \Big(\mu - \frac{y}{b}\Big)\frac{\partial \mu}{\partial \xi} = \frac{1}{2}\omega\big(\xi, y(\tau)\big), \quad \omega(\xi,y) = \mathrm{e}^{y}\omega_{o_{CJ}}\big(\xi \mathrm{e}^{y}\big) > 0, \quad \text{(D 1)}$$

$$\xi = 0 : \mu = 1 + 2y(\tau)/b, \qquad \xi = \xi_b = -\mathrm{e}^{-y(\tau)} : \ \mu = \mu_b(\tau),\ 0 < y/b \leqslant \mu_b \ll 1, \quad \text{(D 2)}$$

where the reduced velocity at the exit of the reaction zone $\mu_b(\tau)$ is a given function of the time and $\omega_{o_{CJ}}(\xi) > 0$, $\int_{-1}^{0} \omega_{o_{CJ}}(\xi)\mathrm{d}\xi = 1$, denotes the reduced distribution of the rate of heat release in the planar CJ wave ($\mu_b = 0$ and $\overline{y} = 0$) in steady state.

D.1. *Planar overdriven detonations in steady state*

Planar overdriven detonations in steady state, $y = \overline{y}_o$, $\mu = \overline{\mu}_o(\xi, \overline{y}_o)$, $\partial\overline{y}_o/\partial\tau = 0$, $\partial\overline{\mu}_o/\partial\tau = 0$, $\mu_b = \overline{\mu}_{ob} = \text{cst}$, $\overline{\mu}_{ob} - \overline{y}_o/b > 0$ (subsonic condition), are solutions to

$$\left(\overline{\mu}_o - \frac{\overline{y}_o}{b}\right)\frac{\mathrm{d}\overline{\mu}_o}{\mathrm{d}\xi} = \frac{1}{2}\mathrm{e}^{\overline{y}_o}\omega_{o_{CJ}}(\xi\,\mathrm{e}^{\overline{y}_o}) \tag{D 3}$$

$$\xi = 0:\ \overline{\mu}_o = 1 + 2\overline{y}_o/b, \qquad \xi = -\mathrm{e}^{-\overline{y}_o}:\ \overline{\mu}_o = \overline{\mu}_{ob},. \tag{D 4}$$

Introducing the velocity profile of the CJ wave $\mu_{o_{CJ}}(\xi) = \sqrt{\int_{-1}^{\xi}\omega_{o_{CJ}}(\xi')\mathrm{d}\xi'}$ and using the relation $\int_{\xi}^{0}\mathrm{e}^{\overline{y}}\omega_{o_{CJ}}\left(\xi'\mathrm{e}^{\overline{y}}\right)\mathrm{d}\xi' = \int_{\xi\mathrm{e}^{\overline{y}}}^{0}\omega_{o_{CJ}}(\xi'')\mathrm{d}\xi''$, integration of (D 3) from the exit of the reaction zone yields

$$\overline{\mu}_o(\xi) - \overline{y}_o/b = \sqrt{(\overline{\mu}_{ob} - \overline{y}_o/b)^2 + \mu^2_{o_{CJ}}(\xi\mathrm{e}^{\overline{y}_o})}. \tag{D 5}$$

For overdriven detonations $(\overline{\mu}_{ob} - \overline{y}_o/b) > 0$, the model (5.9)-(5.10) leads to the following behavior of the distribution $\overline{\mu}_o(\xi)$ at the end of the reaction zone $0 < (\xi + \mathrm{e}^{-\overline{y}_o}) \ll 1$ of

$$\xi < -\mathrm{e}^{-\overline{y}_o}:\ \overline{\mu}_o(\xi) = \overline{\mu}_{ob},\ \mathrm{d}\overline{\mu}_o/\mathrm{d}\xi = 0 \tag{D 6}$$

$$(\overline{\mu}_{ob} - \overline{y}_o/b) > 0, \quad 0 < \xi\mathrm{e}^{\overline{y}_o} + 1 \ll 1:\ \overline{\mu}_o(\xi) - \overline{\mu}_{ob} \approx \frac{a^2/2}{(\overline{\mu}_{ob} - \overline{y}_o/b)}(\xi\mathrm{e}^{\overline{y}_o} + 1)^2, \tag{D 7}$$

showing the existence of a thin layer at the end of the reaction zone of thickness $\sqrt{\overline{\mu}_{ob}}$ if the detonation is weakly overdriven $0 < \overline{\mu}_{ob} - \overline{y}_o/b \ll 1$. In the limit $\overline{\mu}_{ob} \to 0^+$, the derivative $\mathrm{d}\overline{\mu}_o/\mathrm{d}\xi$ degenerates into the singularity (5.9)-(5.10) of $\mathrm{d}\mu_{o_{CJ}}(\xi)/\mathrm{d}\xi$ at $\xi = -1$ for the planar CJ wave. The propagation velocity $\overline{y}_o$ is obtained and expressed in terms of the flow velocity at the exit of the reaction zone $\overline{\mu}_{ob}$ by the boundary condition at the Neumann state, $1 + \overline{y}_o/b = \sqrt{(\overline{\mu}_{ob} - \overline{y}_o/b)^2 + 1}$

$$\overline{y}_o = (1 + \overline{\mu}_{ob})^{-1} b\,\overline{\mu}^2_{ob}/2, \qquad \overline{y}_o/b \ll 1 \Rightarrow \overline{y}_o \approx b\,\overline{\mu}^2_{ob}/2 = O(1), \tag{D 8}$$

the last relation in (D 8) corresponding to a weakly overdriven regime at the leading order in the limit (4.14), $\overline{y}_o = O(1) \Leftrightarrow 0 < \overline{\mu}_{ob} = O(1/\sqrt{b})$.

D.2. *Planar dynamics of overdriven detonations.*

Subtracting (D 3) from (D 1) takes the form when using the notation $y(\tau) = \overline{y}_o + \delta y(\tau)$, $\mu(\xi, \tau) = \overline{\mu}_o(\xi) + \delta\mu(\xi, \tau)$,

$$\frac{\partial\delta\mu}{\partial\tau} + \frac{\partial}{\partial\xi}\left[\left(\overline{\mu}_o - \frac{\overline{y}_o}{b}\right)\delta\mu + \frac{1}{2}\delta\mu^2\right] = \frac{1}{2}\Delta\omega(\xi, y) + \frac{\mathrm{d}\overline{\mu}_o}{\mathrm{d}\xi}\frac{\delta y}{b} + \frac{\delta y}{b}\frac{\partial\delta\mu}{\partial\xi} \tag{D 9}$$

$$\text{where} \qquad \Delta\omega(\xi, y) \equiv \left[\mathrm{e}^{y}\omega_{o_{CJ}}\left(\xi\mathrm{e}^{y}\right) - \mathrm{e}^{\overline{y}_o}\omega_{o_{CJ}}(\xi\,\mathrm{e}^{\overline{y}_o})\right]. \tag{D 10}$$

The fluctuation of the propagation velocity $\delta y(\tau)$ is obtained by solving (D 9) with the boundary conditions (D 2) and (D 4). For a uniform velocity fluctuating in the burnt gas $\mu_b(\tau) = \overline{\mu}_{ob} + \delta\mu_b(\tau)$ where $\overline{\mu}_{ob} = \overline{\mu}(-\mathrm{e}^{-\overline{y}_o})$, the condition at the exit of the reaction zone $\mu(-\mathrm{e}^{-y}) = \mu_b(\tau)$ yields $\overline{\mu}_o(-\mathrm{e}^{-y}) + \delta\mu(-\mathrm{e}^{-y}, \tau) = \mu_b(\tau)$ so that the boundary conditions (D 4) takes the form

$$\delta\mu(0, \tau) = 2\,\delta y(\tau)/b, \qquad \delta\mu(-\mathrm{e}^{-y(\tau)}, \tau) = \delta\mu_b(\tau) - [\overline{\mu}_o(-\mathrm{e}^{-y(\tau)}) - \overline{\mu}_o(-\mathrm{e}^{-\overline{y}_o})]. \tag{D 11}$$

According to (D 6)-(D 7), the expression of the bracket in (D 11) depends on the sign of $\delta y \equiv y(\tau) - \overline{y}_o$ since $\overline{\mu}_o(-\mathrm{e}^{-y(\tau)}) = \overline{\mu}_o(-\mathrm{e}^{-\overline{y}_o})$ for $\delta y \leqslant 0$ so that $\delta\mu(-\mathrm{e}^{-y(\tau)}, \tau) = \delta\mu_b(\tau)$ while the bracket in the second relation in (D 11) is different from zero if $\delta y > 0$ and is continuous and equal to zero at $\delta y = 0$ ($y(\tau) = \overline{y}_o$). According to (3.17), a similar

behavior characterizes the reaction term (D 10), $\xi e^{\overline{y}_o} \leqslant -1 : \Delta\omega = e^{y}\omega_{o_{CJ}}\big(\xi e^{y}\big) > 0$ in the intermediate range $-e^{-y} < \xi < -e^{-\overline{y}_o}$ for $\delta y < 0$. The expression of $\Delta\omega(\xi, y)$ is different for $\delta y > 0$ in the range $-e^{-\overline{y}_o} < \xi < -e^{-y}$ where $\Delta\omega = -e^{\overline{y}_o}\omega_{o_{CJ}}(\xi\, e^{\overline{y}_o}) < 0$ but $\Delta\omega(\xi, y) \equiv 0\ \forall\xi$ when $\delta y = 0$.

In the linear approximation $y(\tau) = \overline{y}_o + \delta y(\tau)$ with $|\delta y|/\overline{y}_o \ll 1$, according to (D 11), the boundary condition at the end of the reaction zone reduces to

$$\delta\mu(-e^{-y}, \tau) = \delta\mu(-e^{-\overline{y}_o}, \tau) = \delta\mu_b(\tau) \tag{D 12}$$

since, according to (D 7), $d\overline{\mu}_o/d\xi|_{(\xi+e^{-\overline{y}_o})=0^+} = d\overline{\mu}_o/d\xi|_{(\xi+e^{-\overline{y}_o})=0^-} = 0$, so that the bracket in (D 11) introduces a quadratic term. Moreover the amplitude of the fluctuation of the position of the end of the reaction is limited to the thin layer mentioned below (D 7). Consider the transit time $\int_{\xi}^{0} d\xi'/[\overline{\mu}_o(\xi') - \overline{y}_o/b]$ of the upward-running acoustic mode for propagating disturbances from a point $\xi < 0$ to the lead shock $\xi = 0$. For overdriven detonations, focusing the attention to $\overline{\mu}_o(\xi) > 0$ larger than $1/b$, see (D 8), and neglecting correction of order $1/b$, the transit time can be written as the absolute value of a new coordinate system $\overline{\zeta}_o(\xi)$,

$$\overline{\zeta}_o(\xi) \equiv -\int_{\xi}^{0} d\xi'/\overline{\mu}_o(\xi') \leqslant 0, \qquad \overline{\zeta}_{ob} \equiv \overline{\zeta}_o(-e^{-\overline{y}_o}) = -\int_{-e^{-\overline{y}_o}}^{0} d\xi'/\overline{\mu}_o(\xi') < 0. \tag{D 13}$$

The distribution $\overline{\mu}_o(\xi)$ being a positive function increasing monotonously with ξ inside the inner structure $\xi \in [-e^{-\overline{y}_o}, 0]$, the relation between ξ and $\overline{\zeta}_o$ is bijective and the inverse function $\xi(\overline{\zeta}_o)$ is well defined. The transit time from the end of the reaction zone to the lead shock is $|\overline{\zeta}_{ob}|$ and one has $\overline{\zeta}_{ob} \leqslant \overline{\zeta}_o(\xi) \leqslant 0$ for $-e^{-\overline{y}_o} \leqslant \xi \leqslant 0$ while

$$\xi \leqslant -e^{-\overline{y}_o} : \qquad \overline{\zeta}_o(\xi) = \overline{\zeta}_{ob} + (\xi e^{\overline{y}_o} + 1)e^{-\overline{y}_o}/\overline{\mu}_{ob}, \tag{D 14}$$

since $e^{\overline{y}_o}\omega_{o_{CJ}}(\xi\, e^{\overline{y}_o}) = 0$ and $\overline{\mu}_o(\xi) = \overline{\mu}_{ob}$.

Neglecting the term $-(\overline{y}_o/b)\partial\delta\mu/\delta\xi$ in front of $\overline{\mu}_o\,\partial\delta\mu/\delta\xi$, linearization of (D 9) and (D 11) after multiplication by $\overline{\mu}_o(\xi)$ yields, according to (D 12),

$$\frac{\partial(\overline{\mu}_o\,\delta\mu)}{\partial\tau} + \frac{\partial(\overline{\mu}_o\,\delta\mu)}{\partial\overline{\zeta}_o} = f(\xi, y), \quad f(\xi, y) \equiv \overline{\mu}_o(\xi)\left[\frac{1}{2}\Delta\omega(\xi, y) + \frac{1}{b}\frac{d\overline{\mu}_o}{d\xi}\delta y\right] \tag{D 15}$$

$$\xi = 0 :\ \delta\mu = 2\,\delta y(\tau)/b, \qquad \xi = -e^{-y(\tau)} :\ \delta\mu = \delta\mu_b(\tau). \tag{D 16}$$

where ξ in $f(\xi, y)$ is the function of $\overline{\zeta}_o$, $\xi(\overline{\zeta}_o)$ obtained by inversion of (D 13). Using the relation $d\overline{\zeta}_o(\xi) = d\xi/\overline{\mu}_o(\xi)$, the instantaneous propagation velocity $\delta y(\tau)$ obtained from (D 15)-(D 16) is, according to (C 12), solution to the following integral equation,

$$2\overline{\mu}_o(0)\delta y(\tau) = \int_{-e^{-y(\tau_b)}}^{0}\left[\frac{b}{2}\Delta\omega\big(\xi, y(\tau + \overline{\zeta}_o(\xi))\big) + \frac{d\overline{\mu}_o}{d\xi}\delta y(\tau + \overline{\zeta}_o(\xi))\right]d\xi$$
$$+ b\overline{\mu}_{ob}\delta\mu_b\big(\tau + \overline{\zeta}_o(-e^{-y(\tau_b)})\big), \tag{D 17}$$

where $\tau_b = \tau + \overline{\zeta}_o(-e^{-y(\tau_b)})$. In the linear approximation

$$y(\tau_b) \approx \overline{y}_o + \delta y(\tau + \overline{\zeta}_{ob}) \approx y(\tau + \overline{\zeta}_{ob}), \tag{D 18}$$

$$-e^{-y(\tau_b)} \approx -e^{-y(\tau+\overline{\zeta}_{ob})} \approx -e^{-\overline{y}_o}[1 - \delta y(\tau + \overline{\zeta}_{ob})], \tag{D 19}$$

where $\zeta_{ob} \equiv \overline{\zeta}_o(-e^{-\overline{y}_o})$, the function $\delta\mu_b\big(\tau + \overline{\zeta}_o(-e^{-y(\tau_b)})\big)$ in the last term on the right-hand side of (D 17) can be replaced by $\delta\mu_b(\tau + \overline{\zeta}_{ob})$ and the lower bound of the integral can be replaced by $-e^{-y(\tau+\overline{\zeta}_{ob})}$. Consider first the case $\delta y(\tau + \overline{\zeta}_{ob}) < 0$, $y(\tau + \overline{\zeta}_{ob}) < \overline{y}_o$,

$-\mathrm{e}^{-y(\tau+\overline{\zeta}_{ob})} < -\mathrm{e}^{-\overline{y}_o}$. Starting the ξ-integration from the lower bound, there is a small ξ-range adjacent to $\xi = -\mathrm{e}^{-\overline{y}_o}$ of thickness $\mathrm{e}^{-\overline{y}_o}|\delta y(\tau+\overline{\zeta}_{ob})|$,

$$-\mathrm{e}^{-y(\tau+\overline{\zeta}_{ob})} < \xi < -\mathrm{e}^{-\overline{y}_o} \tag{D 20}$$

where the unperturbed reaction rate $\mathrm{e}^{\overline{y}_o}\omega_{o_{CJ}}(\xi\,\mathrm{e}^{\overline{y}_o})$ is identically zero so that, according to (D 10), $\Delta\omega\big(\xi, y(\tau+\overline{\zeta}_o)\big) = \mathrm{e}^{y(\tau+\overline{\zeta}_o(\xi))}\omega_{o_{CJ}}(\xi\,\mathrm{e}^{y(\tau+\overline{\zeta}_o(\xi))})$. According to (3.17), this term $\Delta\omega$ is linear in ξ in the small range (D 20), $\Delta\omega \approx c\,\mathrm{e}^{y(\tau+\overline{\zeta}_{ob})}[\xi\,\mathrm{e}^{y(\tau+\overline{\zeta}_{ob})}+1]$ so that the integral $\int_{-\mathrm{e}^{-y(\tau_b)}}^{-\mathrm{e}^{-\overline{y}_o}} \Delta\omega\big(\xi, y(\tau+\overline{\zeta}_o)\big)\mathrm{d}\xi$ yields a quadratic term $\propto |\delta y(\tau+\overline{\zeta}_{ob})|^2$ which is thus negligible in the linear analysis. A similar conclusion holds for $\delta y(\tau+\overline{\zeta}_{ob}) > 0$ since $\Delta\omega = \mathrm{e}^{\overline{y}_o}\omega_{o_{CJ}}(\xi\,\mathrm{e}^{\overline{y}_o}) \approx c\,\mathrm{e}^{\overline{y}_o}[\xi\,\mathrm{e}^{\overline{y}_o}+1]$ in the small ξ-range $-\mathrm{e}^{-\overline{y}_o} < \xi < -\mathrm{e}^{-y(\tau+\overline{\zeta}_{ob})}$. Therefore the lower bound of the integral in (D 17) can be taken equal to $-\mathrm{e}^{-\overline{y}_o}$. The linear version of equation (D 17) then takes the form,

$$2\overline{\mu}_o(0)\delta y(\tau) = \int_{-\mathrm{e}^{-\overline{y}_o}}^{0} g_o(\xi)\delta y\big(\tau+\overline{\zeta}_o(\xi)\big)\mathrm{d}\xi + b\overline{\mu}_{ob}\delta\mu_b(\tau+\overline{\zeta}_{ob}) \tag{D 21}$$

$$\text{where}\quad g_o(\xi) \equiv \frac{b}{2}\frac{\partial}{\partial y}\big[\mathrm{e}^y\omega_{o_{CJ}}(e^y\xi)\big]_{y=\overline{y}_o} + \frac{\mathrm{d}\overline{\mu}_o(\xi)}{\mathrm{d}\xi} \tag{D 22}$$

$$= \frac{b}{2}\mathrm{e}^{\overline{y}_o}\big[\omega_{o_{CJ}}(\xi\,\mathrm{e}^{\overline{y}_o}) + \xi\,\mathrm{e}^{\overline{y}_o}\omega'_{o_{CJ}}(\xi\,\mathrm{e}^{\overline{y}_o})\big] + \frac{\mathrm{d}\overline{\mu}_o(\xi)}{\mathrm{d}\xi} \tag{D 23}$$

where $\omega'_{o_{CJ}}(\xi) \equiv \mathrm{d}\omega_{o_{CJ}}(\xi)/\mathrm{d}\xi$. The lower bound of the integral $-\mathrm{e}^{-\overline{y}_o}$ in (D 21) can be set equal to $-\infty$ since $g_o(\xi) = 0$ for $\xi \leqslant -\mathrm{e}^{-\overline{y}_o}$ and $\int_{-\infty}^{0} g_o(\xi)\mathrm{d}\xi = \overline{\mu}_o(0) - \overline{\mu}_{ob}\ \forall b$ yielding $\int_{-\infty}^{0} g_o(\xi)\mathrm{d}\xi \approx \overline{\mu}_o(0)\ \forall b$ for a weakly overdriven regime ($\overline{\mu}_{ob} \ll 1$). The linear stability of weakly overdriven detonations sustained by a distribution of reaction rate satisfying (3.17) is obtained from (D 21) for $\delta\mu_b = 0$. This leads to the same equation as that derived by Clavin & Williams (2002) near the CJ regime for a distribution of reaction rate $\omega_{o_{CJ}}(\xi)$ and its derivative $\mathrm{d}\omega_{o_{CJ}}(\xi)/\mathrm{d}\xi$ decreasing continuously to zero at the end of the reaction $\lim_{\xi\to-\infty}\omega_{o_{CJ}}(\xi) = 0$,

$$2\,\overline{\mu}_o(0)\delta y(\tau) = \int_{-\infty}^{0} g_o(\xi)\delta y\big(\tau+\overline{\zeta}_o(\xi)\big)\mathrm{d}\xi, \qquad \int_{-\infty}^{0} g_o(\xi)\mathrm{d}\xi = \overline{\mu}_o(0) \quad \forall b. \tag{D 24}$$

Detonations are unstable to planar disturbances when b is sufficiently large. For typical reaction rates, the threshold of instability corresponds to b of order unity, see appendix B of Clavin & Denet (2018) where a slightly different notation has been used $\overline{\mu}(\xi)g(\xi) \to g(\overline{\zeta})$. Near the instability threshold, assuming that the dominant nonlinear mechanisms stabilizing the instability are the chemical kinetics, the nonlinear pulsation of weakly unstable detonations is solution to a nonlinear equation extending (D 24) when $g_o(\xi)\delta y$ is replaced by its nonlinear version $W_o(\xi, y)$,

$$2\,\overline{\mu}_o(0)\delta y(\tau) = \int_{-\infty}^{0} W_o\big(\xi, y(\tau+\overline{\zeta}_o(\xi)\big)\mathrm{d}\xi, \tag{D 25}$$

$$W_o(\xi, y) \equiv \frac{b}{2}\left[\mathrm{e}^y\omega_{o_{CJ}}\big(\xi\mathrm{e}^y\big) - \mathrm{e}^{\overline{y}_o}\omega_{o_{CJ}}(\xi\,\mathrm{e}^{\overline{y}_o})\right] + \frac{\mathrm{d}\overline{\mu}_o(\xi)}{\mathrm{d}\xi}(y-\overline{y}_o). \tag{D 26}$$

A similar equation was derived previously in the opposite limit of strongly overdriven detonations with a large Mach number, see Clavin & He (1996).

D.3. *CJ regime. The hot boundary difficulty*

The hot boundary difficulty is associated with the sonic condition at the end of the reaction of a CJ wave, $\xi = -1 : \overline{\mu}_{o_{CJ}}(\xi) = 0$, $\overline{y}_{o_{CJ}} = 0$ so that the transit time from the end of the reaction of the upwards-running acoustic mode diverges. This divergence is weak for the model (3.17)-(5.10) as shown now. Consider a weakly overdriven regime, $\overline{\mathrm{m}}_{ob}^2 \equiv b\overline{\mu}_{ob}^2/2 = O(1)$, for which the small parameter $1/\sqrt{b}$ characterizes the proximity of the CJ regime,

$$\overline{\mu}_{ob} = O(1/\sqrt{b}), \quad \overline{y}_o \approx \overline{\mathrm{m}}_{ob}^2 = O(1), \quad \overline{\mu}_o(\xi, \overline{y}_o) \approx \sqrt{2\,\overline{\mathrm{m}}_{ob}^2/b + \mu_{o_{CJ}}^2(\xi \mathrm{e}^{\overline{\mathrm{m}}_{ob}^2})}, \qquad \text{(D 27)}$$

the explicit dependence on the detonation velocity $\overline{y}_o$ being now incorporated into the expression of the velocity distribution $\overline{\mu}_o(\xi, \overline{y}_o)$. Inside the inner structure of the detonation for $\xi \mathrm{e}^{\overline{\mathrm{m}}_{ob}^2} + 1$ not close to zero, namely for $\overline{\mu}_o(\xi, \overline{y}_o) \approx \mu_{o_{CJ}}(\xi \mathrm{e}^{\overline{\mathrm{m}}_{ob}^2}) > 0$ of order unity, the time delay $|\overline{\zeta}_o(\xi)|$ is also of order unity. It increases and becomes as large as $\ln \sqrt{b}$ in a thin layer near the end of the reaction zone ($\xi \mathrm{e}^{\overline{\mathrm{m}}_{ob}^2} + 1) = O(1/\sqrt{b})$ and diverges logarithmically when approaching the CJ regime (limit $\overline{\mathrm{m}}_{ob} \to 0$). This is checked by considering a point ξ_m outside the thin layer so that the integral $\int_0^{\xi_m}$ in (D 13) is finite (of order unity) and by computing $\int_{\xi_m}^{\xi}$ for ξ inside the thin layer, $\mu_{o_{CJ}}(\xi \mathrm{e}^{\overline{\mathrm{m}}_{ob}^2}) \approx a \left(\xi \mathrm{e}^{\overline{\mathrm{m}}_{ob}^2} + 1\right) = O(1/\sqrt{b})$

$$-\int_{\xi}^{\xi_m} \frac{\mathrm{d}\xi'}{\overline{\mu}_o(\xi')} = -\sqrt{b/2}\frac{\mathrm{e}^{-\overline{\mathrm{m}}_{ob}^2}}{\overline{\mathrm{m}}_{ob}} \int_{\xi \mathrm{e}^{\overline{\mathrm{m}}_{ob}^2}}^{\xi_m \mathrm{e}^{\overline{\mathrm{m}}_{ob}^2}} \frac{\mathrm{d}\xi''}{\sqrt{1 + b(\xi''+1)^2 a^2/(2\,\overline{\mathrm{m}}_{ob}^2)}}. \qquad \text{(D 28)}$$

A change of variable $Y'' = \sqrt{b}\,(\xi''+1)a/(\sqrt{2}\,\mathrm{m}_b)$ leads to

$$-\int_{\xi}^{\xi_m} \frac{\mathrm{d}\xi'}{\overline{\mu}_o(\xi')} = -\frac{\mathrm{e}^{-\overline{\mathrm{m}}_{ob}^2}}{a} \int_{Y}^{Y(\xi_m)} \frac{\mathrm{d}Y''}{\sqrt{1+Y''^2}} = -\frac{\mathrm{e}^{-\overline{\mathrm{m}}_{ob}^2}}{a} \ln\left(Y'' + \sqrt{1+Y''^2}\right)\Big|_Y^{Y_m},$$

where $Y \equiv \sqrt{b}\,(\xi \mathrm{e}^{\overline{\mathrm{m}}_{ob}^2} + 1)a/(\sqrt{2}\,\overline{\mathrm{m}}_{ob})$, $Y(\xi) = O(1)$ inside the thin layer and $Y(\xi_m) \gg 1$ of order $\sqrt{b}$ outside. Moreover, using the limit $\lim_{\sqrt{b}\,(\xi \mathrm{e}^{\overline{\mathrm{m}}_{ob}^2}+1) \to 0^+} Y = 0\ \forall\, \overline{\mathrm{m}}_{ob}$, the time delay $|\overline{\zeta}_o(\xi)|$ at the end of the reaction zone behaves like

$$-\frac{\mathrm{e}^{-\overline{\mathrm{m}}_{ob}^2}}{a} \ln\left[\frac{\sqrt{2\,b}}{\overline{\mathrm{m}}_{ob}}\left(\xi_m \mathrm{e}^{\overline{\mathrm{m}}_{ob}^2} + 1\right)\right] \quad \text{where} \quad \xi_m \mathrm{e}^{\overline{\mathrm{m}}_{ob}^2} + 1 = O(1), \qquad \text{(D 29)}$$

showing an order of magnitude equal to $\ln(\sqrt{b})$ inside the thin layer and a logarithmic divergence when approaching the CJ regime ($\overline{\mathrm{m}}_{ob} \to 0^+$),

$$\lim_{\overline{\mathrm{m}}_{ob} \to 0} |\overline{\zeta}_o(\xi)|_{\sqrt{b}\,(\xi+1)=0^+} \propto \ln(\sqrt{b}/\,\overline{\mathrm{m}}_{ob}). \qquad \text{(D 30)}$$

Thanks to the rapid decease of the reaction rate at the end of the reaction zone, equations (D 24) and (D 26) still work for the CJ regime despite the divergence of the transit time.

Appendix E. Time lag along a straight trajectory

Considering a trajectory with a detonation velocity decreasing toward the CJ velocity, $\mathrm{d}y/\mathrm{d}\tau < 0$, an analytical expression of the time lag z_b can be obtained by using the piecewise-linear model for $\mu_{o_{CJ}}(\xi)$ in figure 8 where $h_\mu > 1$, (typically $h_\mu \approx 1.5 - 2$). To obtained $z_b(\tau)$ from (8.30), two cases have to be considered depending on the sign of

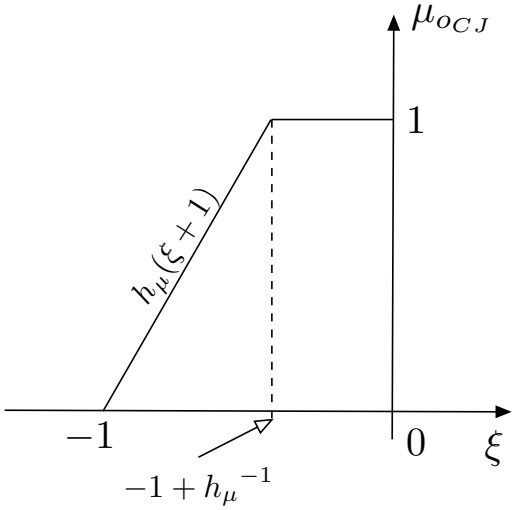

FIGURE 8. Model of constant reaction rate during a finite time after the induction delay

$-\mathrm{e}^{-[y(\tau-z_b)-\overline{y}_{CJ}]}+1-h_\mu^{-1}$:

-i) Consider first conditions for which $y(\tau-z_b)$ is not too far from the CJ regime, so that that the difference $y(\tau-z_b)-\overline{y}_{CJ}$ is such that,

$$-1<-\mathrm{e}^{-[y(\tau-z_b)-\overline{y}_{CJ}]}<-1+h_\mu^{-1} \quad \Rightarrow \quad y(\tau-z_b)-\overline{y}_{CJ}<\ln[h_\mu/(h_\mu-1)], \tag{E 1}$$

$-\mathrm{e}^{-[y(\tau-z_b)-\overline{y}_{CJ}]}<-1+h_\mu^{-1}$, where $\ln[h_\mu/(h_\mu-1)]\approx 0.7$ for $h_\mu\approx 2$. This implies that $y(\tau)-\overline{y}_{CJ}$ is also not too large

$$y(\tau)<y(\tau-z_b) \quad \Rightarrow \quad y(\tau)-\overline{y}_{CJ}<\ln[h_\mu/(h_\mu-1)]. \tag{E 2}$$

Then, according to (8.30), one gets the following equation for the delay z_b in the form

$$(h_\mu \mathrm{e}^{\overline{y}_{CJ}})z_b=a-\ln\left(1-\mathrm{e}^{-[y(\tau-z_b)-\overline{y}_{CJ}]}\right), \quad a\equiv(h_\mu-1)-\ln h_\mu>0,\ a\approx 0.3. \tag{E 3}$$

Consider a decreasing velocity larger than the CJ velocity, $\mathrm{d}y(\tau)/\mathrm{d}\tau<0$ and $y(\tau)-\overline{y}_{CJ}>0$, equation (E 3) has a single and finite root $z_b>0$ since the right-hand side is an increasing function of z_b from $(h_\mu-1)-\ln h_\mu<0$ at $z_b=\infty$ $(y(\tau+\zeta_b)=\infty)$ to a smaller value at $\zeta_b=0$. For consistency the solution should satisfy (E 1). For the sake of simplicity, consider a straight trajectory approaching the CJ regime from above (constant deceleration of the blast wave $A>0$)

$$y(\tau)=\overline{y}_{CJ}+A(\tau_{CJ}-\tau), \qquad A>0, \qquad (\tau_{CJ}-\tau)>0 \tag{E 4}$$

$$y(\tau-z_b)-\overline{y}_{CJ}=[y(\tau)-\overline{y}_{CJ}]+Az_b \tag{E 5}$$

$$(h_\mu \mathrm{e}^{\overline{y}_{CJ}})z_b=a-\ln\left(1-\mathrm{e}^{-[y(\tau)-\overline{y}_{CJ}]-Az_b}\right) \tag{E 6}$$

where the parameter $A>0$ is the non dimensional deceleration, τ_{CJ} is the time at which the trajectory intersects the CJ peninsula ($\tau<\tau_{CJ}$) and the parameter $a>0$ is given in (E 3). Introducing $X=y(\tau-z_b)-\overline{y}_{CJ}>0$ and the parameter $B>0$ characterizing the reduced velocity $y(\tau)$ at time τ,

$$X=[y(\tau)-\overline{y}_{CJ}]+Az_b\geqslant 0, \qquad B=[y(\tau)-\overline{y}_{CJ}]+Aa/(h_\mu \mathrm{e}^{\overline{y}_{CJ}})\geqslant 0, \tag{E 7}$$

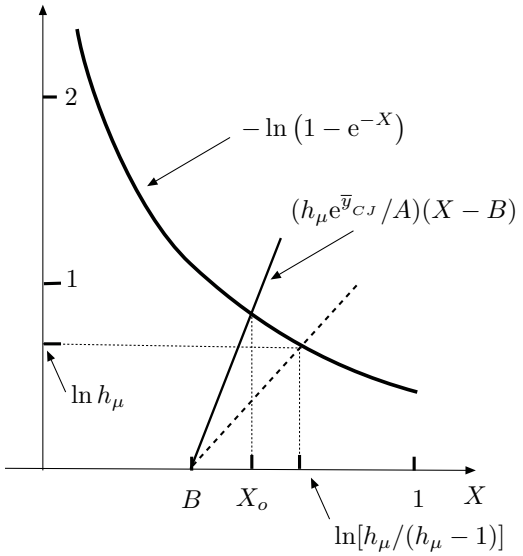

FIGURE 9. Graphic solution of equation (E 8) for $h_\mu \approx 2$. The dot line denotes the limit of the straight line whose intersection with the curve $-\ln(1-\mathrm{e}^{-X})$ determines the solution X_o.

equation (E 6) for z_b at time τ takes the form

$$\frac{h_\mu \mathrm{e}^{\overline{y}_{CJ}}}{A}[X-B] = -\ln\left(1-\mathrm{e}^{-X}\right). \tag{E 8}$$

For consistency with (E 1), the root X_o of (E 8) should be smaller than $ln[h_\mu/(h_\mu-1)] \approx 0.7$, so that the parameter B should be sufficiently small $B < 0.7$ since $B < X_o < ln[h_\mu/(h_\mu-1)]$, see figure 9. These conditions on X_o imply that the slope of the straight line in figure 9, $h_\mu \mathrm{e}^{\overline{y}_{CJ}}/A$ is larger than $\ln h_\mu/[\ln\left(h_\mu/(h_\mu-1)\right)-B]$ yielding a maximum value A_m of the deceleration A

$$A \leqslant A_m, \quad \frac{A_m}{\mathrm{e}^{\overline{y}_{CJ}}}\frac{(h_\mu-1)}{h_\mu} = \ln\left(\frac{h_\mu}{h_\mu-1}\right) - \left(y(\tau)-\overline{y}_{CJ}\right) \tag{E 9}$$

corresponding to a maximum X_m of X_o, $X_m = \ln[h_\mu/(h_\mu-1)]$, $A_m z_b + (y(\tau)-\overline{y}_{CJ}) = \ln[h_\mu/(h_\mu-1)]$ and to a delay $z_b = (h_\mu-1)/h_\mu \mathrm{e}^{\overline{y}_{CJ}}$. For a deceleration of order unity, $A = O(1)$, the solution of (E 8) and the time delay $z_b(\tau)$ are of order unity and the latter varies weakly when approaching the CJ regime $[y(\tau)-\overline{y}_{CJ}] \ll 1$.

Consider now a small deceleration of the blast wave $A \ll 1$. The limit of a small slope of the trajectory $A \to 0^+$, $X_o \to B$, requires some attention. If one considers the limit $A \to 0^+$ for a fixed and nonzero value of $y(\tau)-\overline{y}_{CJ} = A(\tau-\tau_{CJ}) \neq 0$, the parameter B in (E 7) keeps on nonzero $B \to y(\tau)-\overline{y}_{CJ} \neq 0$, and the limit $X_o \to B$ shows that the delay still goes to a value of order unity $z_b \to a/h_\mu \mathrm{e}^{\overline{y}_{CJ}}$. To summarize, at a finite distance from the CJ regime at time τ, the time delay z_b is still of order unity. The limit of a small deceleration $A \to 0^+$ is different when the propagation velocity $y(\tau)$ reaches the CJ velocity at finite time $\tau = \tau_{CJ} : y(\tau) = \overline{y}_{CJ}$, $X = Az_b$ and $B = Aa/(h_\mu \mathrm{e}^{\overline{y}_{CJ}})$, $\lim_{A\to 0^+} B = 0$. Then, equation (E 8) yields

$$\tau = \tau_{CJ} \quad A \to 0^+ : \qquad h_\mu \mathrm{e}^{\overline{y}_{CJ}} X = -A\ln\left(1-\mathrm{e}^{-X}\right) \to 0^+, \tag{E 10}$$

showing that the delay z_b diverges weakly when the slope of the trajectory decreases to

zero, $z_b = X/A \to \infty$, $z_b \approx \ln A^{-1}$ in a way reminiscent of (D 30).

-ii) Consider now the case opposite to (E 1)

$$-1 + h_\mu^{-1} < -\mathrm{e}^{-[y(\tau - z_b) - \overline{y}_{CJ}]} \quad \Rightarrow \quad \ln[h_\mu/(h_\mu - 1)] < y(\tau - z_b) - \overline{y}_{CJ}. \quad \text{(E 11)}$$

Equations (8.30) then yields $z_b = \mathrm{e}^{-y(\tau - z_b)}$. Using (E 4) and $X = Az_b$ this gives

$$X\mathrm{e}^X = A\mathrm{e}^{-A(\tau_{CJ} - \tau)}. \quad \text{(E 12)}$$

For a decreasing trajectory $A > 0$ with $y(\tau) > y_{CJ}$, the delay $z_b(\tau)$ at time $\tau < \tau_{CJ}$ increases with the time to a maximum value $X_m\mathrm{e}^{X_m} = A$ (when reaching the CJ velocity, $\tau = \tau_{CJ}$) and decreases quickly to zero in the past, $z_b \approx \mathrm{e}^{-A(\tau_{CJ} - \tau)}$ for $A(\tau_{CJ} - \tau) \gg 1$.

For an increasing trajectory, $\mathrm{d}y/\mathrm{d}\tau > 0$, $A < 0$, equation (E 12) has no root or the solution for z_b is multivalued. This is in agreement with the fact that, according to § 9.2, causality is not satisfied.

REFERENCES

Clavin, P. & Denet, B. 2018 Decay of plane detonation waves to the self-propagating chapman-jouguet regime. *J. Fluid. Mech.* **845**, 170–202.

Clavin, P. & He, L. 1996 Stability and nonlinear dynamics of one-dimensional overdriven detonations in gases. *Journal of Fluid Mechanics* **306**, 353–378.

Clavin, P. & Searby, G. 2016 *Combustion waves and fronts in flows*. Cambridge University Press.

Clavin, P. & Williams, F.A. 2002 Dynamics of planar gaseous detonations near Chapman-Jouguet conditions for small heat release. *Combustion Theory and Modelling* **6**, 127–129.

Clavin, P. & Williams, F.A. 2009 Multidimensional stability analysis of gaseous detonations near chapman-jouguet conditions for small heat release. *Journal of Fluid Mechanics* **624**, 125–150.

Döring, W. 1943 On detonation processes in gases. *Ann. Phys.* **43**, 421–436.

Eckert, C.A., Quirk, J.J. & Shepherd, J.E. 2000 The role of unstedeadness in direct initiation of gaseous detonations. *J. Fluid. Mech.* **42**, 147–183.

Faria, L., Kasimov, A. & Rosales, R. 2015 Theory of weakly nonlinear self-sustained detonations. *Journal of Fluid Mechanics* **784**, 163–198.

Fickett, W. & Davis, W.C. 1979 *Detonation*. University of California Press.

He, L. 1996 Theoretical determination of the critical conditions for the direct initiation of detonations in hydrogen-oxygen mixtures. *Combust. Flame* **104**, 401–418.

He, L. & Clavin, P. 1994 On the direct initiation of gaseous detonations by an energy source. *Journal of Fluid Mechanics* **277**, 227–248.

Korobeinikov, P.V. 1971 Gas dynamics of explosions. *Annual Review of Fluid Mechanics* **3**, 317–346.

Lee, J.H.S. 1977 Initiation of gaseous detonations. *Ann. Rev. Phys. Chem.* **28**, 75–104.

Lee, J.H.S. 1984 Dynamic parameters of gaseous detonations. *Ann. Rev. Fluid. Mech.* **16**, 311–336.

Lee, J.H.S. & Higgins, A.J. 1999 Comments on criteria for direct initiation of detonation. *Phil. Trans. R. Soc. Lond. A* **357**, 3503–3521.

Liñan, A., Kurdyumov, V. & Sanchez, A.L. 2012 Initiation of reactive blast waves by external energy source. *Comptes Rendus Mécanique* **340**, 829–844.

Sedov, L.I. 1946 Propagation of strong blast waves. *Prikl. Mat. Meckh.* **10**, 241–250.

Short, M. & Bdzil, J. B. 2003 Propagation laws for steady curved detonations with chain-branching kinetics. *Journal of Fluid Mechanics* **479**, 39–64.

Stewart, D. S. & Kasimov, A.R. 2005 Theory of detonation with an embedded sonic locus. *SIAM J. Appl. Math.* **66** (2), 384–407.

Taylor, G. I. 1950*a* The dynamics of combustion products behind plane and spherical detonation fronts. *Proc. R. Soc. London* **A 200**, 235–247.

Taylor, G. I. 1950*b* The formation of a blast wave by a very intense explosion. *Proc. R. Soc. London* **A 201**, 159–174.

Vieille, P. 1900*b* Structure des detonations. *C.R. Acad. Sci. Paris* **131**, 413.

Von Neumann, J. 1942 Theory of detonation waves. Progress Report OSRD-549. National Defense Research Committee Div. B.

Wood, W. W. & Kirkwood, J.G. 1954 Diameter effect in condensed explosives. the relation between velocity and radius of the detonation wave. *Journal of Chemical Physics* **22**, 1920–1924.

Yao, J. & Stewart, D. S. 1995 On the normal shock velocity curvature relationship for materials with large activation energy. *Combustion and Flame* **100** (519-528).

Zeldovich, Ya. B. 1940 On the theory of the propagation of detonations in gaseous systems. *Zhur. Eksp. Teor. Fiz.* **10**, 542–568.

Zeldovich, Ya. B. 1942 On the distribution of pressure and velocity in products of detonation blasts, in particular for spherical propagating detonation waves. *Zhur. Eksp. Teor. Fiz.* **12**, 389–406.

Zeldovich, Ya. B., Kogarko, S.M. & Simonov, N 1956 An experimental investigation of spherical detonations of gases. *Sov. Phys. Tech. Phys.* **1** (8), 1689–1713.

Zeldovich, Ya. B. & Kompaneets, A. S. 1960 *Theory of detonation*. Academic Press.